Mapping **A**rchitecture **C**oncept for **U**niversal **L**anding **A**utomation

MACULA

Customer: Jeffrey Thayer & Brian Argrow, University of Colorado Boulder AES

Faculty Advisor: Jay McMahon

Team Members:

Trevor Arrasmith, Brett Bender, Chris Brown, Nick Dawson, David Emmert,
Bryce Garby, Russell Gleason, Matthew Hurst, Jared Levin, Ansel Rothstein-Dowden

Agenda

Project Description	Nick
Baseline Design	Matt
Hardware Feasibility	Bryce, Ansel
Software Feasibility	Ansel
Test Feasibility	Chris
Budget/Schedule	Chris

PROJECT DESCRIPTION

Motivation

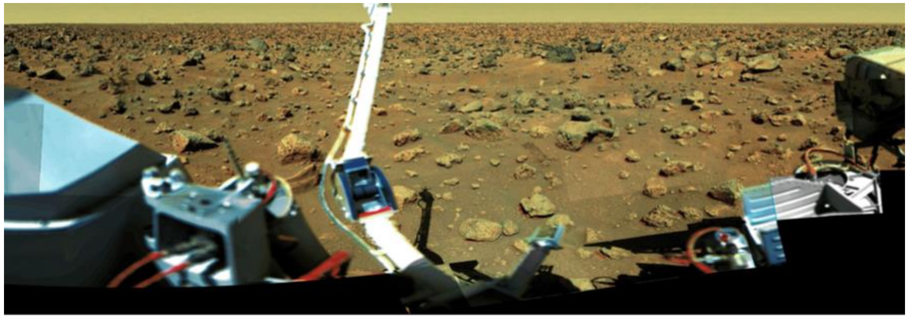

Rocks on the Martian surface

http://geology.isu.edu/wapi/Geo_Pgt/Mod09_Mars/images/VIEWFRMLANDER2VLFMOS21.gif

Landing zones for spacecraft must be pre-determined as "safe," and can be far from areas of scientific interest

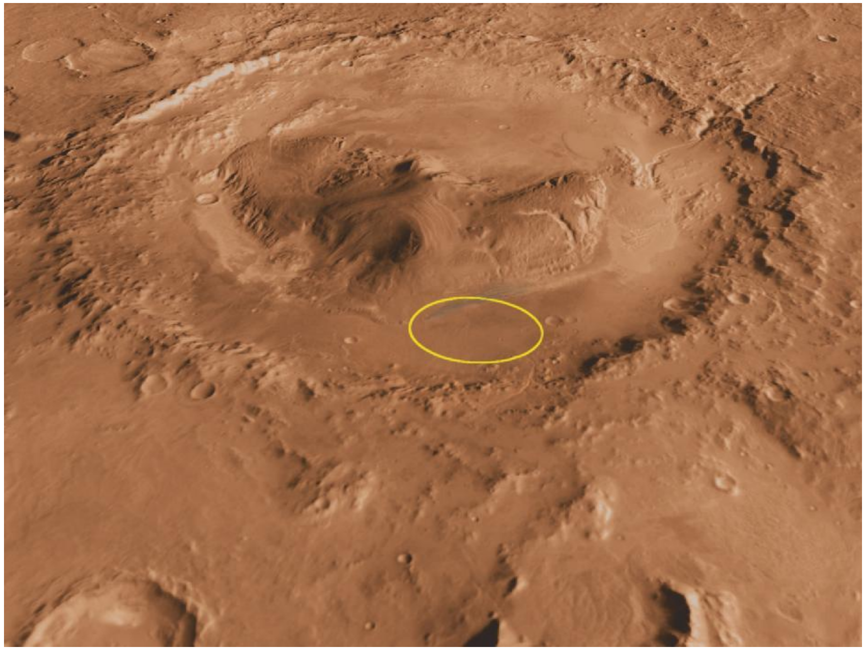

Curiosity's error ellipse on Mars (20 km minor, 25 km major axis)

http://www.nasa.gov/images/content/573652main_pia14294-anno-43_946-710.jpg

CubeSat Lander Concept

- Landing hazard definition based on hypothetical CubeSat lander dimensions
- Hazards (obstacles and gradients) identified where the lander could land more than 15° off of vertical
- Scanning resolution of 10 cm selected to detect ~98% of potential hazards

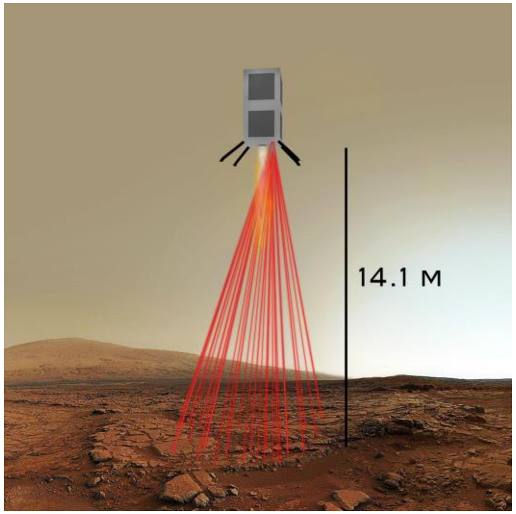

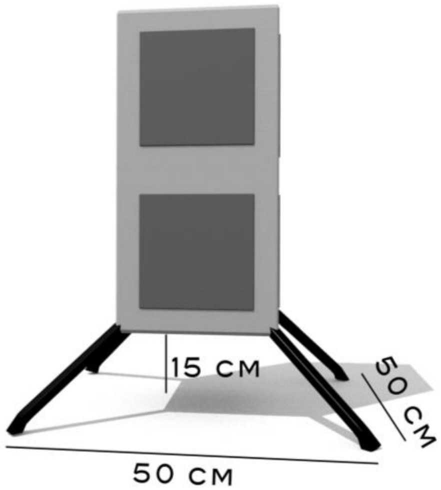

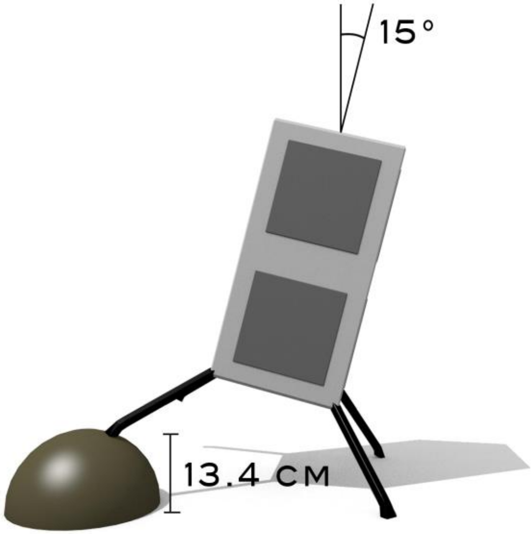

Project Objectives

Design, **manufacture**, and **test** a **proof-of-concept** light detection and ranging (lidar) **scanning system** for a landing spacecraft

Success Levels:

1. Lidar sensor and scanning mechanism, mounted on a stationary platform, shall **record correlated range and attitude measurements** at a 0.1 m spatial resolution from a nadir distance of 14.1 m with a maximum 20° off nadir
2. System shall scan a known test scene and **project measurements into a 3D point cloud**
3. System shall scan a landing-zone mockup and **analyze the 3D point cloud for hazards**
4. System shall **select a safe landing zone**; if no safe landing zone is found, hazard definition will be loosened until a landing zone is found

Concept of Operations

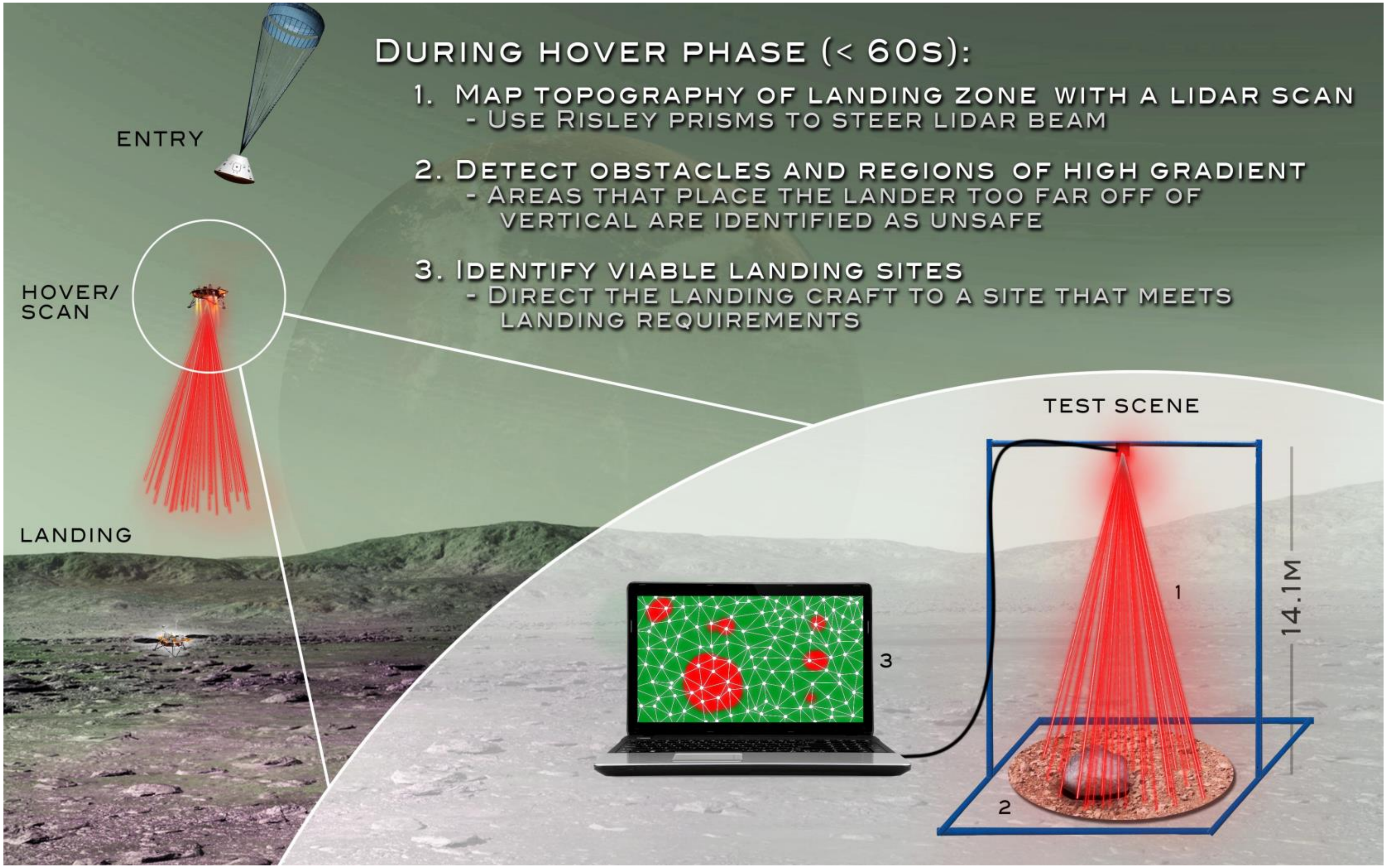

Functional Block Diagram

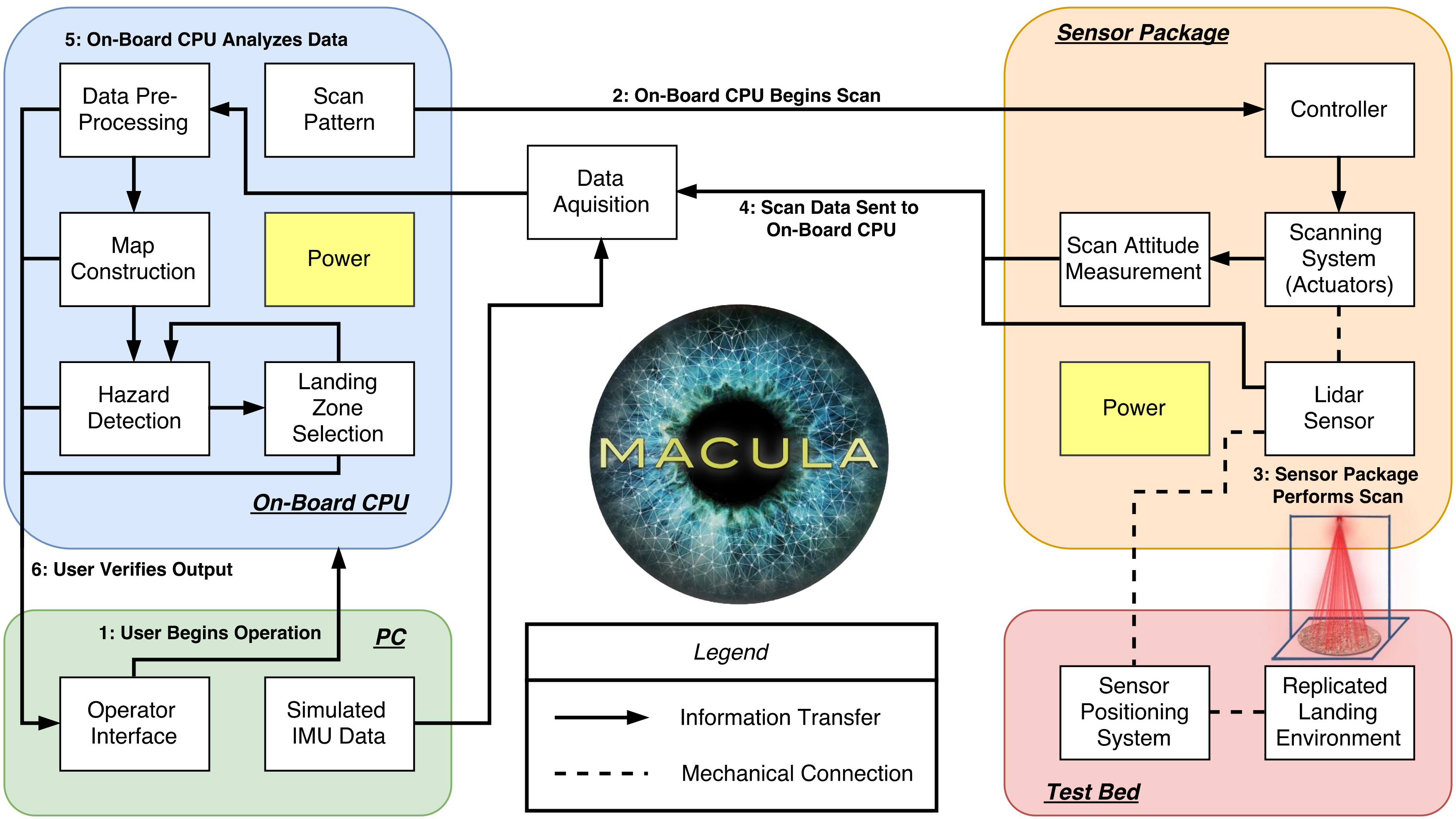

Functional Requirements

FR1: The system shall implement a proof-of-concept landing assist system for a CubeSat lander

DRs: 14.1 m range, 20° half angle, 0.1 m spatial resolution, 60 seconds

FR2: The on-board processor shall receive commands and data from a user-operated PC

FR3: The on-board processor shall command the sensor package, made up of the lidar and the scanning system

FR4: The sensor package shall utilize lidar to obtain range measurements at known orientations

FR5: The sensor package shall transmit data to an on-board processor or DAQ

FR6: The on-board processor shall translate the range and attitude data into a three-dimensional point cloud

FR7: The on-board processor shall analyze the 3D point cloud for hazards

FR8: The on-board processor shall select an acceptable landing site

FR9: The system shall generate output readable by the PC

Baseline Design

Baseline Design Overview

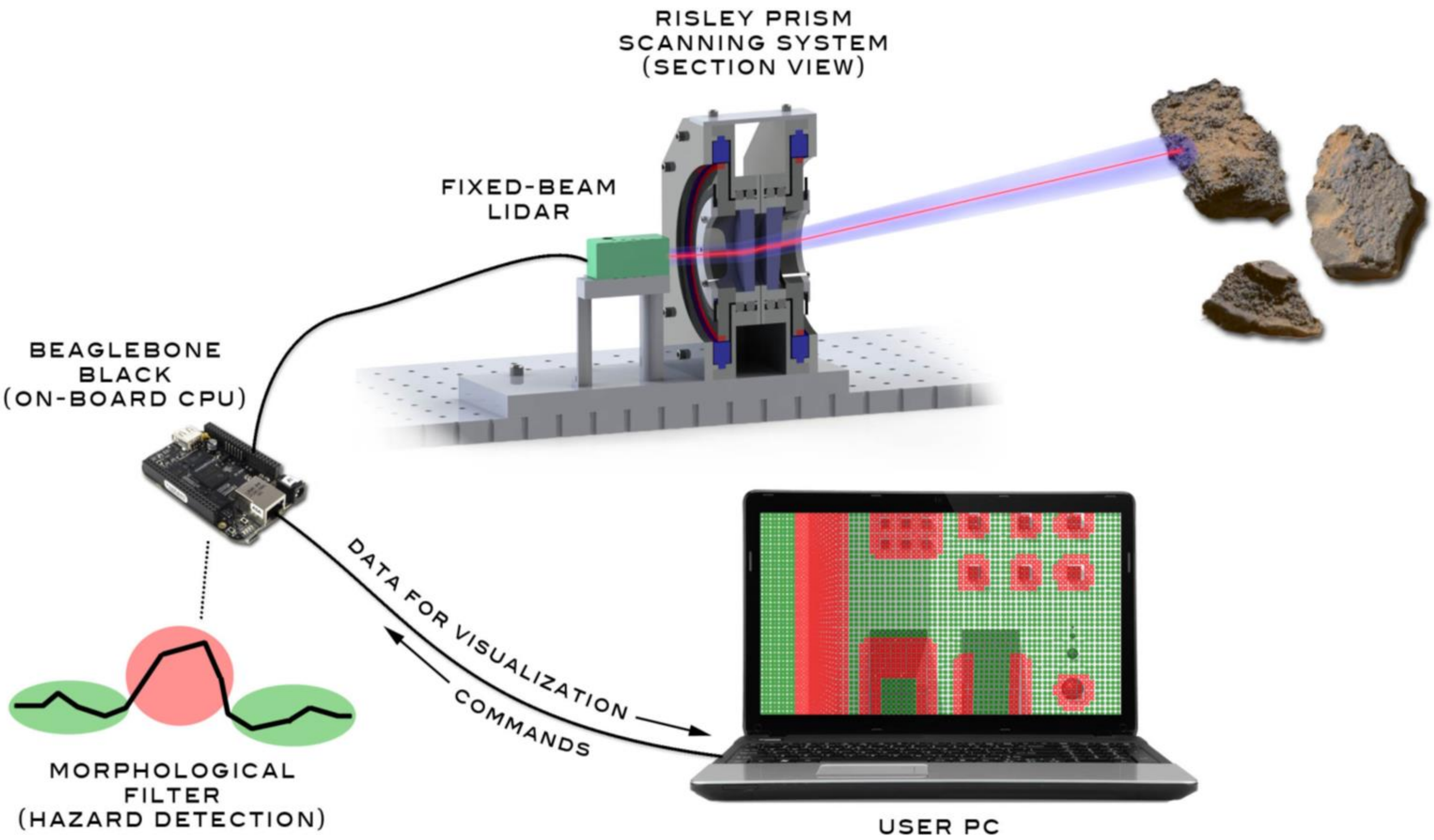

not to scale

Baseline Design: Lidar Sensor

<u>Fixed-Beam Lidar</u>

- Emits and detects laser pulses for range measurement in single direction
- Sensor does not change pointing direction
  - Beam must be steered to scan planar surface
- Attitude and range measurements can be projected into a 3D topographic map

not to scale

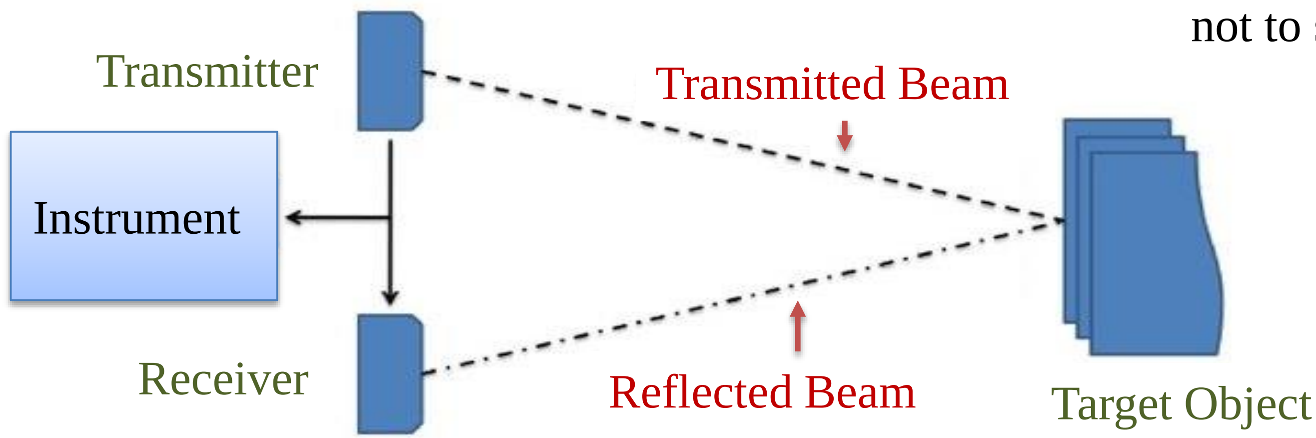

https://www.quora.com/How-does-LIDAR-work

First Principle: Refraction

- Prisms refract incident light at an angle
- Snell's Law: $n_1 \sin(\theta_i) = n_2 \sin(\theta_f)$

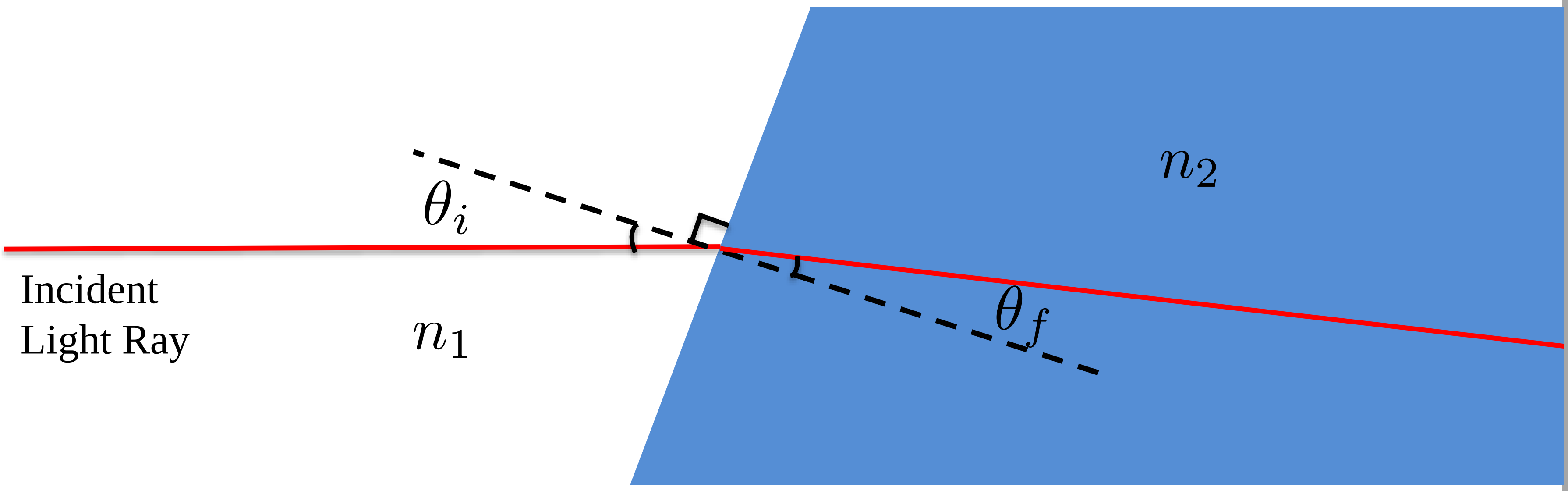

Multiple Refraction: Risley Prisms

- This concept can be extended to multiple prisms
- Two adjacent prisms are called Risley prisms
- Controlling the orientation of these prisms allows the refracted ray to be directed

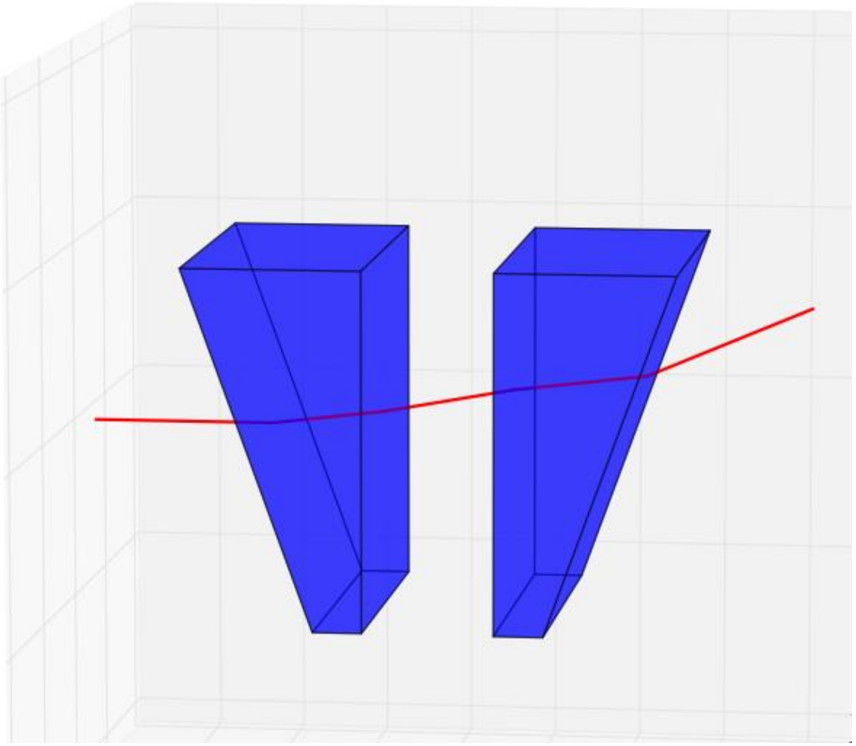

Risley Prisms

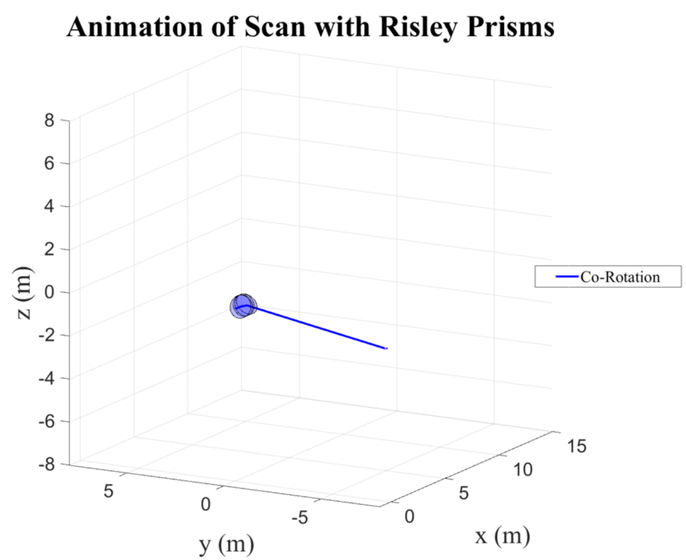

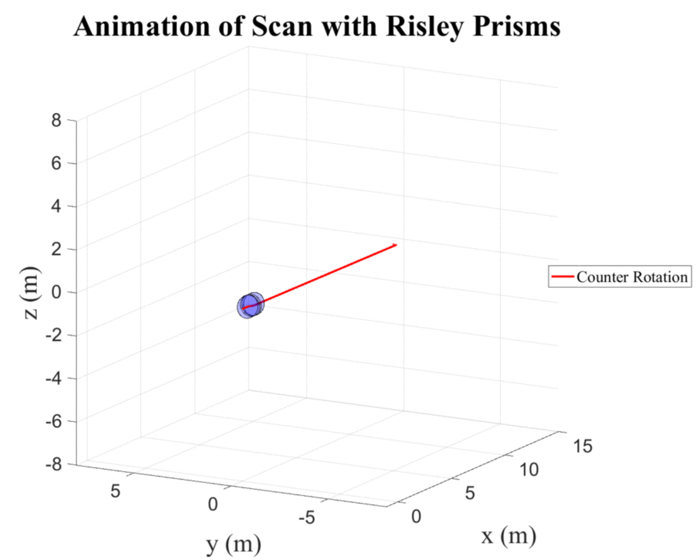

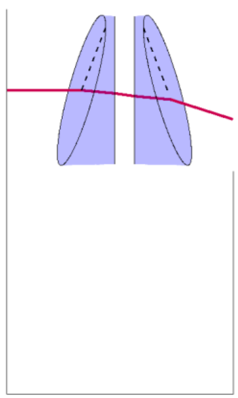

Co-rotation sweeps full-sized circles

Counter-rotation sweeps half-sized circles

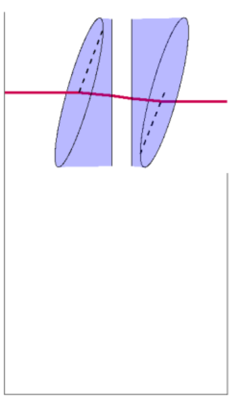

Spiral Scan Pattern

- Risley prisms ➔ polar coordinates

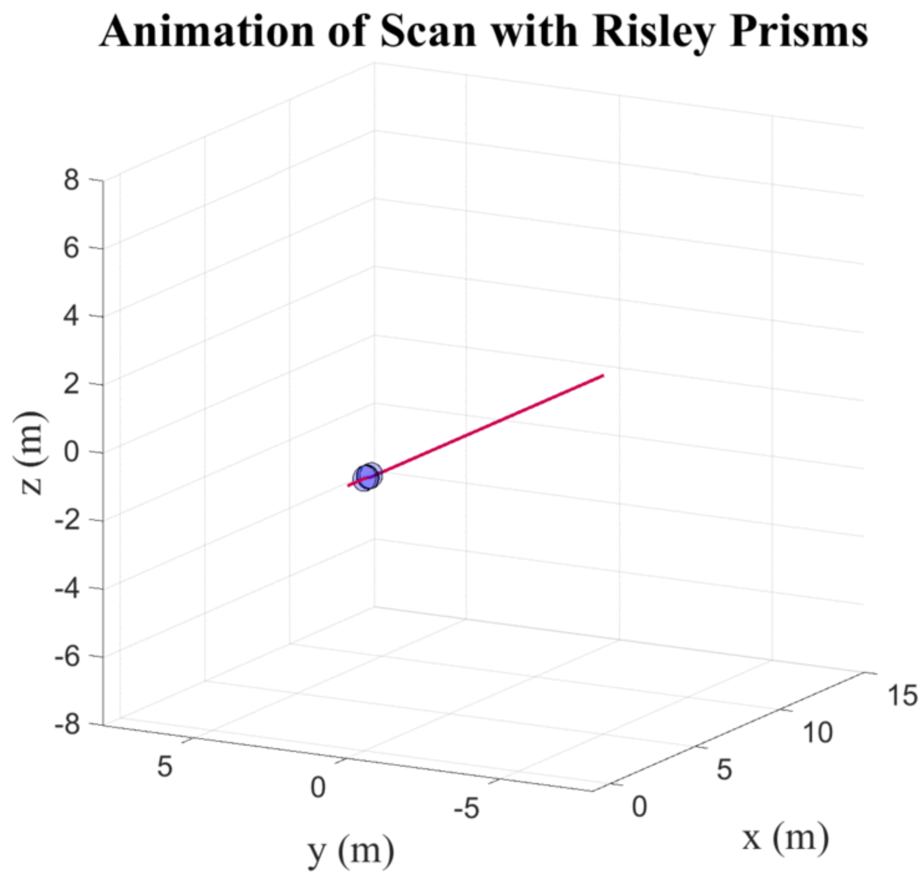

Hardware Architecture Diagram

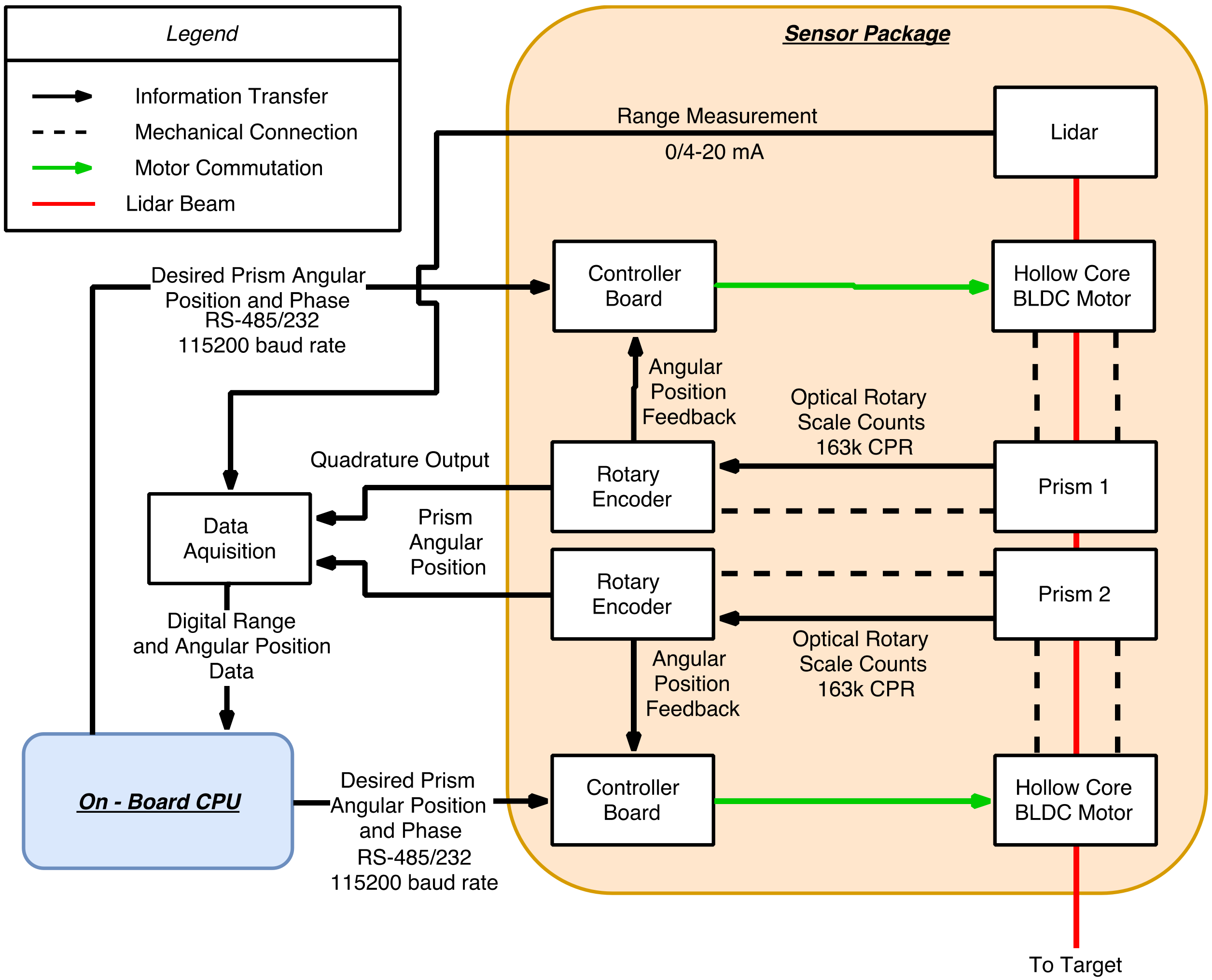

Software

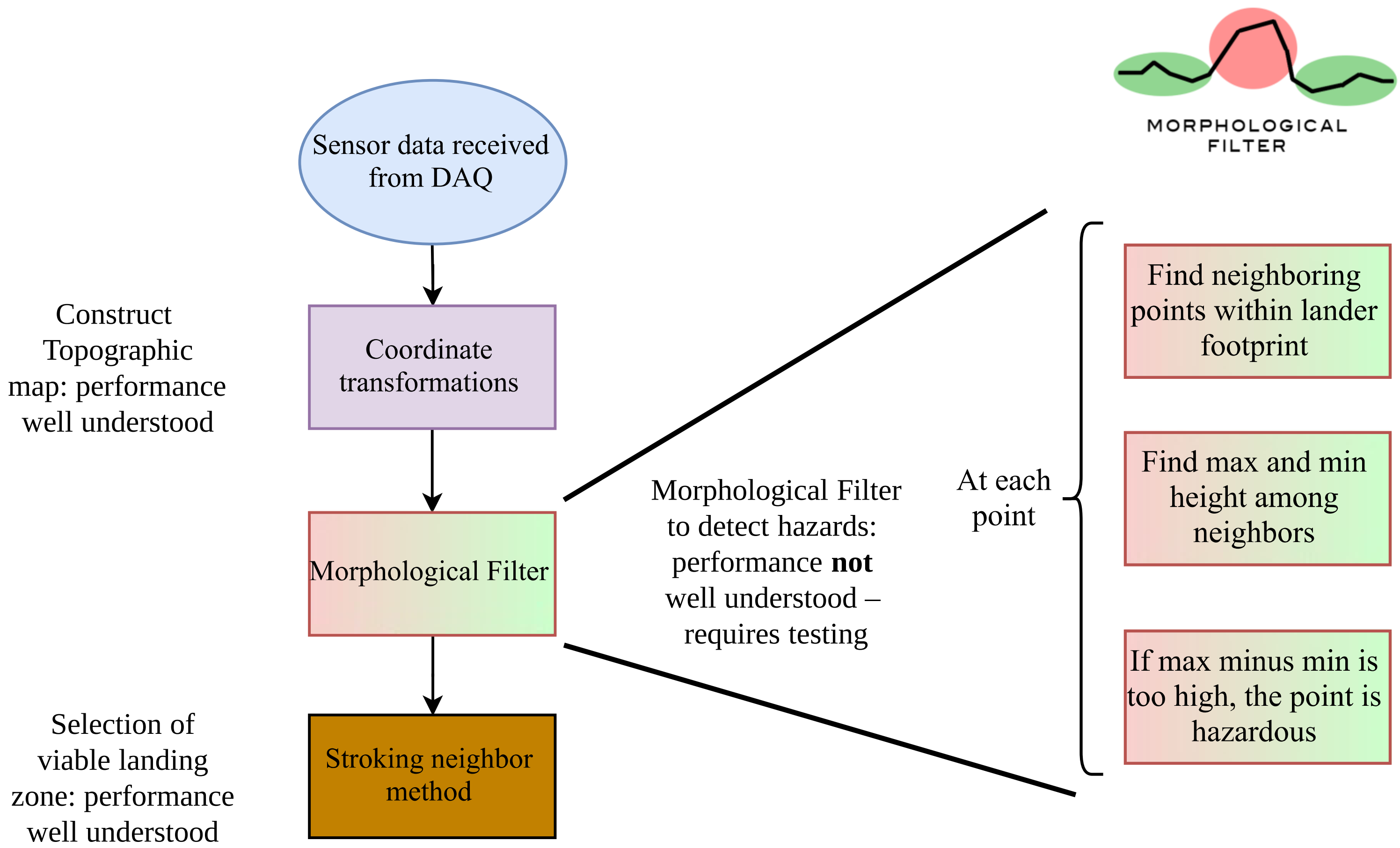
MORPHOLOGICAL FILTER
Sensor data received from DAQ
Coordinate transformations
Morphological Filter
Stroking neighbor method
Construct Topographic map: performance well understood
Selection of viable landing zone: performance well understood
Morphological Filter to detect hazards: performance **not** well understood – requires testing
At each point
Find neighboring points within lander footprint
Find max and min height among neighbors
If max minus min is too high, the point is hazardous

Baseline Verification

1. Create a mockup landing zone with hardware
2. Re-create the same landing zone in software
3. **Scan the landing zone**
4. Compare the output of the scan to the expected point cloud in software

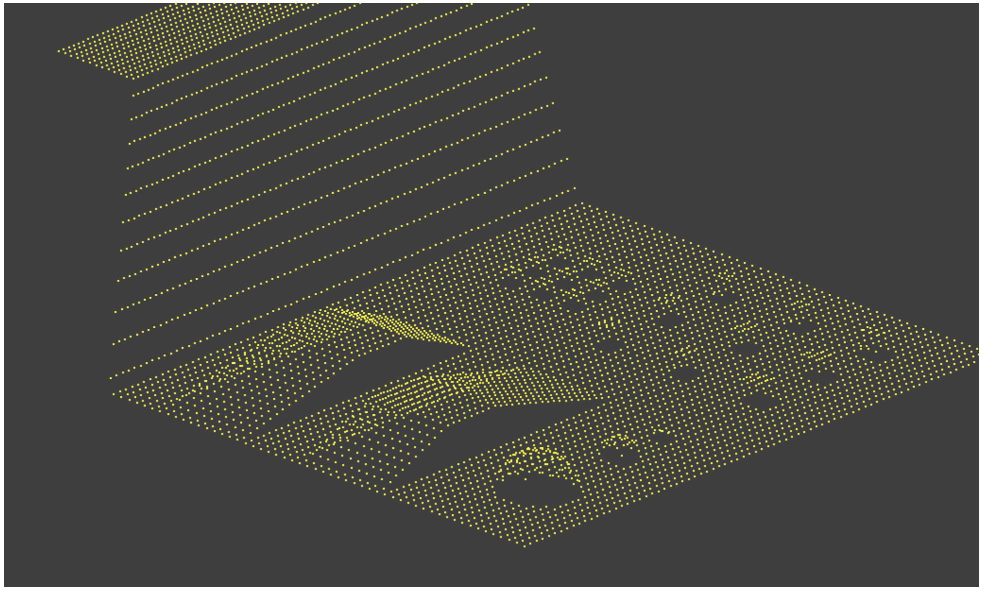

Example map in software

Critical Project Elements

Critical Project Elements

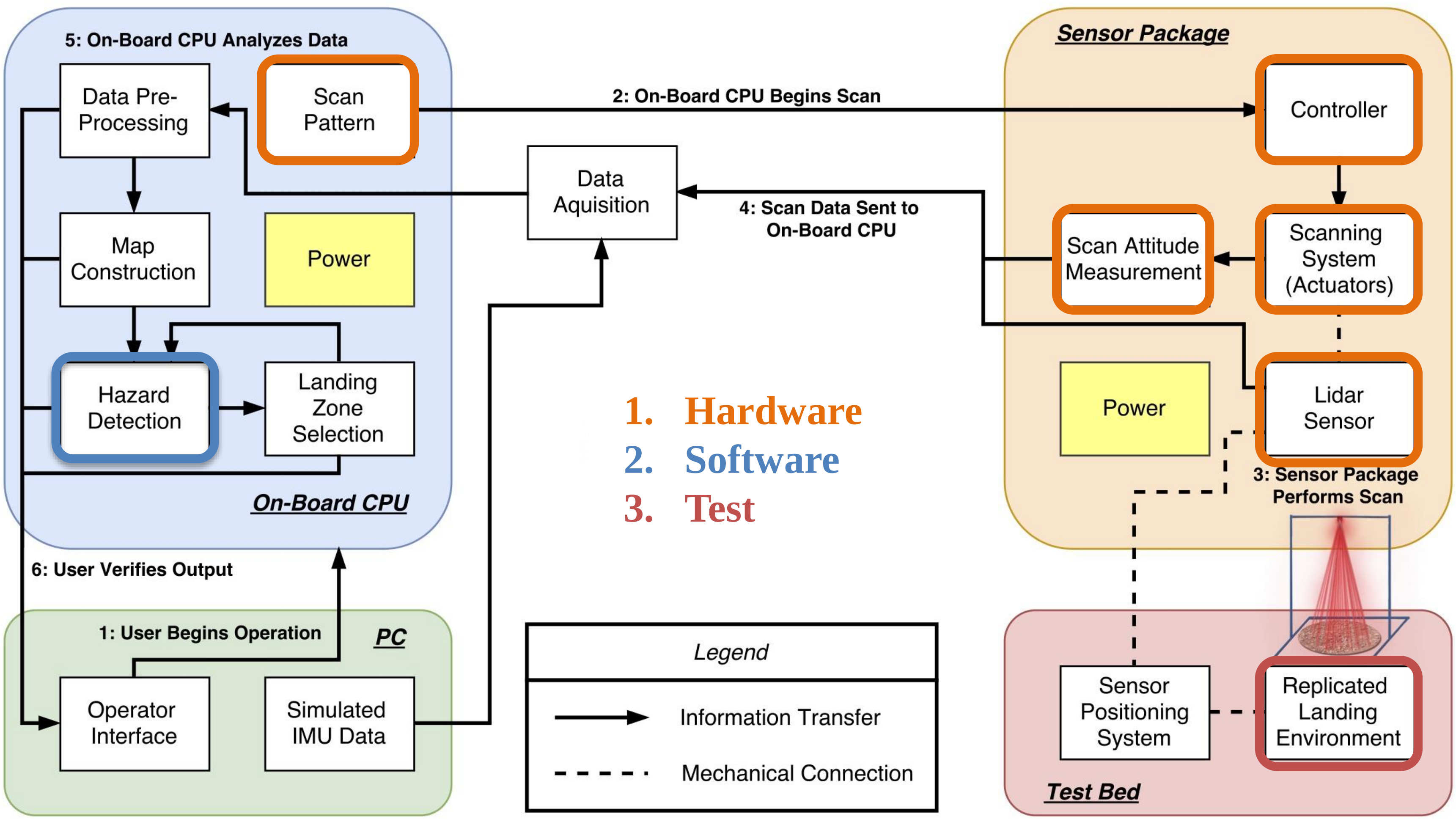

1. Hardware
2. Software
3. Test

Baseline Feasibility: Hardware

Pointing Knowledge

Driving requirement: 10 cm spatial resolution

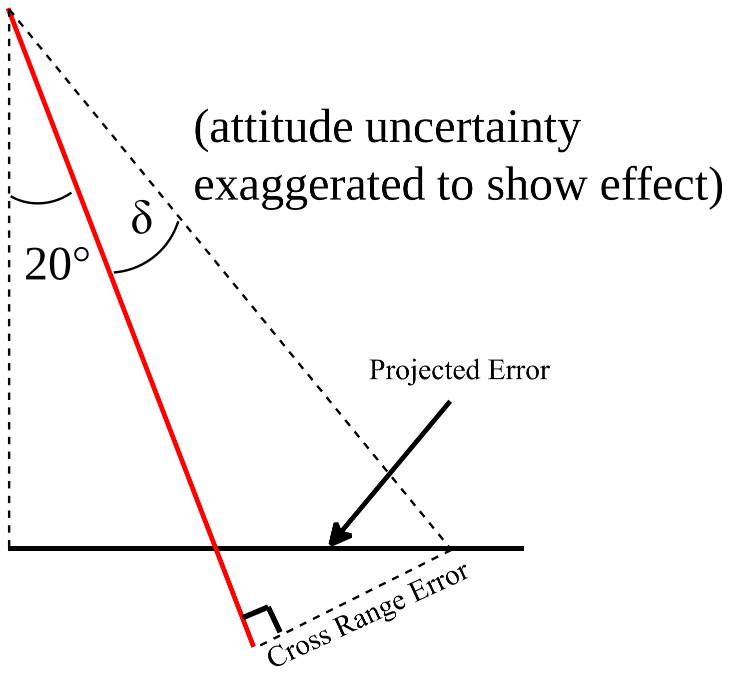

- Total attitude uncertainty must give rise to projected error of less that 5 cm so that uncertainties do not overlap
- Pointing knowledge is most critical hardware requirement
- Total uncertainty is a combination of each component uncertainty

Lidar Sensor Selection

Pepperl+Fuchs VDM28

- FR4: The sensor package shall utilize lidar to obtain range measurements at known orientations

	Design Req.	Pepperl+Fuchs
Range	12 m - 15 m	0.2 - 15 m
Range Error	<0.05 m	0.025 m
Cross Range Error	<0.045 m	0.0080 m

Cost: ~$500
Sampling Frequency: 100 Hz
Wavelength: 660 nm

Lidar Sensor Selection

Pepperl+Fuchs VDM28:

- COTS sensor that meets requirements and budget constraints

Sensor shortcomings:

- 100 Hz sampling frequency
- Time-averages over 10 ms (takes 2500 samples in that interval)

Possible solution:

- Custom-built sensor with higher sampling frequency and no time-averaging
  - Cost estimate: ~$10,000

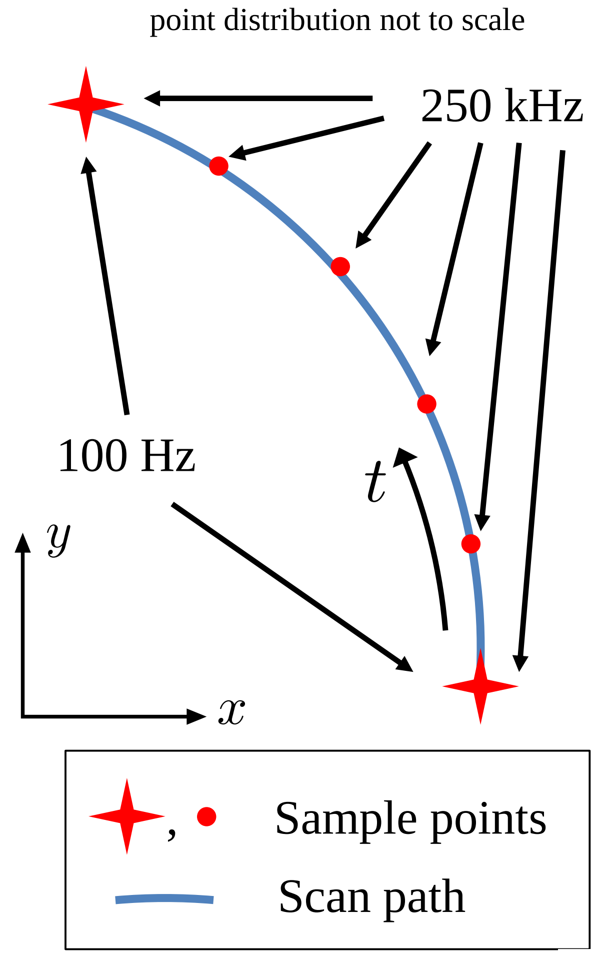

Risley Prism Feasibility

- Suitable for wide range of wavelengths
  - 450 nm - 2000 nm
- Coatings available for 660 nm
  - Reflectance of about 1%, resulting in above 90 % transmissivity
- Cost:
  - $100 each uncoated
  - Additional $5 for coated

Ideal Scan Pattern

Resolution

- Spiral Spacing: 8.66 cm
- Arc-point Spacing: 10 cm

Minimum frequency

- Total points: 9,550
- f_{min} = 159 Hz

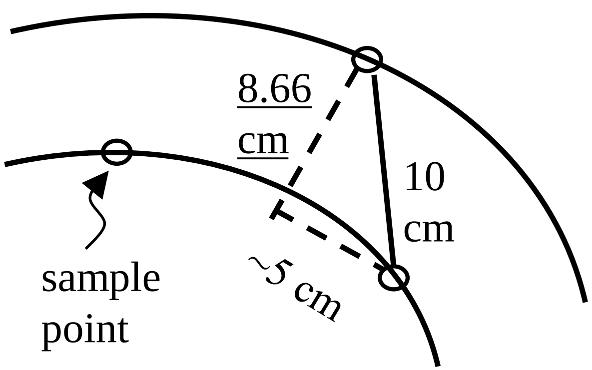

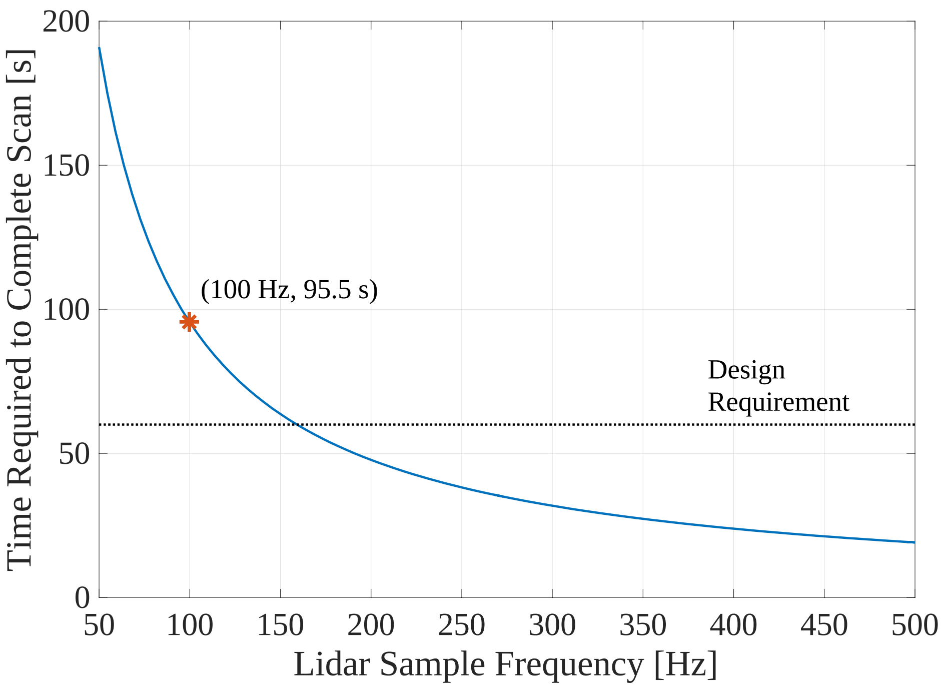

Scan Time vs. Scan Resolution

0.1 m spatial resolution at 14.1 m nadir range with 20° maximum scan angle

Scan process completed in less than 60 seconds

Problem: These two closely coupled objectives cannot be completed concurrently due to financial limitations on the lidar sensor

Scan Pattern Feasibility

Solution: Perform two system-level tests:

1. Verify that the sensor package can obtain measurements with the required resolution in a longer period of time
2. Verify the ability of the system to perform a 60-second scan/analysis, even though the required resolution cannot be met

<u>Resolution requirement test:</u>

- Lidar frequency: 100 Hz
- Point spacing (exterior): 2.5 cm
- Exterior spiral arc length: 32.32 m
- Time to complete scan: ~12 min
- Maximum prism angular acceleration
- Required angular velocity: **4.6536 rpm**
- Maximum prism angular acceleration: 4.8e-6 rad/s^2

<u>Time requirement test:</u>

- Spiral spacing of 8.66 cm gives 59 total spirals
- Time: 50 seconds (leaving margin for analysis)
- Required lidar frequency: 382 Hz
- Required angular velocity: **71.0763 rpm**
- Maximum prism angular acceleration: 3.76e-6 rad/s^2

Direct Drive Conceptual Design

Exploded View

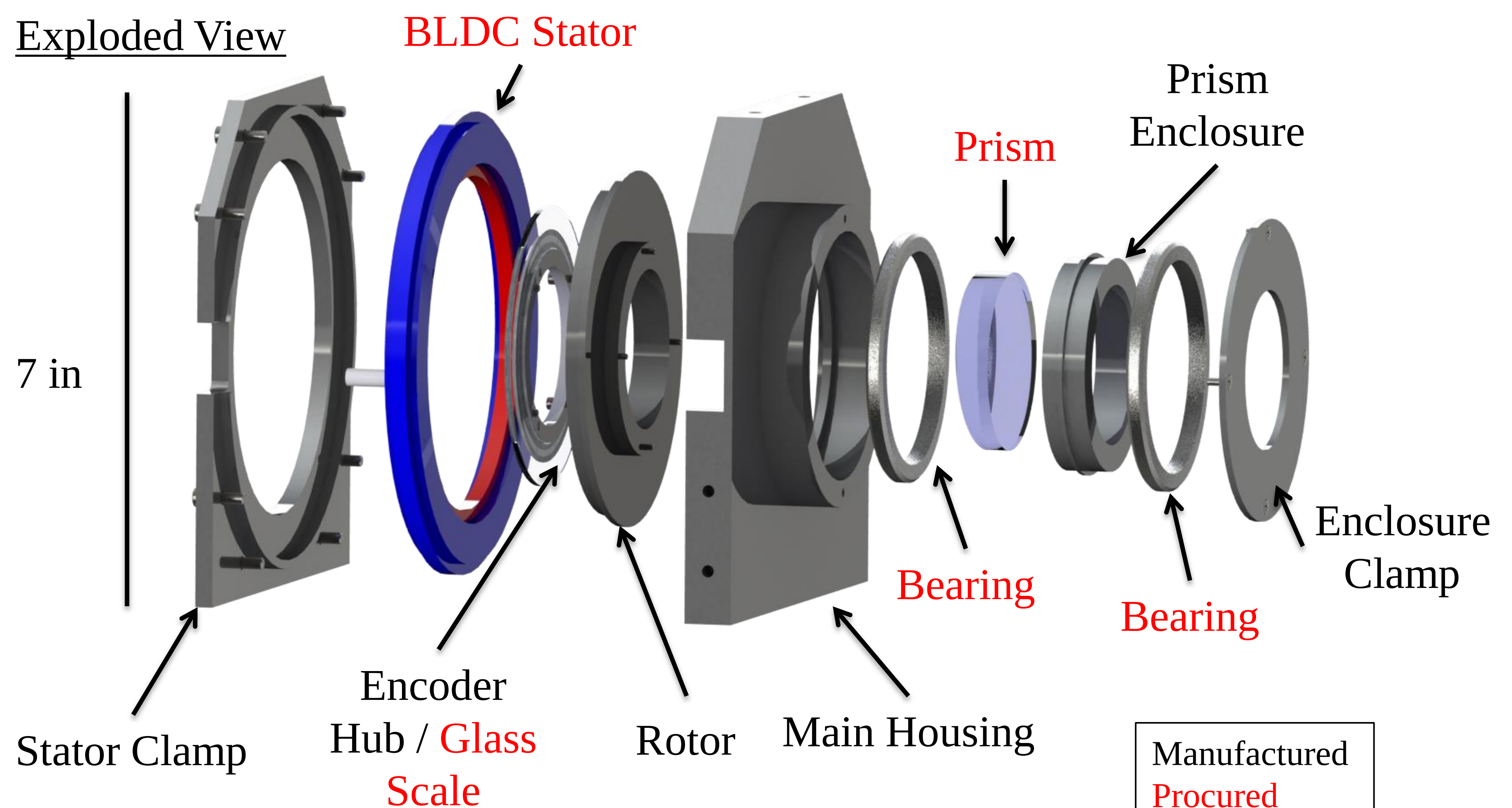

Manufactured
Procured

Direct Drive Conceptual Design

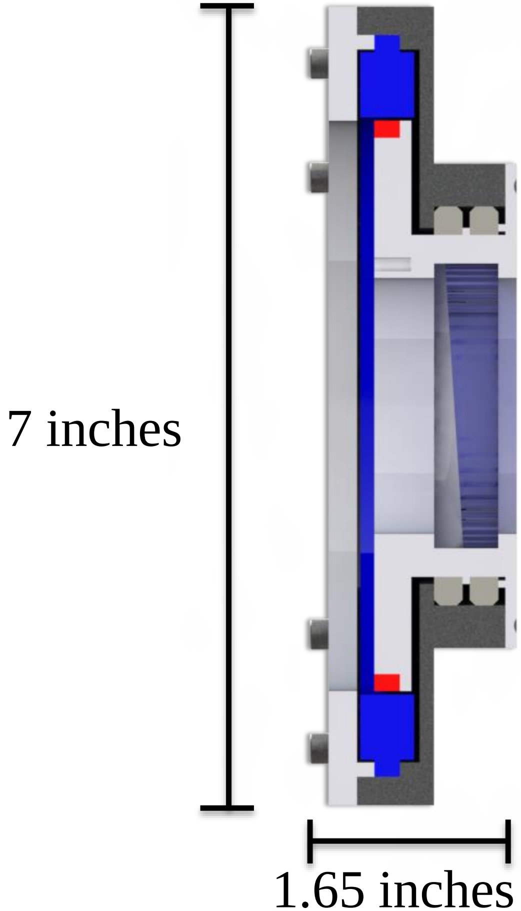

Collapsed View

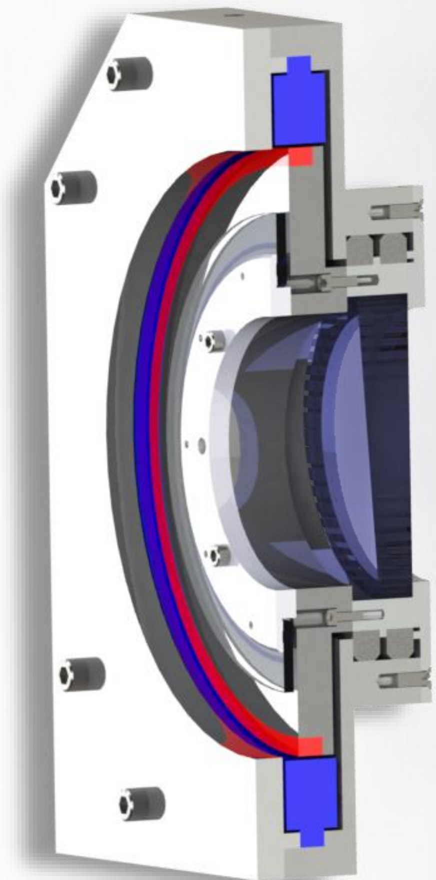

Direct Drive Conceptual Design

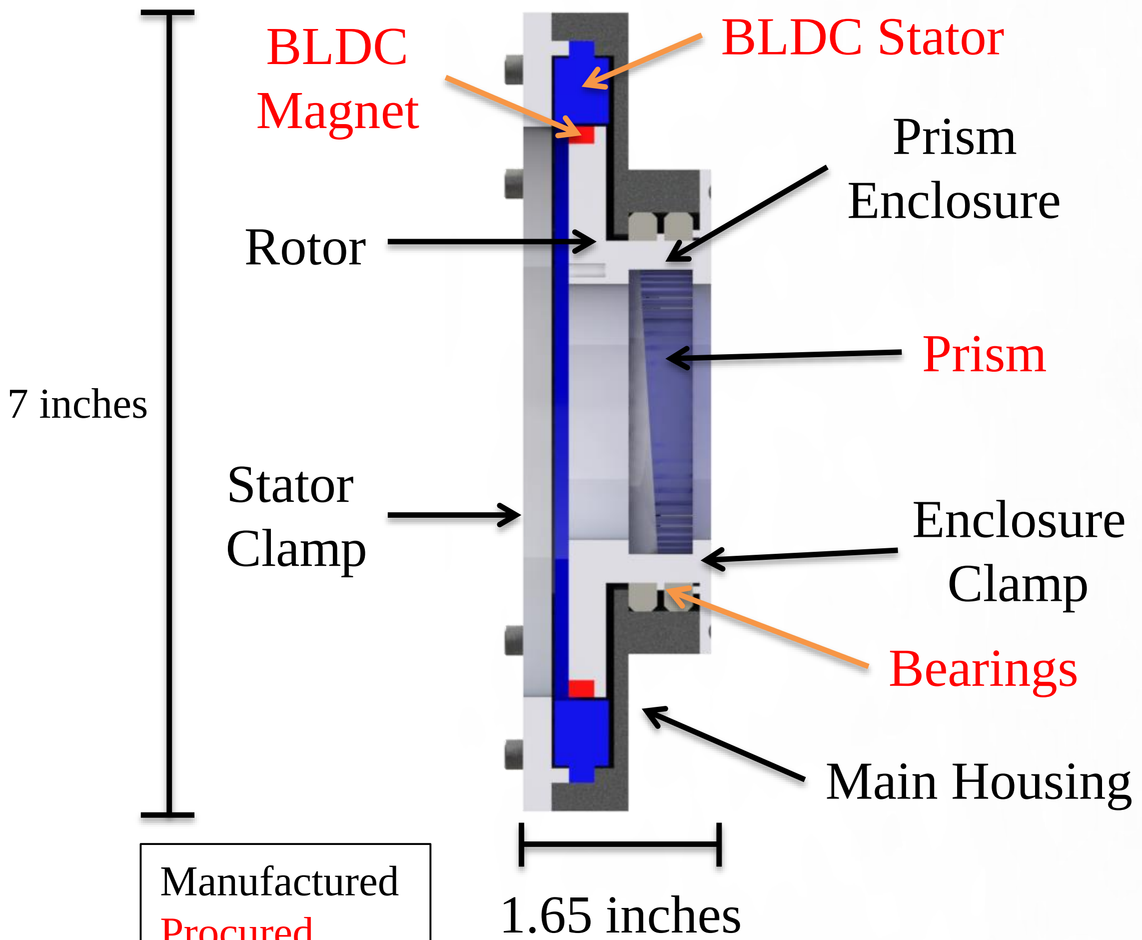

Manufactured
Procured

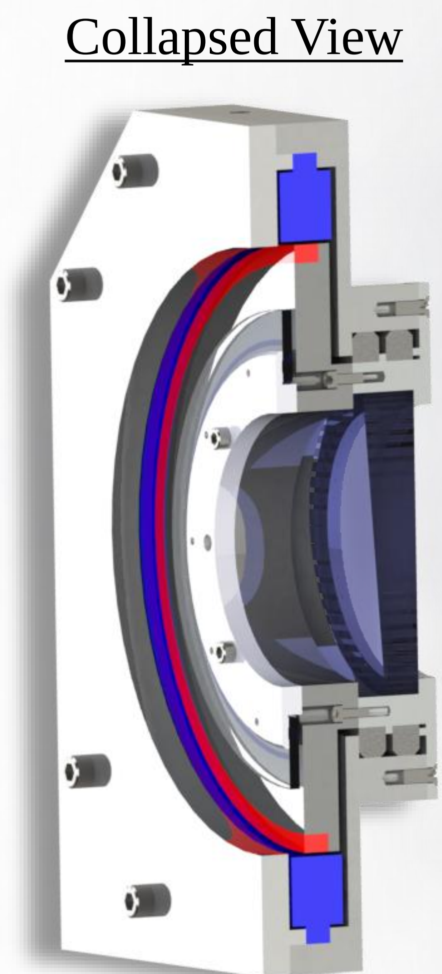

Sources of Error

Sources of Error

Must be Calibrated
System Inherent

	Expected Final Uncertainty
Lidar:	
– Translational deviations	+/- 0.030 in (ALL directions)
– Rotational deviations	+/- 0.05°
– Beam divergence	0.06°

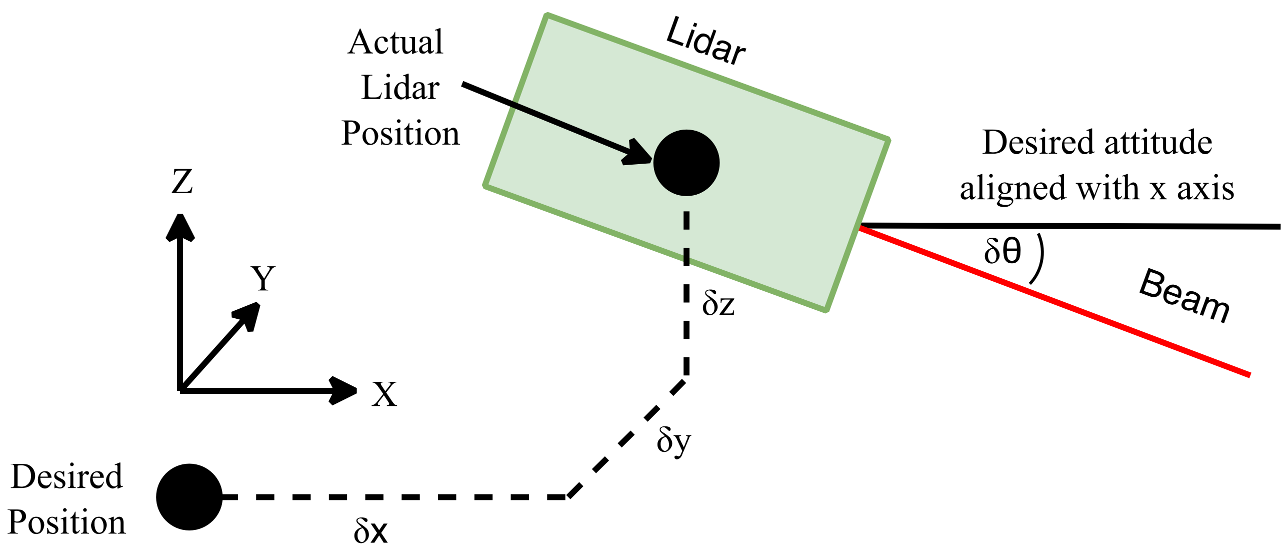

Sources of Error

Prisms:

Expected Final Uncertainty

- Uncertainty in wedge angle +/- 0.008°
- Uncertainty in index of refraction +/- 0.000277

Acceptable / Easily Mitigated
Must be Calibrated

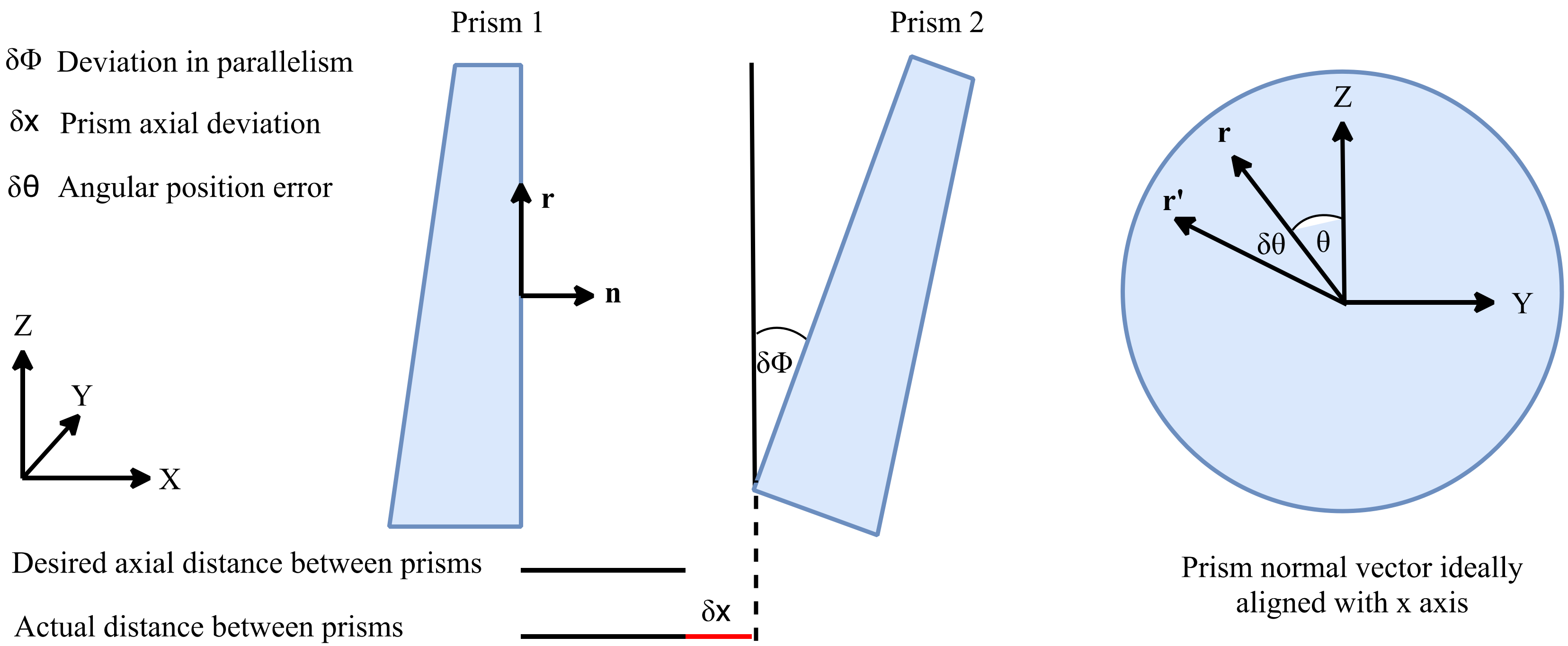

Sources of Error

Prisms:

Expected Final Uncertainty

- Uncertainty in angular position +/- 0.1°
- Deviation from parallelism +/- 0.05°
- Translational deviations

  X: +/- 0.050 in Y: +/- 0.025 in Z: +/- 0.025 in

Acceptable / Easily Mitigated
Must be Calibrated

$\delta\Phi$ Deviation in parallelism

δx Prism axial deviation

$\delta\theta$ Angular position error

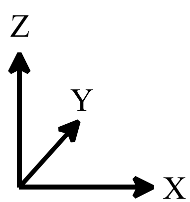

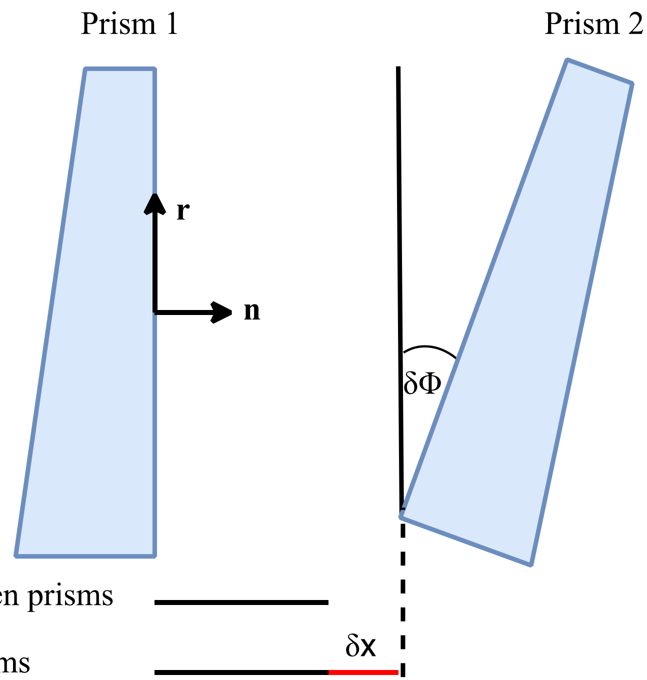

Desired axial distance between prisms

Actual distance between prisms

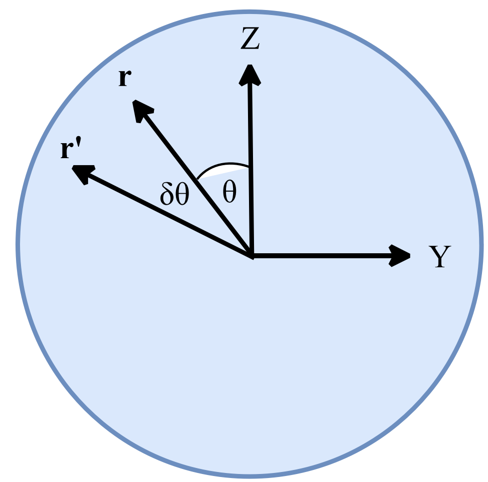

Prism normal vector ideally aligned with x axis

Predicted Performance

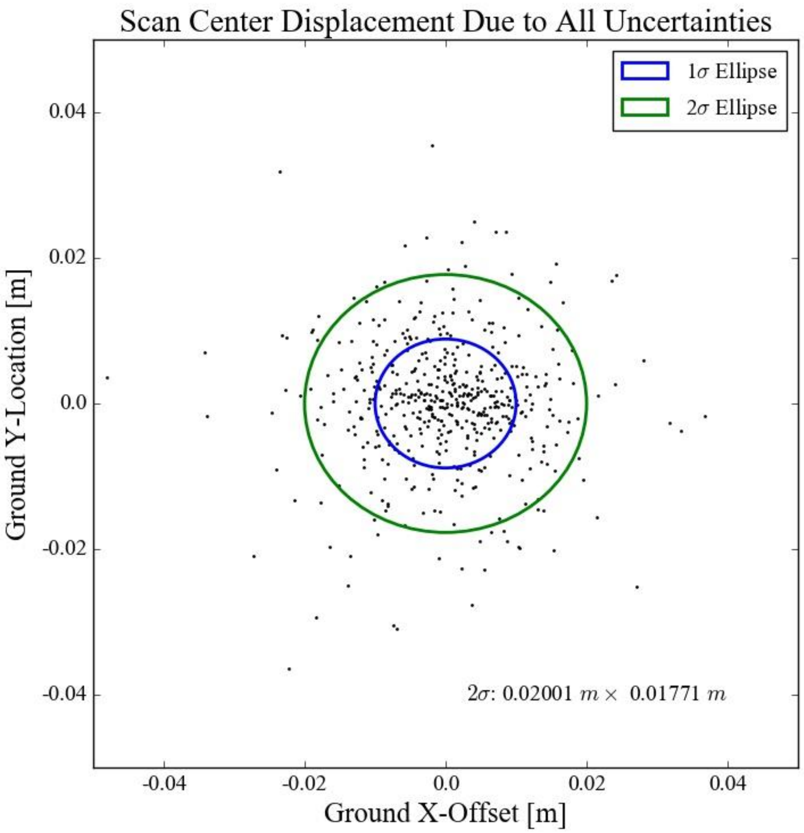

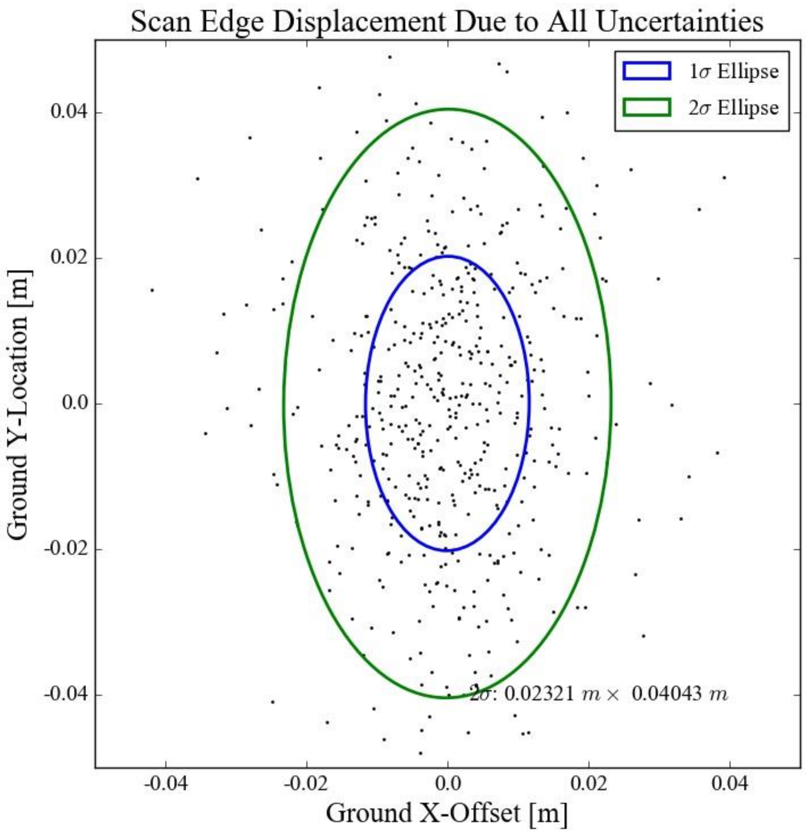

Scanning System Concept

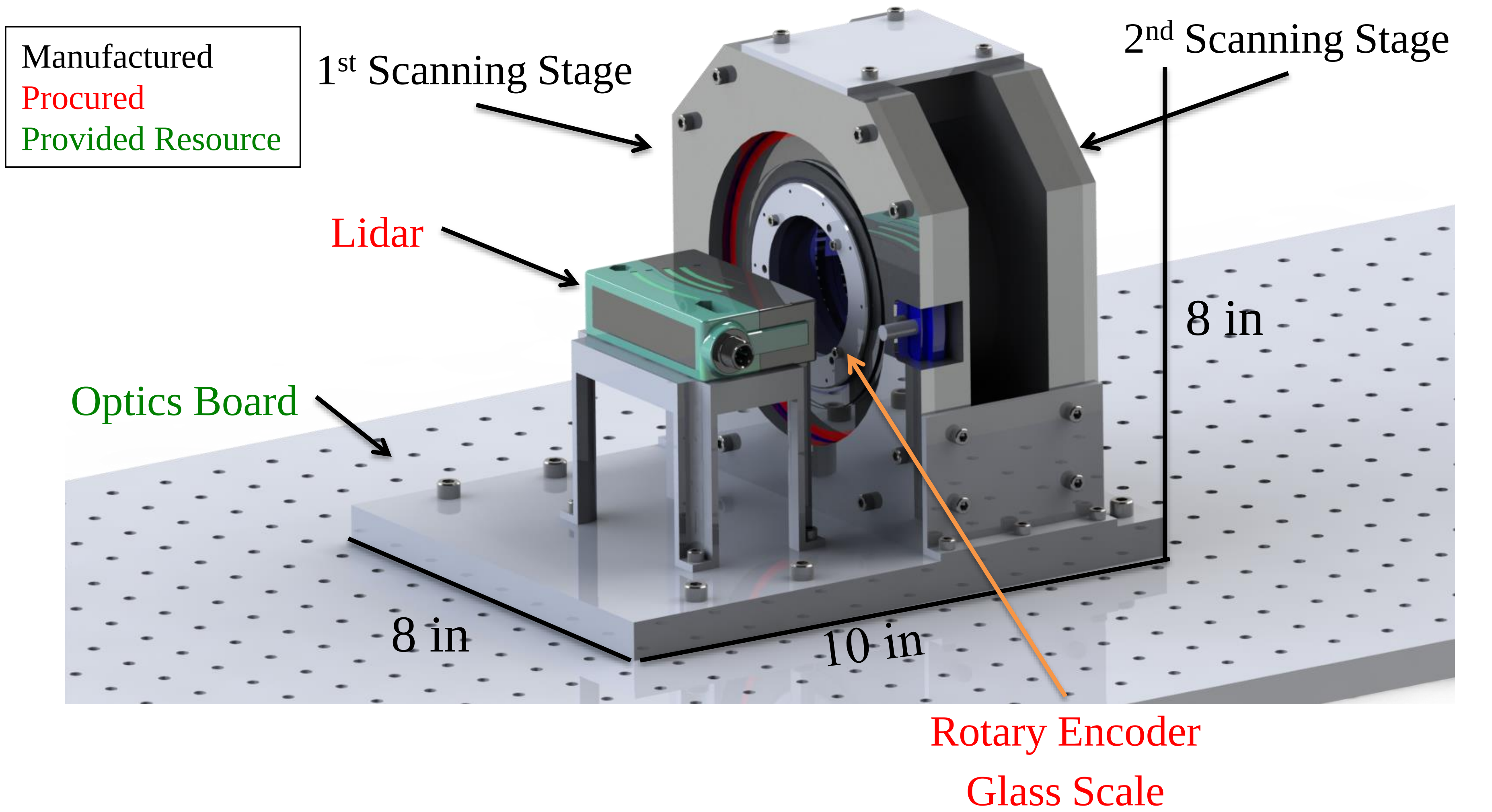

Embedded System

Driving BLDCs
- Position Feedback

Lidar analog output
- ADC

Communication with user PC

Memory to store point cloud

Position Feedback: Encoder

- 0.1° Resolution
- Incremental
- Absolute

Below components fit needs:

Motor Driver: DZRALTE-020L080
- Incremental Encoder Input

Encoder: OPS Incremental Rotary Encoder
- Quadrature output, 0.002209° resolution

Microcontroller: BeagleBone Black
- 12 bit ADC, quadrature decoders, USB, Ethernet, UART, 512 MB DDR3L

BASELINE FEASIBILITY: SOFTWARE

Blender Lidar Simulator

- Blender is an open-source program for 3D modeling
- Projects points onto any arbitrary face or object to simulate a lidar scan
- Can extract 3D data by running Python scripts within Blender

Example Blender artwork

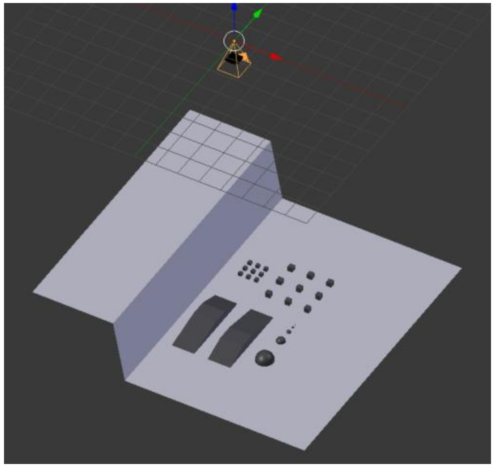

Blender Lidar Simulator

- Scan pattern is defined on the plane of the ground, and projected backward onto a sphere centered on the lidar (Blender camera)
- The pattern is then projected outward from the lidar location onto the modeled map
- A Python script exports the point cloud to a CSV file

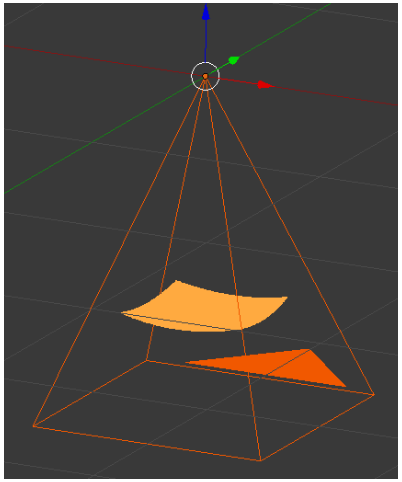

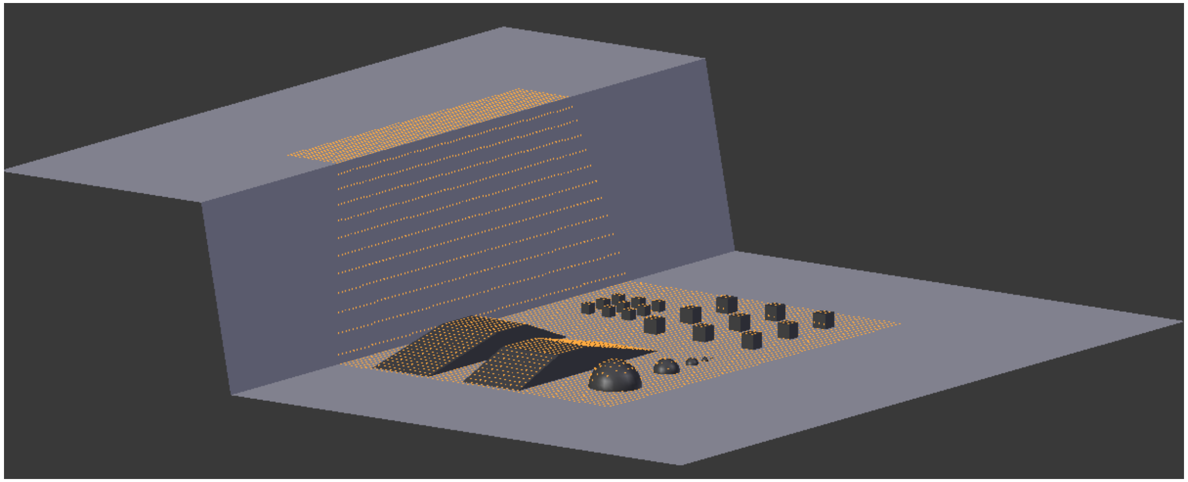

Hazard Detection Algorithms

Morphological Filter

- Identifies hazards by height differences between neighboring points
- Time to run on laptop: 0.31 sec for 10 cm grid

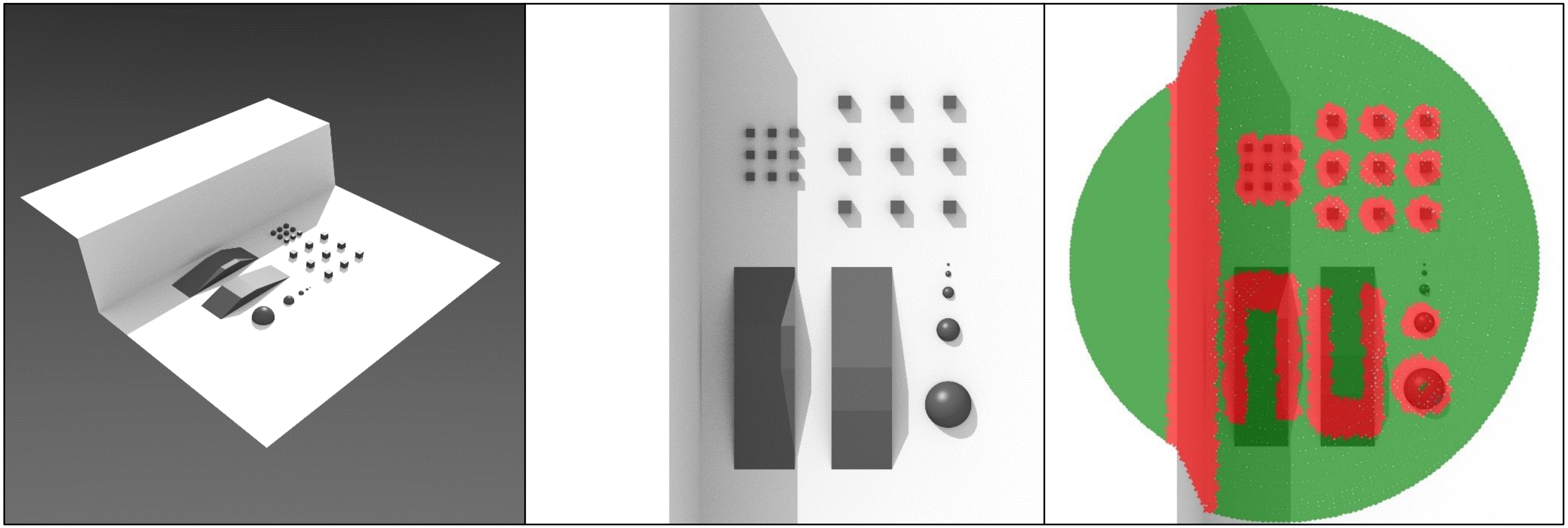

Time Estimates

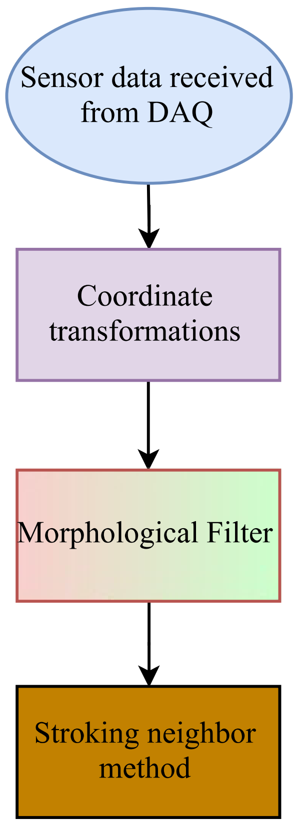

Estimated time: 0.33 s

Estimated time: 0.31 s

Estimated time: 0.026 s

Estimated total time for software elements when run in Python on a personal laptop: about **0.666 s**

Analysis shows that the BeagleBone will run ~10.24 times slower (**6.83 s**). Given our 10 s margin, we will be well within the time requirement even after porting to the microprocessor. More computationally expensive functions may be written in C for speed improvements.

Baseline Feasibility: Test

Modularity

- At 14.1 m nadir
  - Area = 82.36 m^2
  - Diameter = 10.24 m
    - This would be large and cumbersome to move
- Alternate method
  - 2 m × 2 m test bed
  - Scan at nadir position
    - Verify algorithm output only at nadir
  - Scan at 20° slant angle
    - Verify algorithm output only at slant angle
  - Together, this verifies full capability

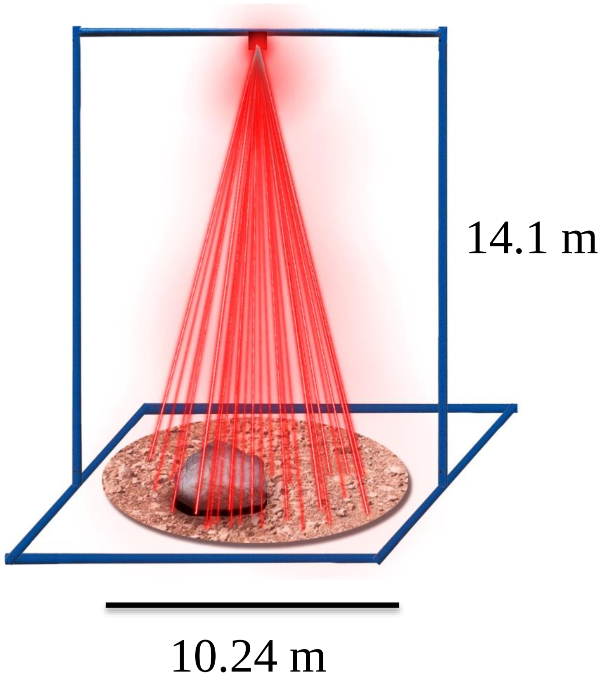

Test Orientation

- Vertical
  - Directly matches system implementation
- Horizontal
  - Simpler logistically and less dangerous
  - Does not sacrifice ability to verify requirements
  - Opens up testing locations

Locations

- <u>Balch Fieldhouse</u>
  - Length = 72.0 m
  - Height = 14.8 m

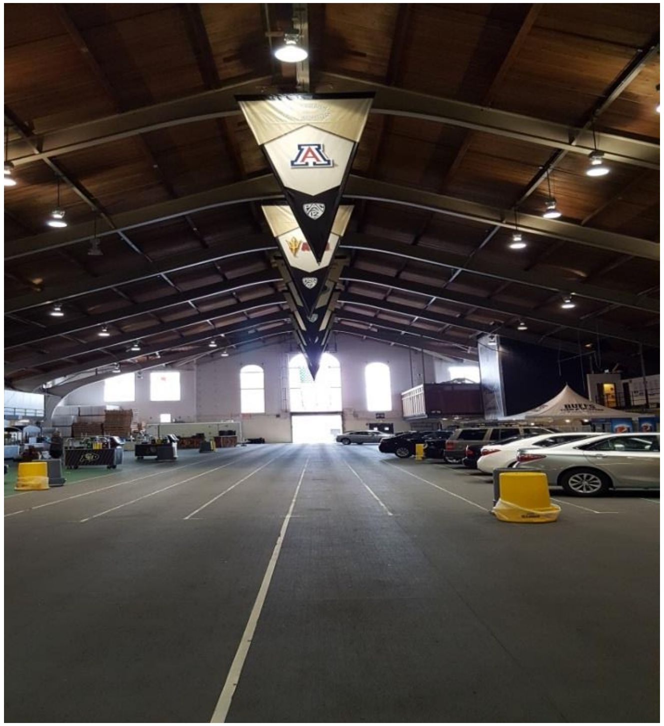

- <u>RECUV Lab</u>
  - Length = 21.7 m
  - Height = 9.5 m

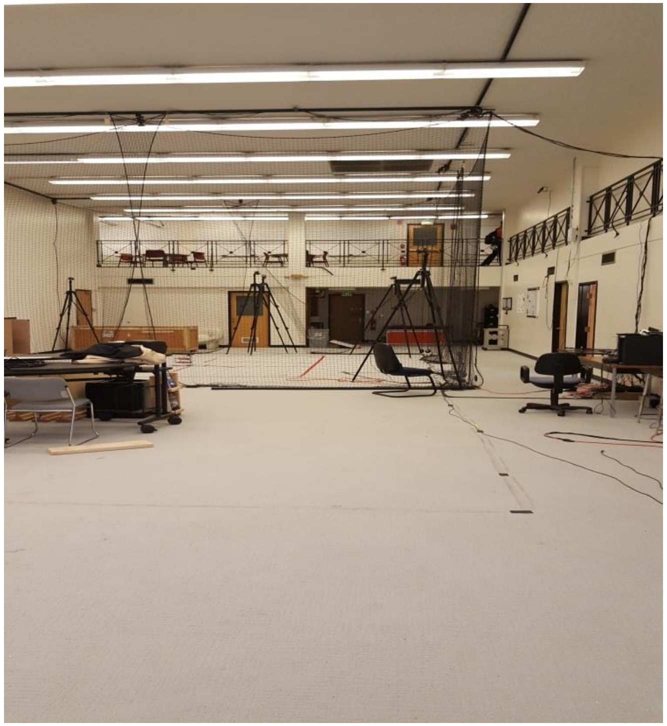

FEASIBILITY RECAP

Feasibility Summary

	Feasibility Shown	Next Steps
Hardware	• Lidar sensor capabilities • Risley prism scanning and scan pattern • Bounding of error • Embedded systems • Power requirements	• Prove motor control feasibility • Confirm negligibility of thermal effects • Finalize integration of scanning components • Design optomechanical adjustment methods • Design passive seating alignment features
Software	• Detection of hazards • Completion of computations in required time	• Implement real-time computations with incoming point stream • Propagate uncertainties in hazard detection
Testing	• Utility of multiple potential locations • Orientation and scale of test	• Secure full-scale test location

BUDGET & SCHEDULE

Budget

Item	Quantity	Cost per (USD)	Total cost (USD)
Lidar:			
Pepperl-Fuchs VDM28-15-L-IO/73c/110/122	1	470.17	470.17
Motors:			
ULT100B11AH000 (without halls)	1	833	833
Encoders:			
OPS read head (OD 3.937" ID 2.756")	2	560	1120
Bearings:			
VA030CP0 Thin Section Bearing 3"x3 1/2"x1/4" inch Open	4	81.77	327.08
Microprocessor:			
BeagleBone Black Rev C.1	1	55	55
Test setup:			
Manufactured in-house	1	100	100
Motor Drivers:			
DZRALTE - 010B080	2	400	800
Risley prism:			
P-WRC059 coated with BBAR 400-700 nm	2	108	216
Materials			
			500
Shipping			210
Total			**4631.25**
Budget			**5000**
Percent Margin			**7.375**

GANTT CHART

Preliminary Design

Lidar Sensor Critical Design

Mechanical System Critical Design

Software Critical Design

Test Planning

Critical Design Review

Finance

Fall Final Report

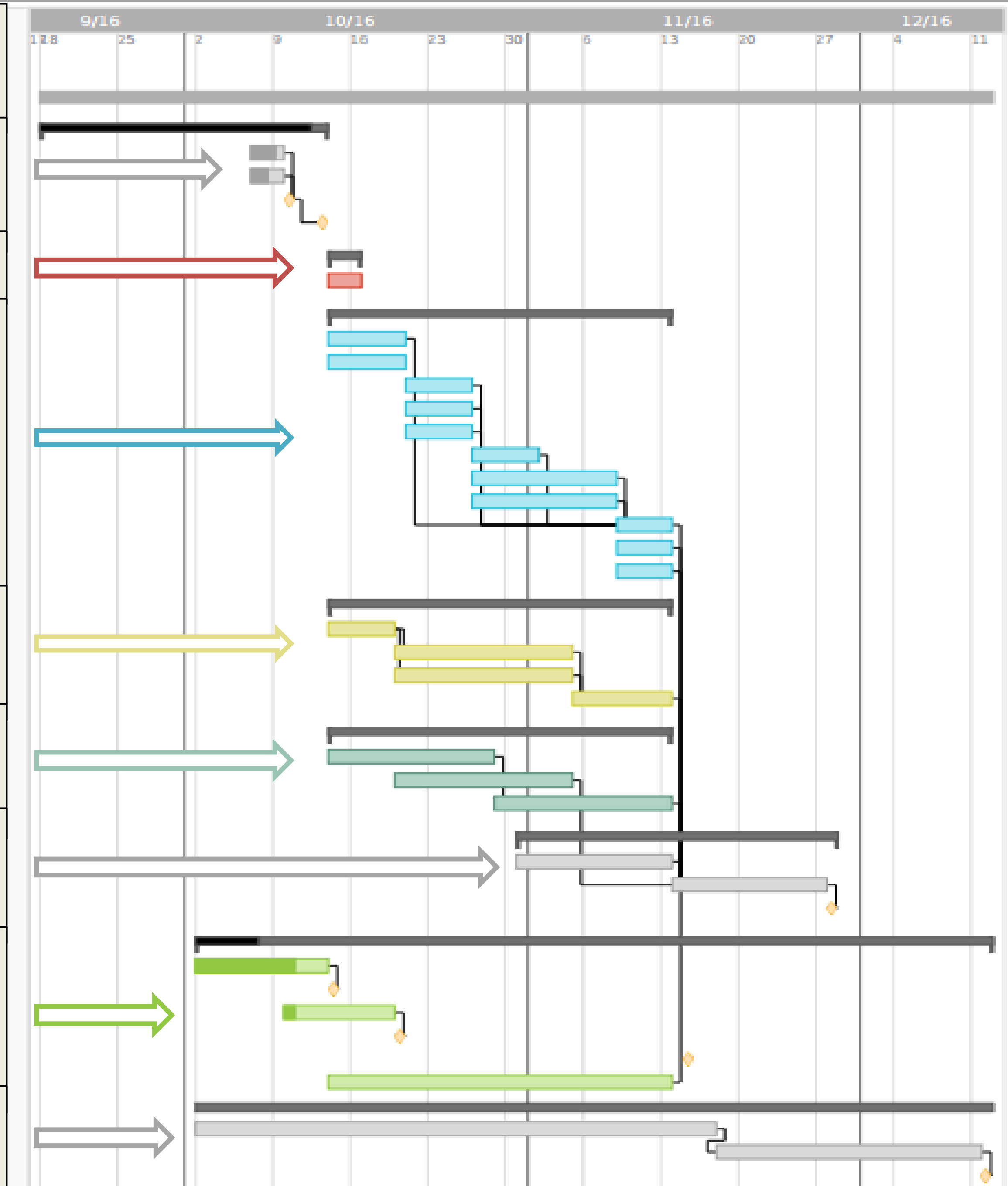

Gantt Chart

margin
lidar

MACULA	**0h**	**19%**
Preliminary Design	**0h**	**94%**
PDR Slide Revision 2	0	75%
PDR Dry Runs	0	50%
PDR Slides DUE	0	0%
PDR Presentation	0	0%
LiDAR Sensor Critical Design	**0h**	**0%**
Select LiDAR Sensor	0	0%

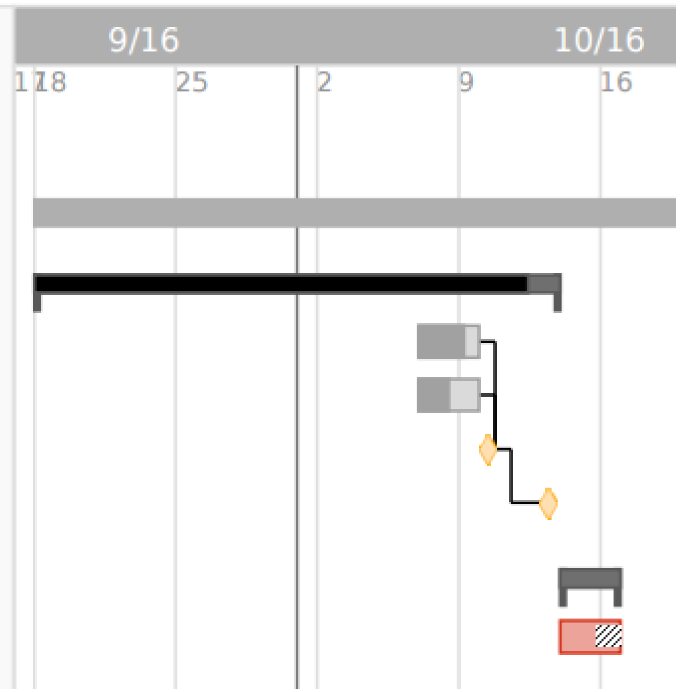

Gantt Chart

margin
mechanical

Mechanical System Critical Design	**0h**	**0%**
Finalize Sizing	0	0%
Finalize Bearing Implementation	0	0%
Finalize encoder integration design	0	0%
Finalize Prism Mounting	0	0%
Finalize Magnet Seating in Rotor	0	0%
Finalize Fasteners	0	0%
Design Passive Seat / Alignment Fea...	0	0%
Design Optomechanical Adjustment ...	0	0%
Make Drawings for All Parts	0	0%
Dimension All Parts	0	0%
Final Mechanical Hardware Review	0	0%

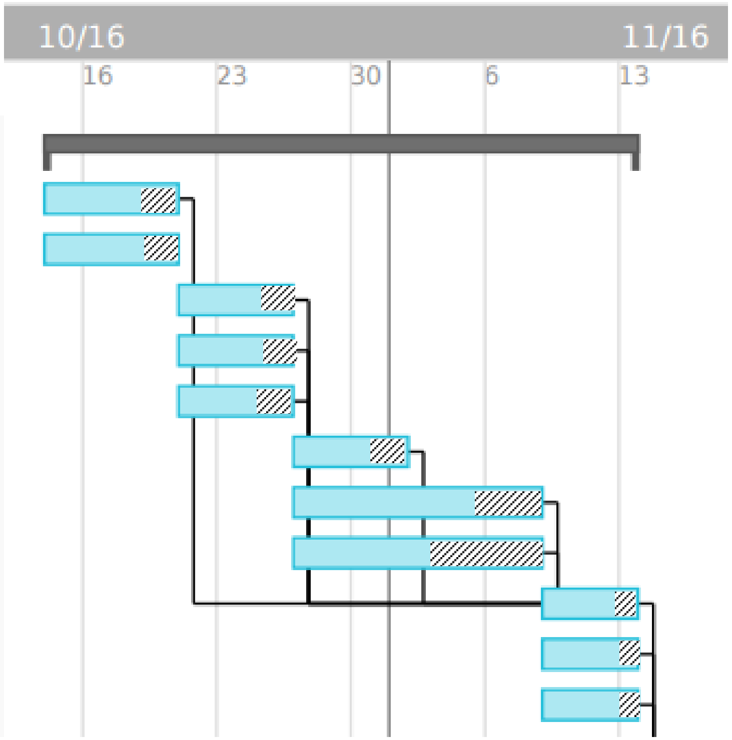

Gantt Chart

margin
software
test

Software Critical Design	**0h**	**0%**
Final Algorithm Selection	0	0%
Optimize Code for Speed	0	0%
Add Real-time Analysis Functionality	0	0%
Port Code to Microprocessor	0	0%
Test Planning	**0h**	**0%**
Secure Test Location	0	0%
Create Subsystem Level Test Plans	0	0%
Create System Level Test Plans	0	0%

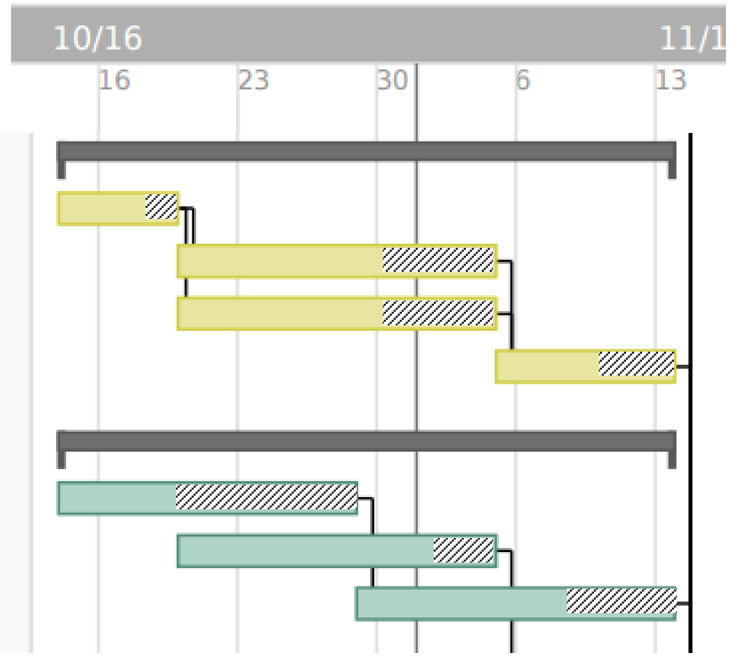

Gantt Chart

margin
documentation
finance

Critical Design Review	**0h**	**0%**
CDR Initial Slide Creation	0	0%
CDR Dry Runs/Revision	0	0%
CDR Due	0	0%
Finance	**0h**	**8%**
UROP Application	0	75%
UROP Due	0	0%
EEF Application	0	10%
EEF Due	0	0%
EEF Decision	0	0%
Budget Determination	0	0%
Fall Final Report	**0h**	**0%**
FFR Draft Writing	0	0%
FFR Revision	0	0%
FFR Due	0	0%

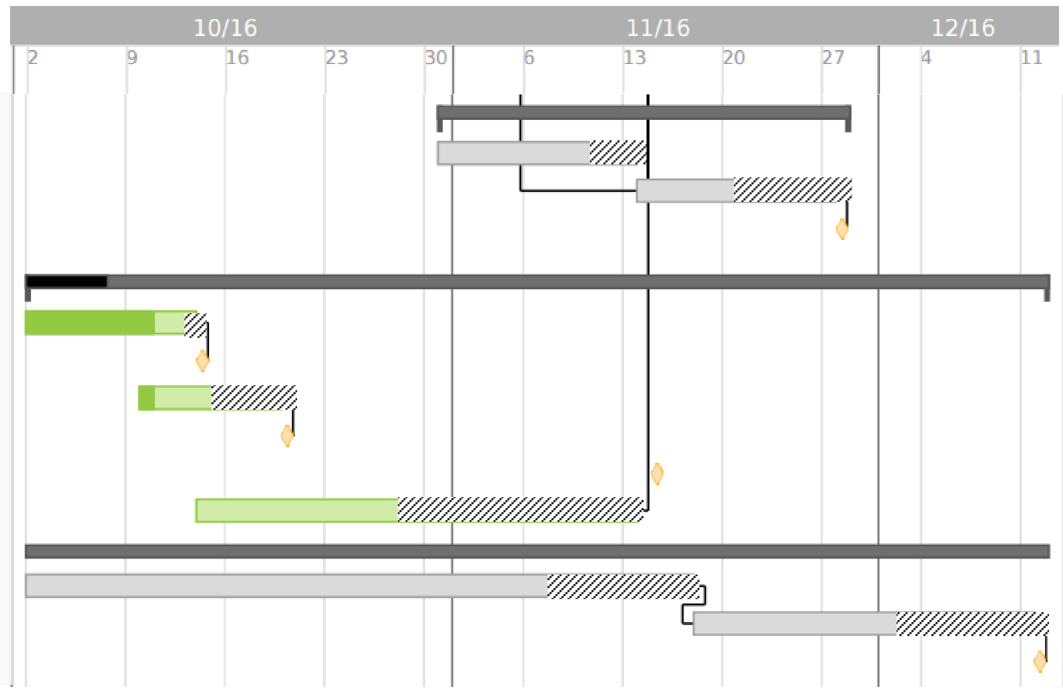

GANTT CHART

Preliminary Design

Lidar Sensor Critical Design

Mechanical System Critical Design

Software Critical Design

Test Planning

Critical Design Review

Finance

Fall Final Report

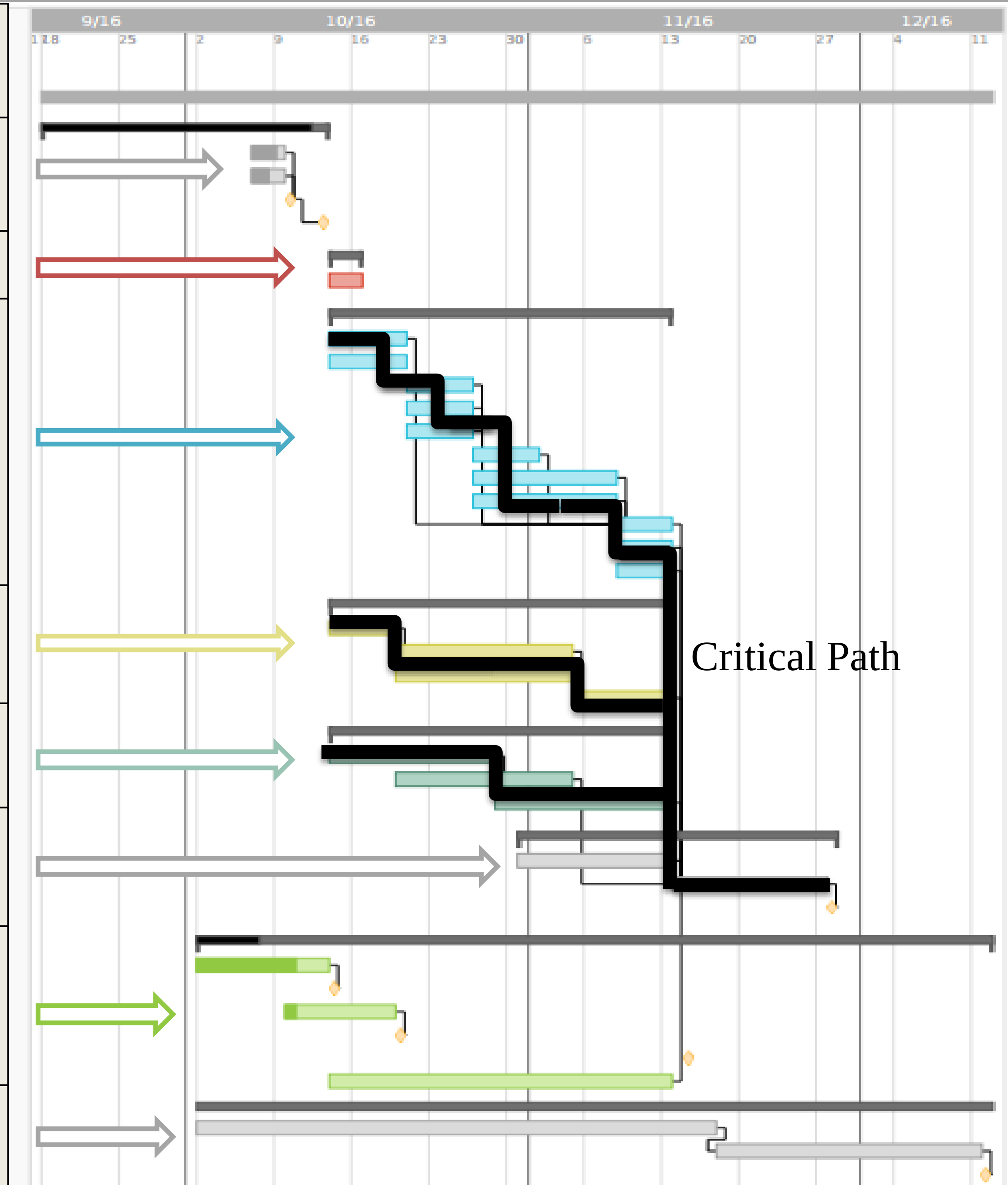

Acknowledgements

Advisor: Jay McMahon

PAB: James Nabity, Kaley Pinover, Brian Argrow, Bobby Hodgkinson, Matt Rhode, Trudy Schwartz, Bob Marshall, Josh Stamps, Jelliffe Jackson

Active Remote Sensing Lab: Jeff Thayer, Rory Barton-Grimley, Bobby Stillwell

Computational and Mechanical Geometry Lab: John Evans, Luke Engvall, Joseph Benzaken

Dale Lawrence

Blue Canyon Technologies: Steve Steg, Matt Carton, Bryce Peters

Special Aerospace Services PEAPOD Team

Tyler Roth (for creative brilliance in coming up with MACULA team name)

And our sponsor: Celestial Seasonings Café

References

"AMG Series Optical Mounts & Gimbals." Aerotech. Aerotech Inc., n.d. Web. 22 Sept. 2016. <https://www.aerotech.com/product-catalog/gimbals-and-optical-mounts/amg.aspx>.

Berg, Mark . Computational Geometry: Algorithms and Applications. Berlin: Springer, 2008. Print.

By FAS — March 23, 2016. "Federation Of American Scientists -." Federation Of American Scientists. N.p., n.d. Web. 24 Sept. 2016.

Cryan, Scott, and Christian, John A. "A Survey of LIDAR Technology and its Use in Spacecraft Relative Navigation." AIAA Guidance, Navigation, and Control (GNC) Conference, Boston, MA, 19-22 Aug. 2013. Web.

Dunbar, Brian. "Lidar Atmospheric Sensing Experiment (LASE): Measuring Water Vapor, Aerosols and Clouds." NASA. NASA, 21 Nov. 2004. Web. 24 Sept. 2016.

Folger, Jean. "Why Curiosity Cost $2.5 Billion." Investopedia, LLC. 5 Sept. 2012. Web.

Hughes, T. J. R, J. Cottrell A., and Y. Bazilevs. "Isogeometric Analysis: CAD, Finite Elements, NURBS, Exact Geometry and Mesh Refinement." Computational Methods in Applied Mechanics and Geometry 194.39-41 (2005): 4135-195. Web.

Gonzales, Rafael C. Digital Image Processing. 3rd ed. N.p.: Pearson Education International, n.d. Print.

"LeddarTech Launches LeddarVu, a New Scalable Platform Towards High-Resolution LiDAR." PR Newswire Association LLC. Quebec City, 7 Sept. 2016. Web.

References

"LiDAR, Laser Scanners and Rangefinders." RobotShop, Inc. 2016. Web. <http://www.robotshop.com/en/lidar.html >

Lynch, Andrew, and Kai Focke. "Beam Manipulation: Prisms vs. Mirrors." Photonik International (n.d.): n. pag. Mar. 2009. Web. 20 Sept. 2016. <http://www.edmundoptics.com/globalassets/resources/articles/beam-manipulation-prisms-vs-mirrors-en.pdf>.

"Puck LiDAR: Our Lightest Yet." Velodyne LiDAR, Inc., 2016. Web. <http://velodynelidar.com/vlp-16-lite.html>

"Round Wedge Prisms." Round Wedge Prisms. THORLABS, n.d. Web. 20 Sept. 2016. <https://www.thorlabs.com/NewGroupPage9.cfm?ObjectGroup_ID=147 >.

Saniee, Kamron. "A Simple Expression for Multivariate Lagrange Interpolation." SIAM (2007): n. pag. Web.

Schwarze, Craig. "A New Look At Risley Prisms." Photonics Spectra (n.d.): n. pag. Photonics Media, June 2006. Web. 20 Sept. 2016.

Shan, Jie, and Charles Toth K. Topographic Laser Ranging and Scanning: Principles and Processing. Boca Raton: CRC/Taylor & Francis Group, 2009. N. pag. Print.

Shewchuk, J. "What is a good linear finite element? interpolation, conditioning, anisotropy, and quality measures (preprint)." University of California at Berkeley 73 (2002).

References

"Technology Overview." Advanced Scientific Concepts, Inc. 2015. Web. <http://www.advancedscientificconcepts.com/technology/technology.html >

Wilsenack, Frank. "Defense & Security." Detecting and Tracking Thin Aerosol Clouds. SPIE, 12 Oct. 2012. Web. 24 Sept. 2016.

Y. Bazilevs et al., Isogeometric analysis using T-splines, Comput. Methods Appl. Mech. Engrg. (2009), doi:10.1016/ j.cma.2009.02.036

Riemersma, Thiadmer. "Candela, Lumen, Lux: the equations." CompuPhase, 2016. Web.

"Standard Test Method for Coefficient of Retroreflection of Retroreflective Sheeting Utilizing the Coplanar Geometry." ASTM International, Designation E 810-03, 2016. PDF.

"Pepperl+Fuchs VDM 28 Photoelectric Sensor Datasheet." Pepperl+Fuchs, 2016. PDF.

"Reflexite Daybright V92 Conspicuity Sheeting." Reflexite America, 2006. PDF.

QUESTIONS?

Backup Master

Top View Martian Rock Analysis

Top view of Martian surface

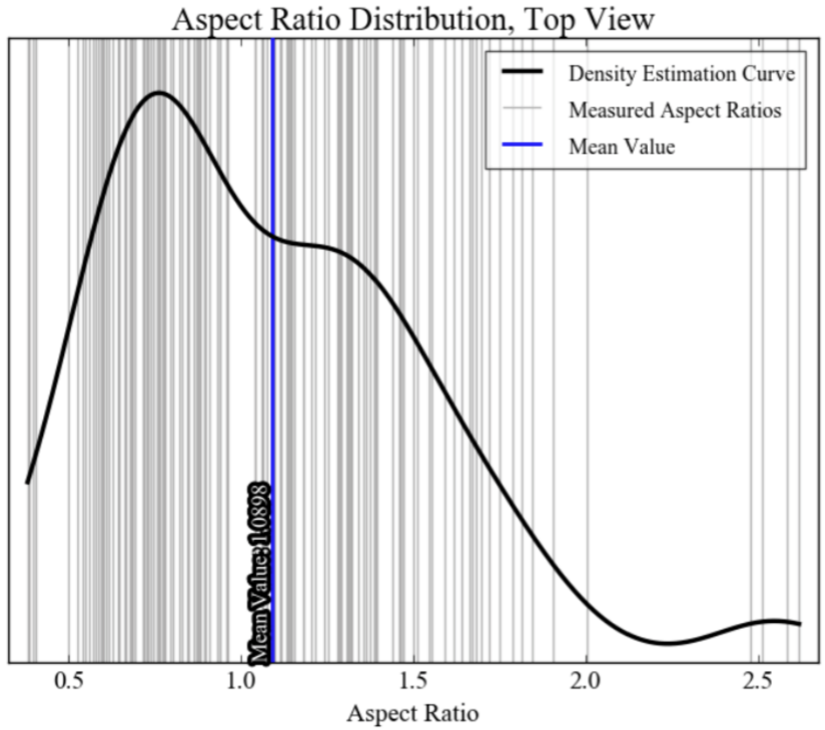

Aspect ratio distribution

Side View Martian Rock Analysis

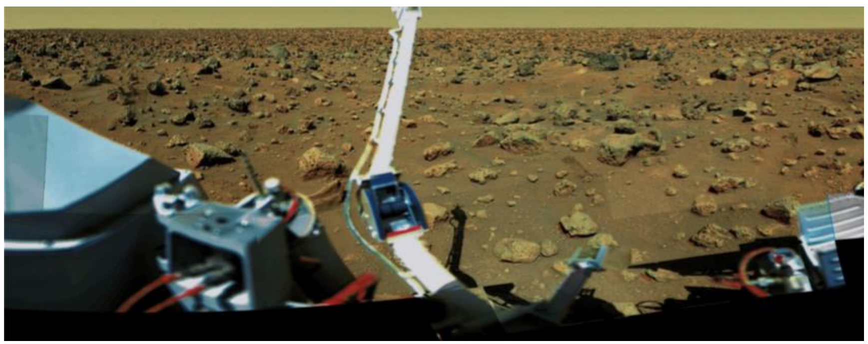

Side view of Martian surface

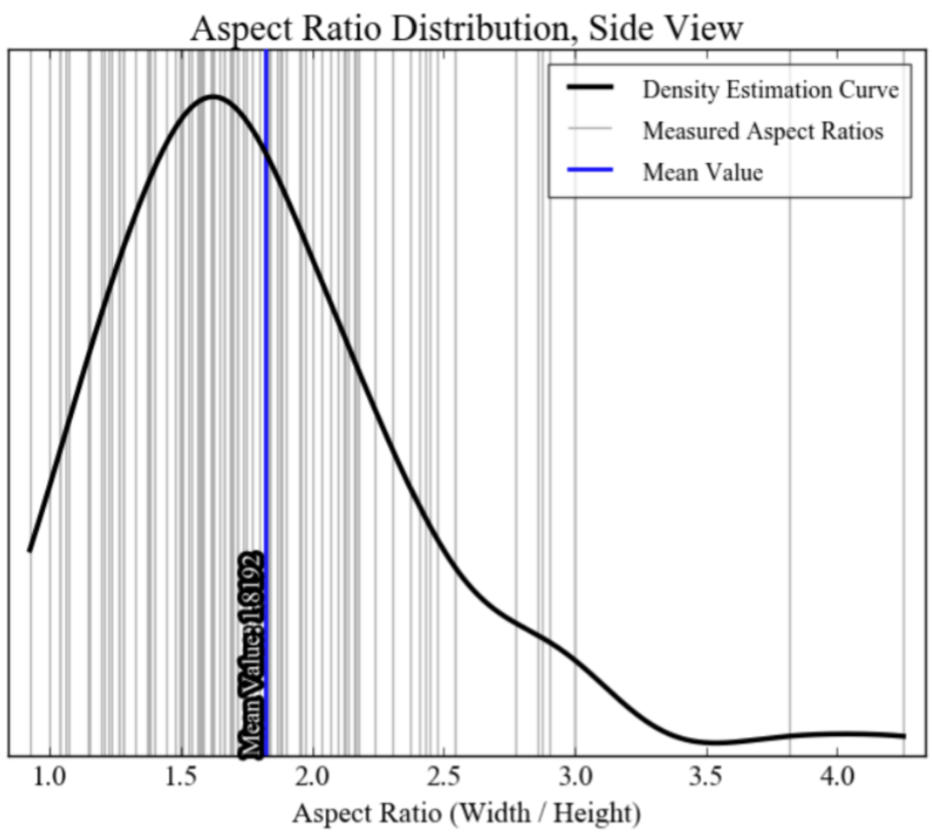

Aspect ratio distribution

Resolution Requirement

- Statistical analysis of rock size/aspect ratios on Mars
- Created a software map of a characteristic landing surface
- Monte Carlo simulation with different scan resolutions
- Determine probability of aliasing over a hazard (failure) vs. scan resolution

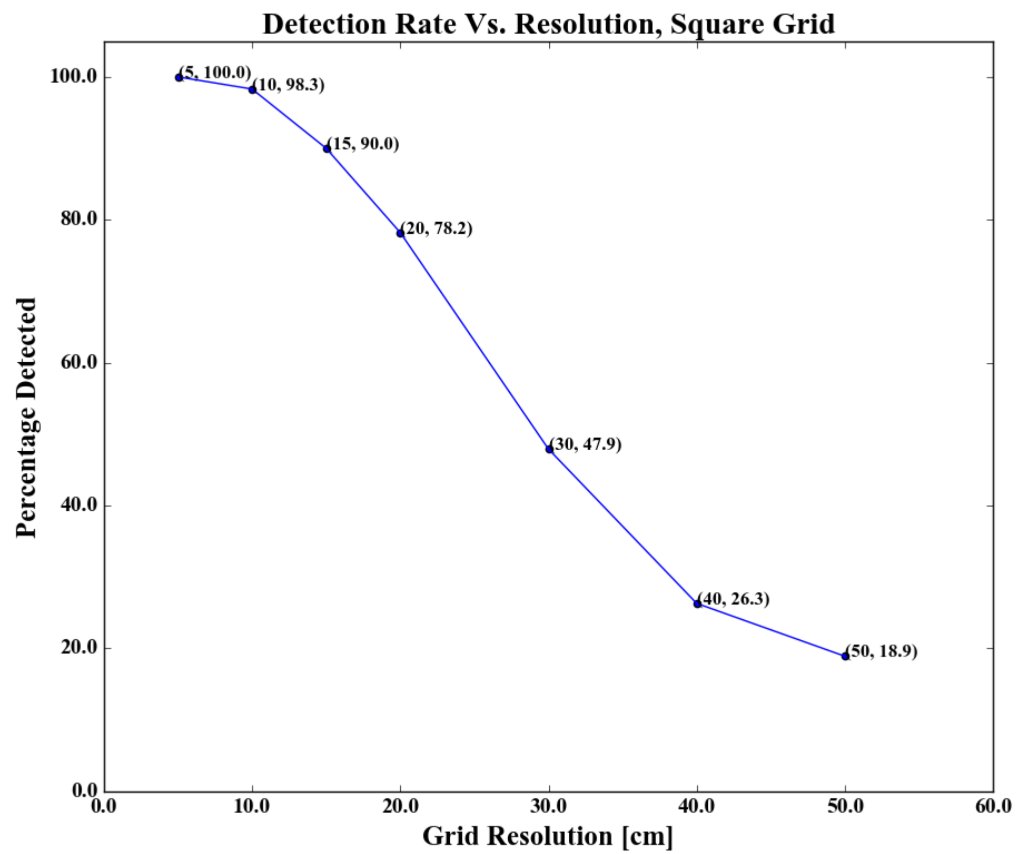

Shadowing

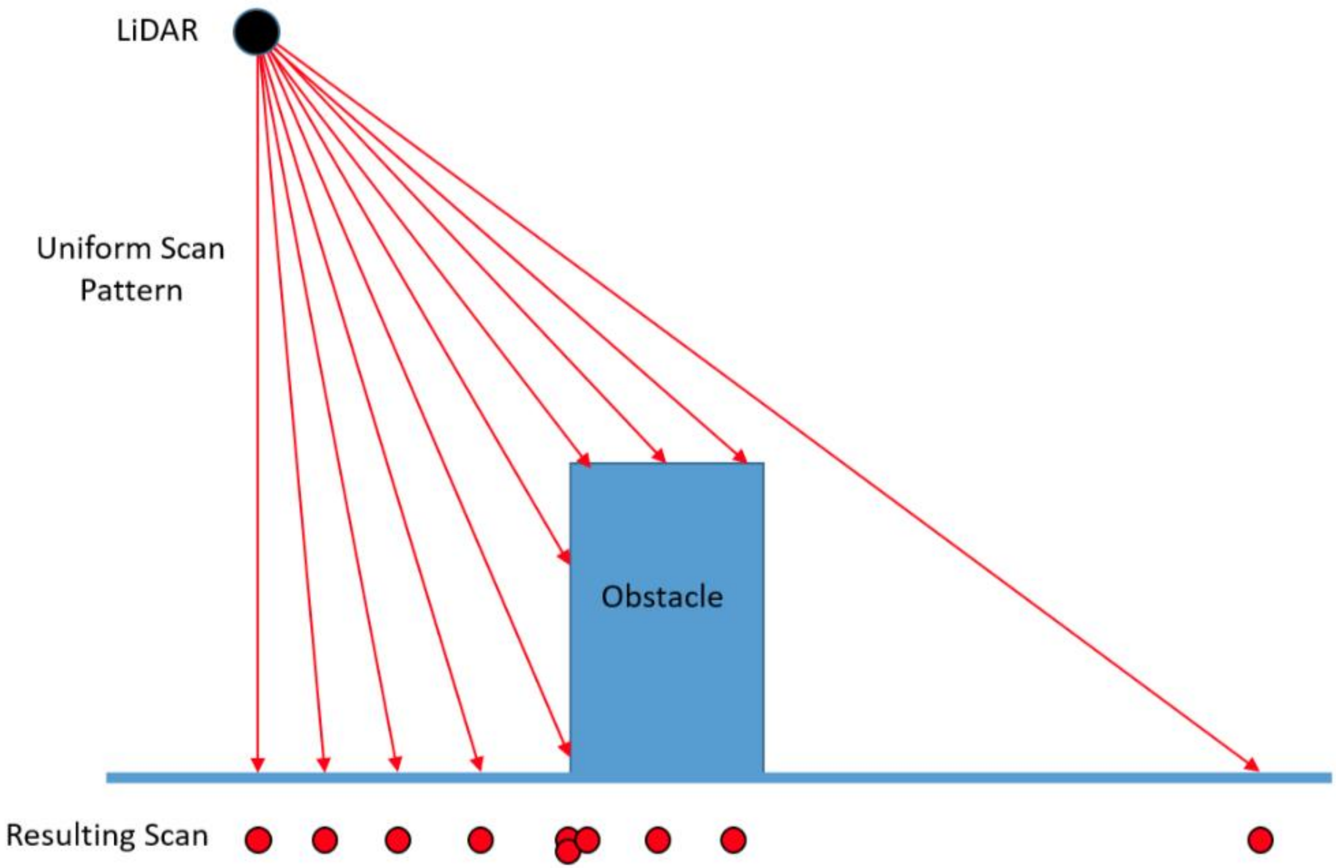

Visualization of shadowing effects

Maximum Scan Angle

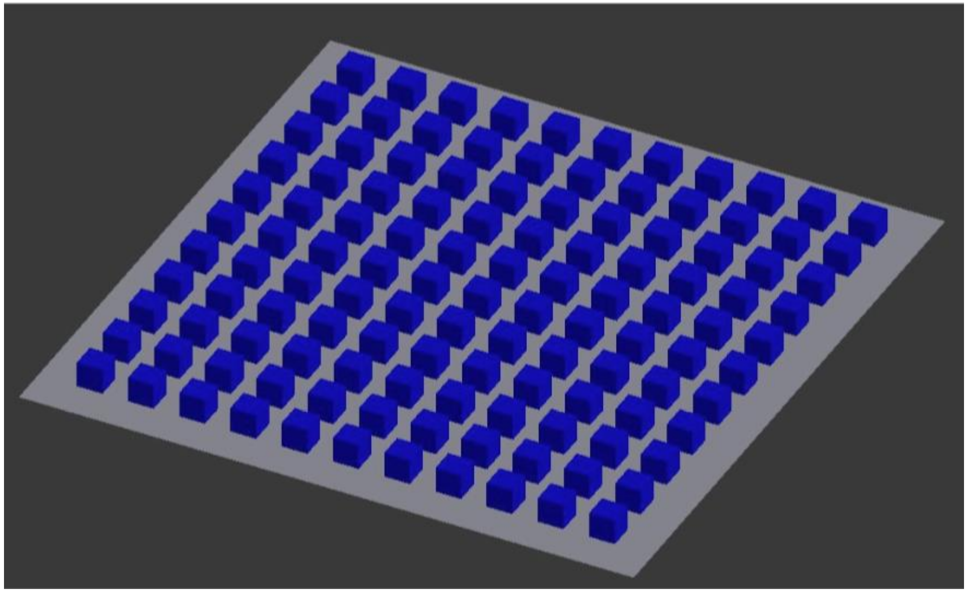

Blender visualization of a test scene

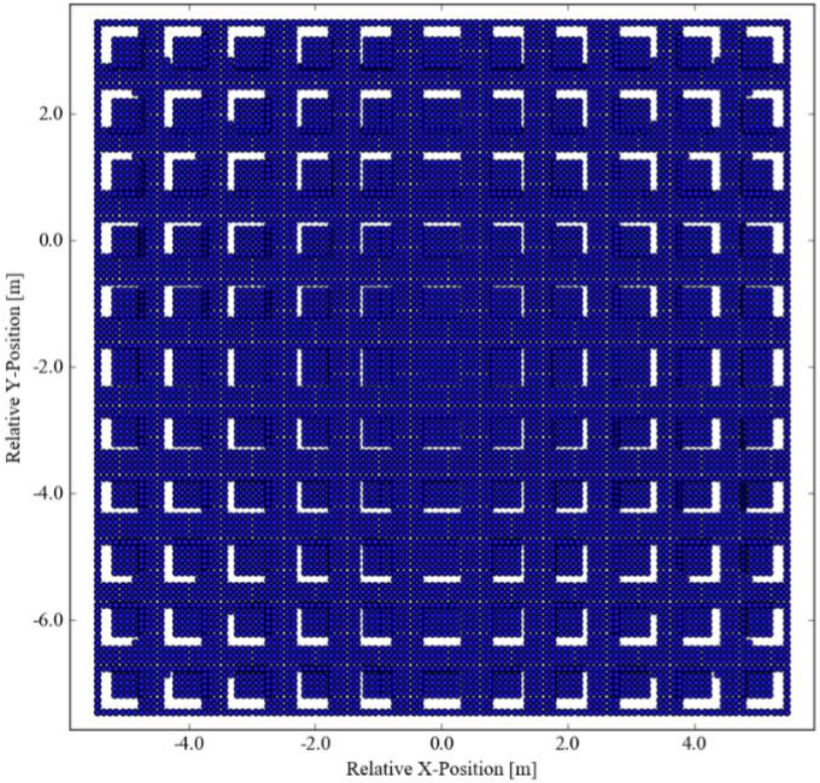

Resulting points with lidar scan

Success Levels

Level	Hardware: Lidar Scanning System	Software Development	Test Bed
1	Lidar sensor and scanning system shall obtain measurements with a $0.1m$ spatial resolution at a $14.1m^*$range and a maximum angle of 20° from nadir	Subsystems shall interact to record and output correlated range and attitude measurements	Stationary platform shall be built to house and operate the lidar scanning system
2	Scanning process shall be completed in less than 60 seconds	Range and attitude measurements with uncertainties shall be projected into a three-dimensional point cloud within the same 60-second time requirement as the hardware scan	Arbitrary test scene with dimensions known to an accuracy better than $0.01m$ shall be scanned with lidar in order to verify mapping accuracy

Success Levels

Level	Hardware: Lidar Scanning System	Software Development	Test Bed
3	-	Topographic map shall be analyzed to create a map of hazards, within the same 60-second requirement	Landing zone mock-up with known hazards shall be constructed with dimensions known to an accuracy better than 0.01m in order to verify hazard detection
4	-	Within the same 60-seconds, hazard map shall be analyzed to determine the nearest safe landing zone; if no safe zones are detected, hazard definitions will be loosened until the first viable landing zone is detected	-

Functional Requirements 1, 2

FR 1 The system shall implement a proof-of-concept landing assist system for a CubeSat lander.

DR 1.1 The system shall be capable of scanning terrain in two dimensions, centered in the nadir direction.

DR 1.2 The system shall have a maximum scan angle of 20° off of nadir.

DR 1.3 The scan target area shall be located at a nadir range of $14.1m$.

DR 1.4 The distance between scanned points shall be less than or equal to $0.1m$.

DR 1.5 The system shall complete the scan and analysis in under 60 seconds.

FR 2 The on-board processor shall receive commands and data from a user-operated PC.

DR 2.1 The system shall receive a command from the PC to initiate operation.

DR 2.2 The system shall terminate operation upon command from the PC.

DR 2.3 The system shall accept simulated Inertial Measurement Unit (IMU) data from the PC.

Functional Requirements 3, 4

FR 3 The on-board processor shall command the sensor package, made up of the lidar and the scanning system.

DR 3.1 The on-board processor shall store logs with timestamps of all commands sent to the lidar and actuator(s).

DR 3.2 The on-board processor shall send actuator commands to control the orientation of the lidar beam.

DR 3.3 The on-board processor shall command the start and stop of lidar data collection.

FR 4 The sensor package shall utilize lidar to obtain range measurements at known orientations.

DR 4.1 The lidar shall have a minimum range of 12*m* or less.

DR 4.2 The lidar shall have a maximum range of 17.25*m* or greater.

DR 4.3 The lidar shall have a range error of less than 0.05*m*.

DR 4.4 The lidar shall have a cross range error of less than 0.05*m*.

DR 4.5 Worst-case return signal angular uncertainty* shall be less than or equal to 0.15°.

DR 4.6 Lidar range and beam attitude measurements shall be taken within one microsecond.

*The worst-case return signal angular uncertainty is defined as the sum of uncertainty due to angular position uncertainty, beam diameter (spot size), and beam divergence. Beam divergence and beam spot size both create angular uncertainty in where the return is measured from.

Functional Requirements 5, 6, 7

FR 5 The sensor package shall transmit data to an on-board processor or DAQ.

DR 5.1 The lidar shall send range data to the on-board processor or DAQ.

DR 5.2 The beam attitude measurement shall be sent to the on-board processor or DAQ.

FR 6 The on board processor shall translate the range and attitude data into a three-dimensional point cloud.

DR 6.1 Range and attitude data shall be transformed into (x, y, z) coordinates.

DR 6.2 Uncertainties in range and attitude shall be propagated into uncertainty in (x, y, z) coordinates.

FR 7 The on-board processor shall analyze the 3D point cloud for hazards.

DR 7.1 Hazardous areas shall be identified if the area contains a hazard with height defined in section C.3 of the appendix, or if touchdown in the selected area would place the lander base more than 15° off of vertical.

Functional Requirements 8, 9

FR 8 The on-board processor shall select an acceptable landing site.

DR 8.1 The selected landing site shall be a square measuring 0.5*m* by 0.5*m* when projected onto the plane of the ground.

DR 8.2 The landing site selected as "safe" (defined in App C.3) shall not contain any terrain or obstacles that exceed the landing safety requirements of the mission.

DR 8.3 In the event that no suitable landing site is found, the acceptable threshold for safety will be lowered until one appears.

FR 9 The system shall generate output readable by the PC.

DR 9.1 The system shall generate health and status information readable by the PC in real time.

DR 9.2 Range measurements from the lidar and attitude measurements from the pointing system shall be readable by the PC.

DR 9.3 The three-dimensional point cloud shall be readable by the PC.

DR 9.4 Identified hazard locations shall be readable by the PC.

DR 9.5 The selected landing location shall be readable by the PC.

Lidar Sensor Trade Study

Metric	1	2	3	4	5
Sample Rate [Hz]	< 100	100 - 199	200 - 299	300 - 399	> 400
Cross Range Error [°]	> 0.4	0.3 - 0.39	0.2 - 0.29	0.1 - 0.19	< 0.1
Range Error [cm]	> 4	3 - 3.99	2 - 2.99	1 - 1.99	< 1
Cost [$]	> 4000	3000 - 3999	2000 - 2999	1000 - 1999	< 1000
Algorithm Implications	Impossible	Difficult	Undesirable	Inconvenient	None
Range	Operational Range does not meet requirements	N/A	N/A	N/A	Operational Range meets requirements
Moment of Inertia	Prohibitive	Large	Moderate	Small	Negligible

Lidar Sensor Trade Study

	Weight	Fixed Beam	Scanning	Optical Segmentation
Sample Rate	25%	3	5	1
Cross Range Error	25%	4	2	1
Range Error	15%	4	3	1
Cost	10%	4	3	5
Algorithm Implications	10%	5	4	2
Range	10%	5	1	5
Moment of Inertia	5%	2	3	4
Sum	100%	**3.85**	3.15	2.05

Scanning System Trade Study

Metric	1	2	3	4	5
Cost	> 2000 USD	1500-2000 USD	1000-1499 USD	500-999 USD	< 500 USD
Actuation Complexity for Desired Scan Pattern	Uncontrollable	Complex	Moderate	Simple	Trivial
Moment of Inertia of Rotating Components	Prohibitive	Large	Average	Small	Negligible
Attitude Error with Constant δ in Motors	$>> \delta$	$> \delta$	$\approx \delta$	$< \delta$	$<< \delta$
Hardware Design Complexity	Overscoped	Involved	Moderate	Simple	Trivial
Technology Readiness Level	Research Based	Under Development	Made and Tested	Used in Real World Scenario	Commercial off the Shelf

Scanning System Trade Study

	Weight	Mechanical-Based	Mirror-Based	Risley Prisms
Cost	10%	2	4	4
Actuation Complexity for Desired Scan Pattern	20%	4	4	2
Moment of Inertia of Rotating Components	15%	2	4	5
Attitude Error with Constant δ in Motors	20%	3	1	4
Hardware Design Complexity	10%	2	3	4
Technology Readiness Level	25%	4	4	3
Sum	100%	3.1	3.3	**3.5**

Scanning System Trade Study

	Weight	Mechanical Based	Mirror Based	Risley Prisms	Mirror/Gimbal Hybrid
Cost	10%	2	4	4	4
Actuation Complexity for Desired Scan Pattern	20%	4	4	2	4
Moment of Inertia of Rotating Components	15%	2	4	5	4
Attitude Error with Constant δ in Motors	20%	3	1	4	2
Hardware Design Complexity	10%	2	3	4	3
Technology Readiness Level	25%	4	4	3	4
Sum	100%	3.1	3.3	**3.5**	3.4

Hazard Detection Algorithm Trade Study

	Weight	Simple Filter	Surface-Based Filter	Morpho-logical Filter	Fourier Decom-position	Image Process-ing	Point Dis-place-ment
Computational Complexity	10%	5	3	4	2	4	5
Robustness	65%	1	3.5	5	3.5	5	4
Calculation with Incoming Point Stream	10%	5	1	5	1	3	5
Low Impact on Mechanical System	15%	5	5	3	3	3	5
Sum	100%	2.4	3.425	4.6	3.025	4.4	4.35

Hazard Detection Unit Tests

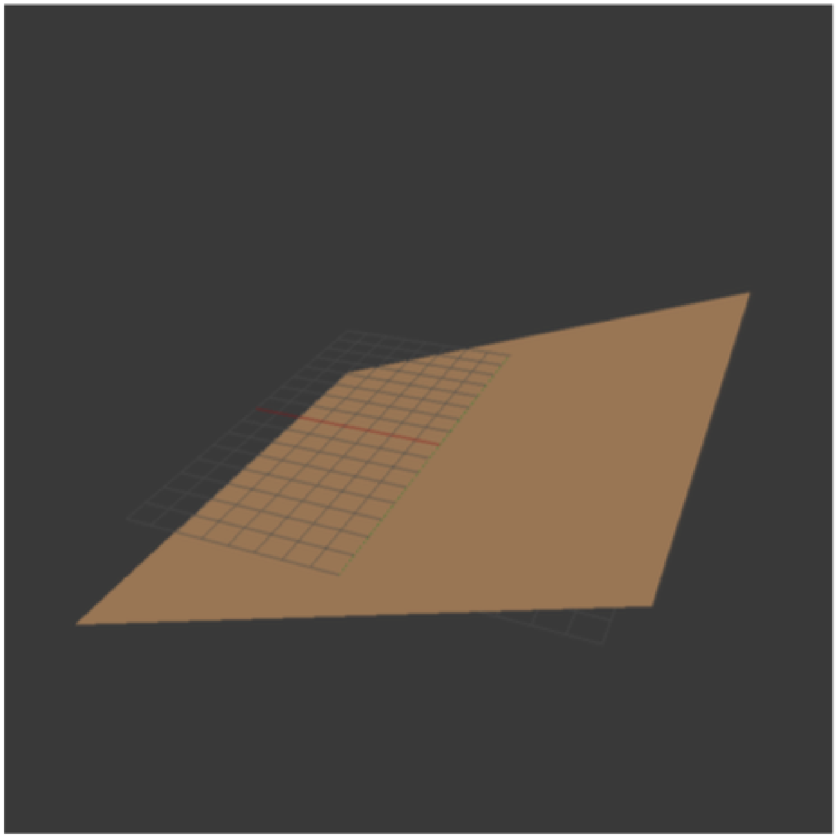

Slanted plane with no obstacles

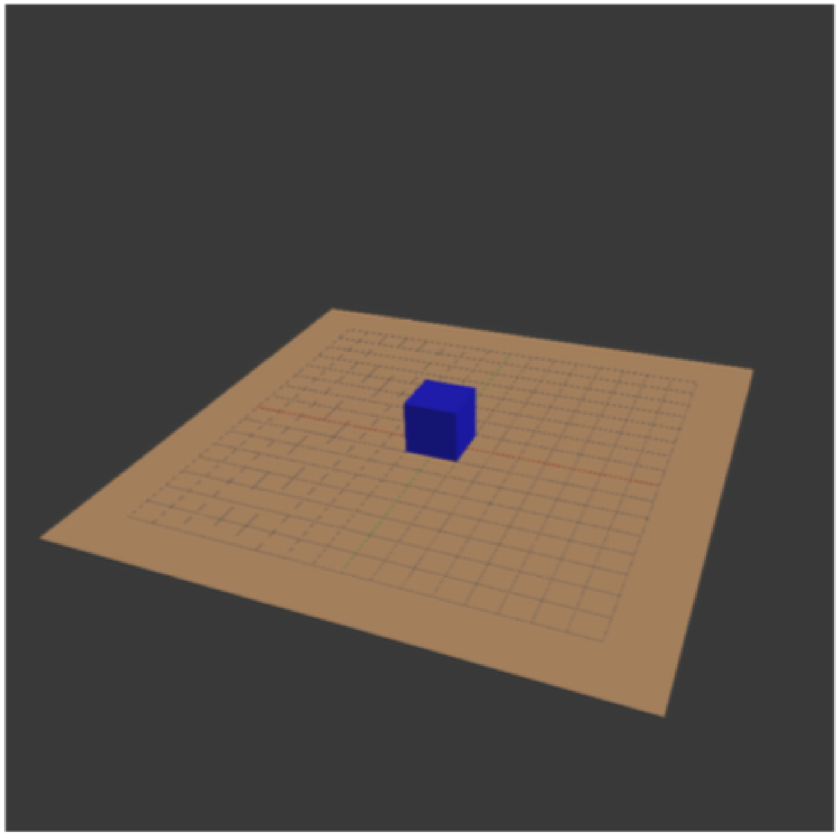

Flat plane with cube in center

Hazard Detection Unit Tests

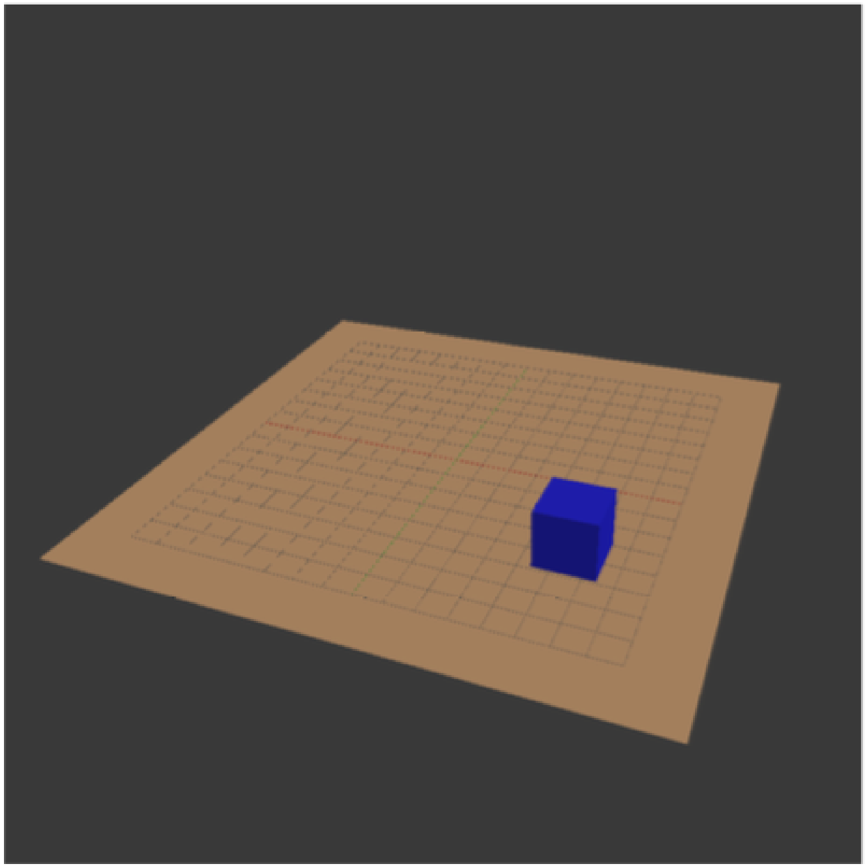

Flat plane with cube not in center

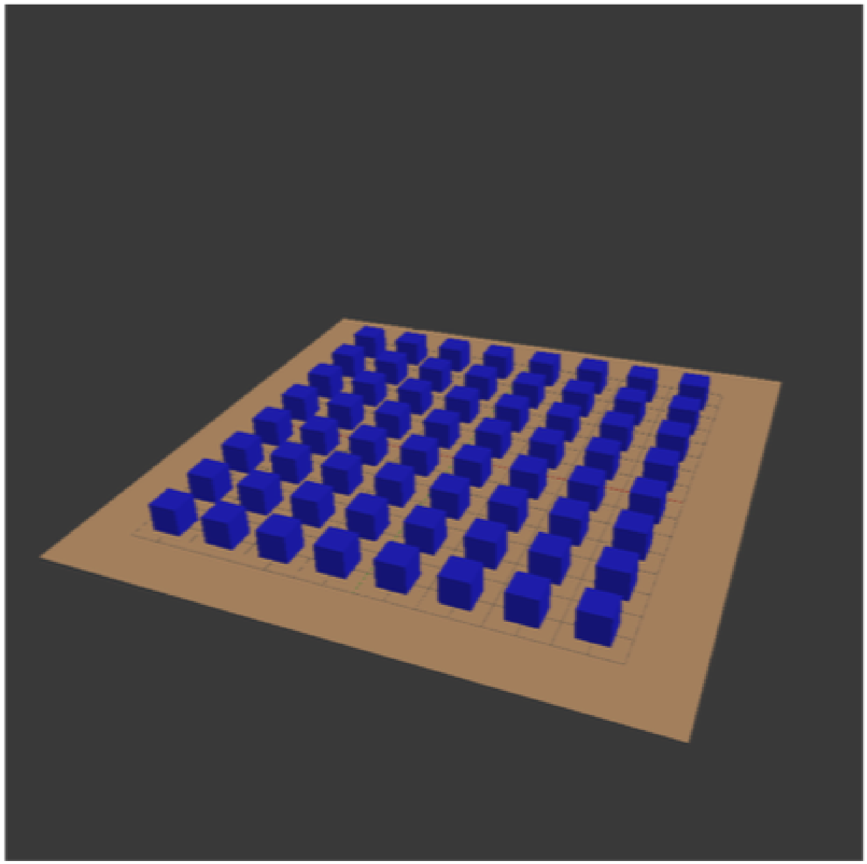

Flat plane with array of spaced cubes

Hazard Detection Unit Tests

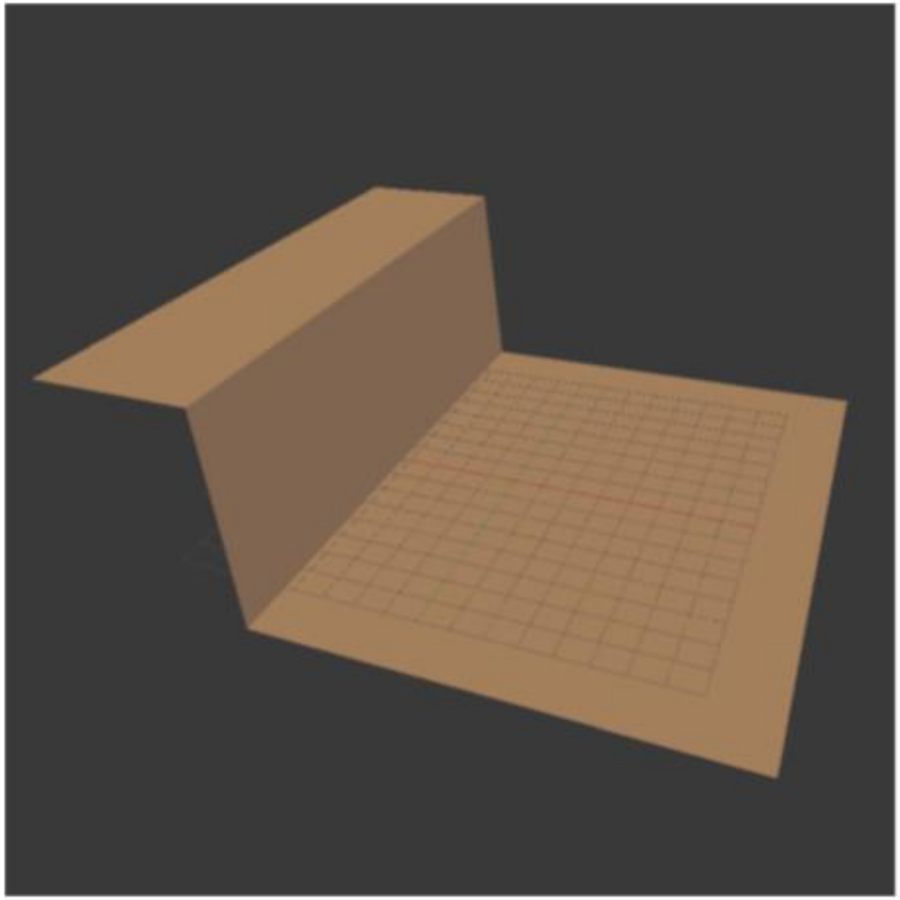

Cliff

Hazard Detection Unit Test

	Failed Algorithms Per Unit Test
Constant Slope	• *Simple Filter:* Only a band in the center will be reported as safe
Centered Cube	• *Simple Filter:* Cube top will be registered as ground level and everything else below it will be registered as hazardous • *Point Displacement:* The point displacement will be small at the edges of the cube since it is located close to nadir
Off-Center Cube	*None*
Spaced Array of Cubes	• *Surface-Based Filter:* The smoothed surface be wavy and the subtraction from the original surface will result in spikes and dips at all edges • *Fourier Decomposition:* Same issue as the Surface-Based filter
Cliff	• *Simple Filter:* Will not register the flat surface on the upper side of the cliff as safe • *Surface-Based Filter:* Half-passed. The smoothed surface will not capture the steepness of the cliff and so there will be zones near the cliff top and bottom that are not registered safe even though they are flat • *Fourier Decomposition:* Same rationale as the Surface-Based Filter

Grid pattern

Problems

- Prisms lend well to polar
- Difficult to control
- Complete stop often

Solution

- Square grid almost identical to equilateral triangle grid

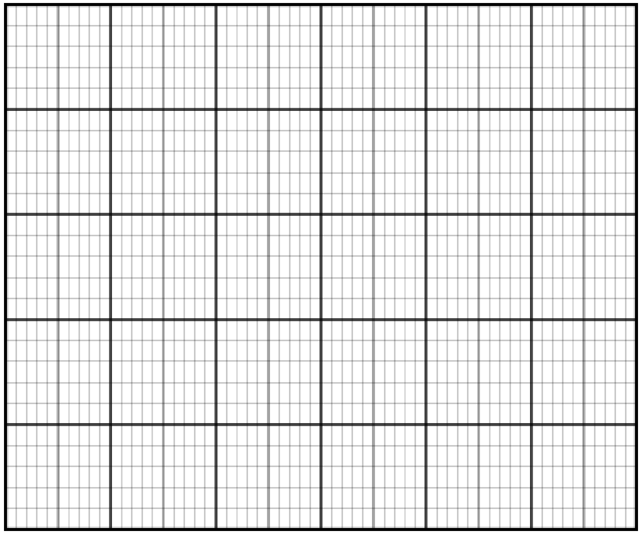

Concentric Circles

Advantages

- Equilateral triangles best capture gradients
- Grid can be represented easily as circles
- Circles are co-rotations of prisms

Disadvantages

- Requires traversal between circles

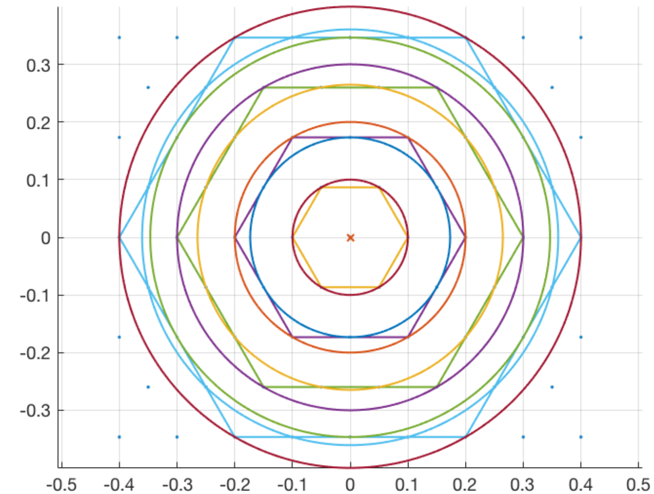

Spirals

<u>Solution: Spirals</u>

- Closely capture concentric circles
- Able to conform to resolution requirements
- Proven method

<u>Issues</u>

- Velocity and alpha spike towards center

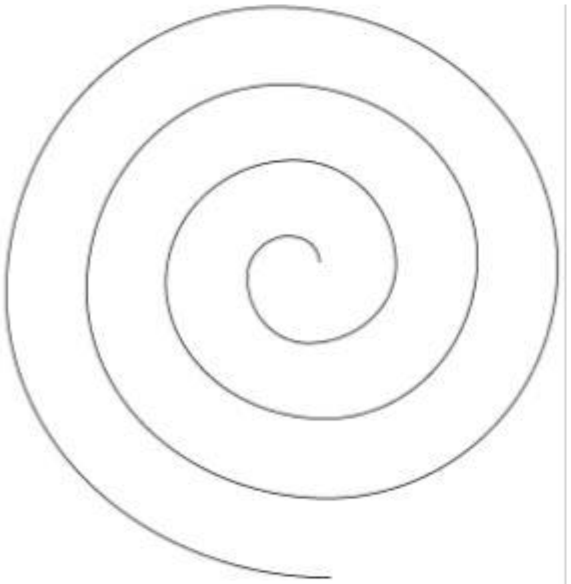

Beam Steering Equations

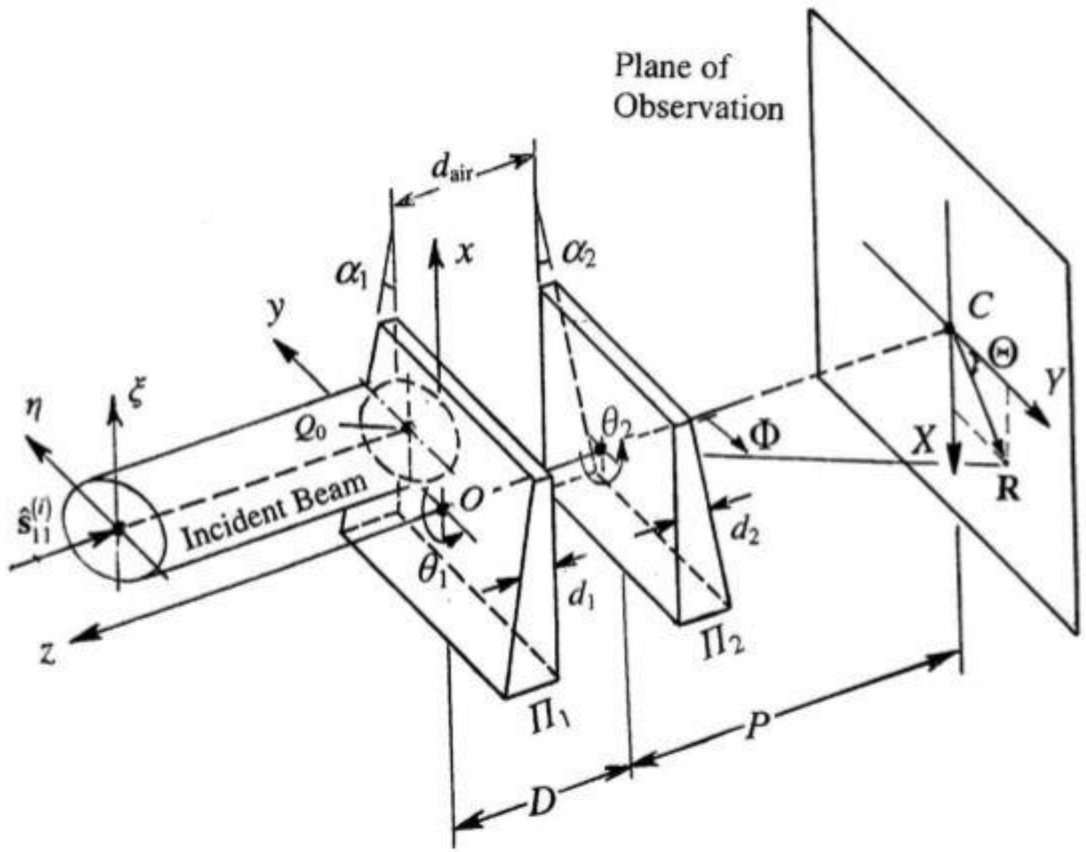

Beam Steering Equations

Variables

- δ_q: Angular deviation from prism
- α: apex angles
- η: refractive index
- θ: Prism rotation angle
- γ: clock angle
- P: distance to nadir point
- ϕ: Apex angle

Beam Steering Equations

<u>Assumptions</u>

- Thin prism approximation
  - First order analysis
  - $\delta_q = (\eta_q - 1)\alpha_q$, ($q$ = 1,2)

Beam Steering Equations

$$x = P[\delta_1 \cos(\theta_1) + \delta_2 \cos(\theta_2)]$$
$$y = P[\delta_1 \sin(\theta_1) + \delta_2 \sin(\theta_2)]$$

First order approximation

$$\phi = \sqrt{(\delta_1 \cos(\theta_1) + \delta_2 \cos(\theta_2))^2 + (\delta_1 \sin(\theta_1) + \delta_2 \sin(\theta_2))^2}$$

$$\gamma = \tan^{-1}\left(\frac{x}{y}\right) = \tan^{-1}\left(\frac{\delta_1 \cos(\theta_1) + \delta_2 \cos(\theta_2)}{\delta_1 \sin(\theta_1) + \delta_2 \sin(\theta_2)}\right)$$

Beam steering equations

- Take the partials of the beam steering equations

$$\frac{\delta\phi}{\delta\theta_2} = \frac{\delta_1\delta_2 sin(\theta_1 - \theta_2)}{\sqrt{\delta_1^2 + 2\delta_1\delta_2 cos(\theta_1 - \theta_2) + \delta_2^2}(\delta_1^2 + 2\delta_1\delta_2 cos(\theta_1 - \theta_2) + \delta_2^2 + 1)}$$

$$\frac{\delta\phi}{\delta\theta_1} = \frac{-\delta_1\delta_2 sin(\theta_1 - \theta_2)}{\sqrt{\delta_1^2 + 2\delta_1\delta_2 cos(\theta_1 - \theta_2) + \delta_2^2}(\delta_1^2 + 2\delta_1\delta_2 cos(\theta_1 - \theta_2) + \delta_2^2 + 1)}$$

$$\frac{\delta\gamma}{\delta\theta_1} = \frac{-\delta_1(\delta_1 + \delta_2 cos(\theta_1 - \theta_2))}{\delta_1^2 + \delta_2^2 + 2\delta_1\delta_2 cos(\theta_1 - \theta_2)} \quad \frac{\delta\gamma}{\delta\theta_2} = \frac{-\delta_2(\delta_2 + \delta_1 cos(\theta_1 - \theta_2))}{\delta_1^2 + \delta_2^2 + 2\delta_1\delta_2 cos(\theta_1 - \theta_2)}$$

Azimuth Angle

Variables

- a: Nadir scan height
- b: Maximum radius
- ϕ: Azimuth angle
- y: Radius over time

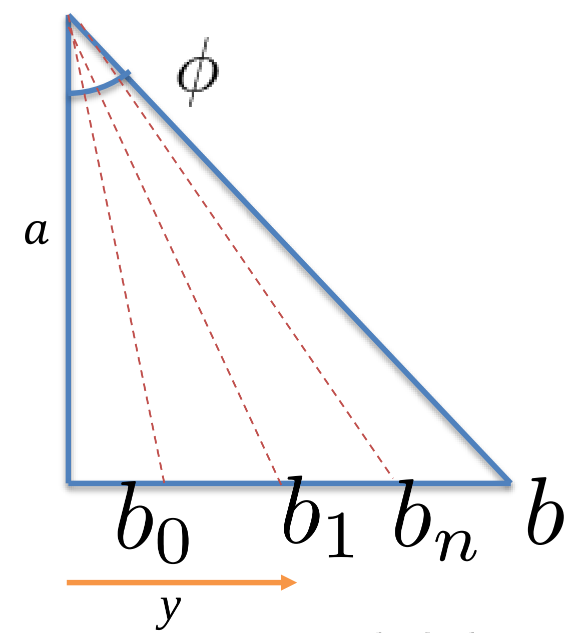

$$\phi_{b_i} = tan^{-1}(\frac{y}{a}) = tan^{-1}(\frac{\Delta b * t}{a})$$

$$\dot{\phi}_{b_i} = \frac{(a)(\Delta b)}{a^2 + (\Delta b^2)(t^2)}$$

Clock Angle

<u>Variables</u>

- l: arch length
- y: radius over time
- γ : Clock angle

$$\Delta\gamma = \frac{l}{y} = \frac{l}{(\Delta b)(\Delta t)}$$

$$\Delta\dot{\gamma} = \frac{-l}{(\Delta b)(\Delta t^2)}$$

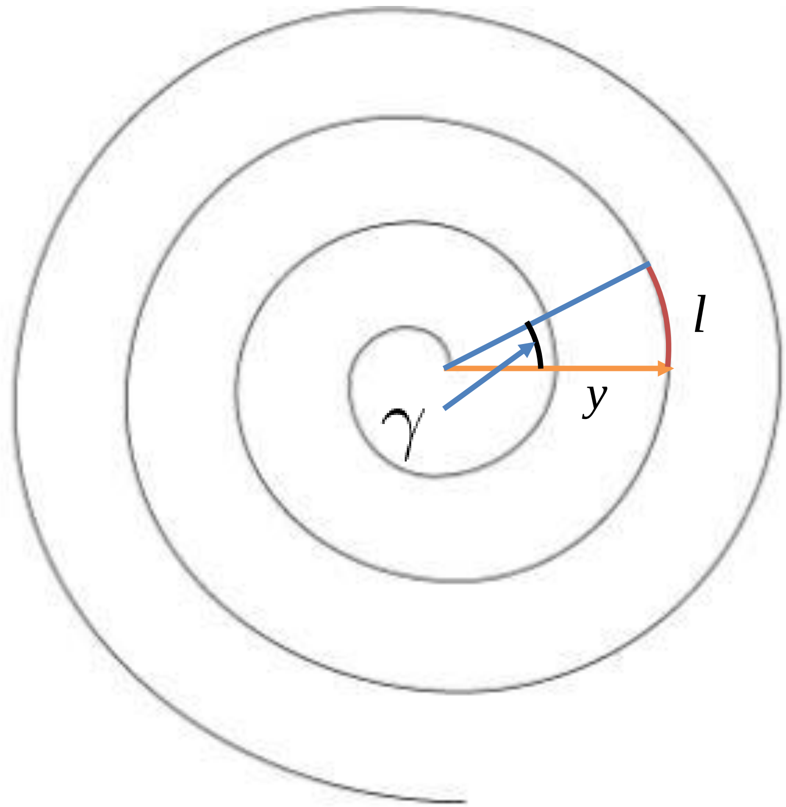

Motor Rate Equations

- We can relate the rates of the beam attitude to the prism angular velocities to find motor rates

$$\begin{pmatrix} \frac{d\theta_1}{dt} \\ \frac{d\theta_2}{dt} \end{pmatrix} = \begin{pmatrix} \frac{\partial\phi}{\partial\theta_1} & \frac{\partial\phi}{\partial\theta_2} \\ \frac{\partial\gamma}{\partial\theta_1} & \frac{\partial\gamma}{\partial\theta_2} \end{pmatrix}^{-1} \begin{pmatrix} \frac{d\phi}{dt} \\ \frac{d\gamma}{dt} \end{pmatrix}$$

Resolution Requirement Test

Spiral angular velocity: **4.6536 rpm**

Risley Prism Rotation Rates:

Maximum rate: 4.6653 rpm
Minimum rate: 4.6419 rpm
Maximum acceleration:
4.7988e-6 rad/s^2

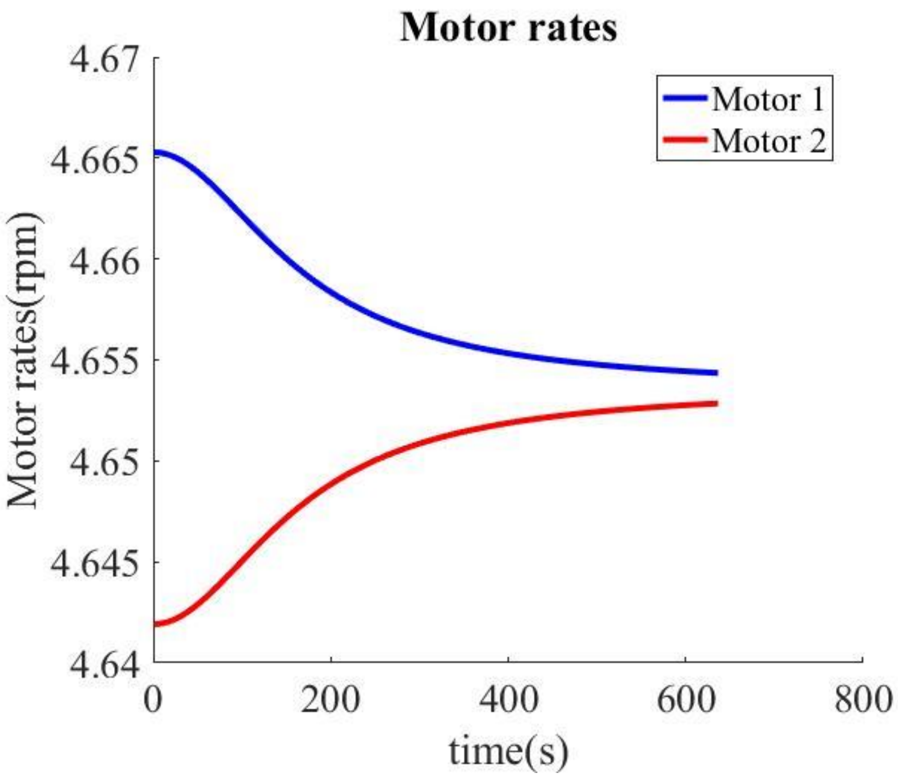

Time Requirement Test

Spiral angular velocity: **71.0763 rpm**

<u>Risley Prism Rotation Rates:</u>

Maximum rate: 71.0881 rpm
Minimum rate: 71.0647 rpm
Maximum acceleration:
3.7575e-6 rad/s^2

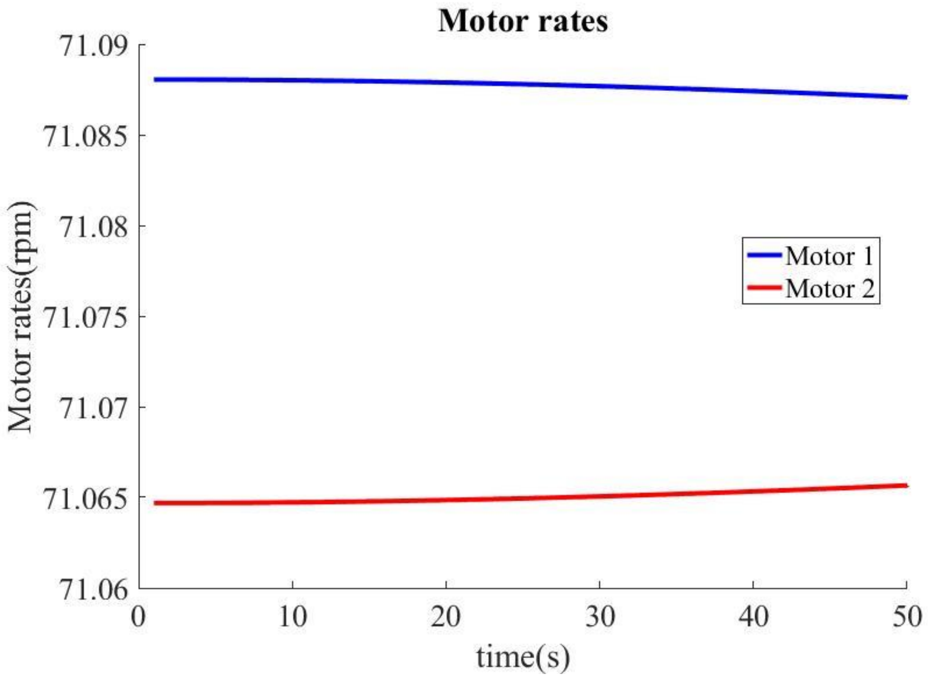

Accelerations: Time Tests

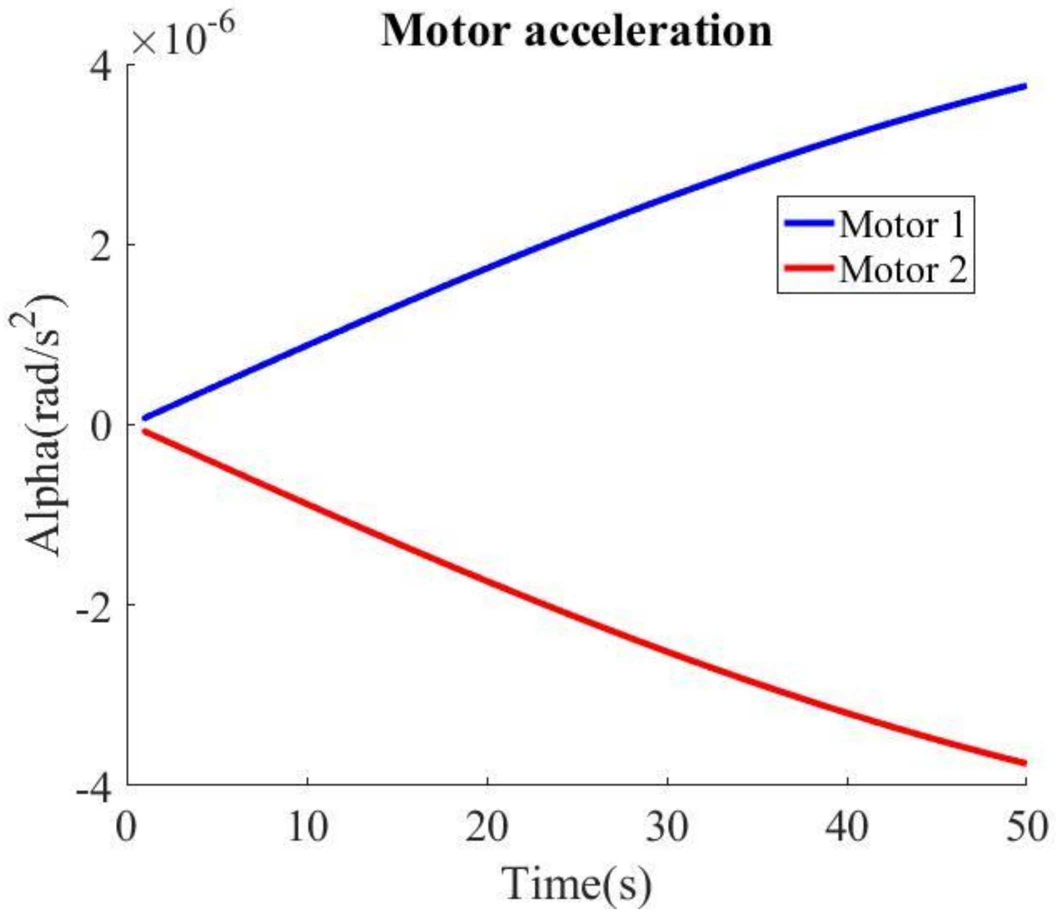

Accelerations: Resolution

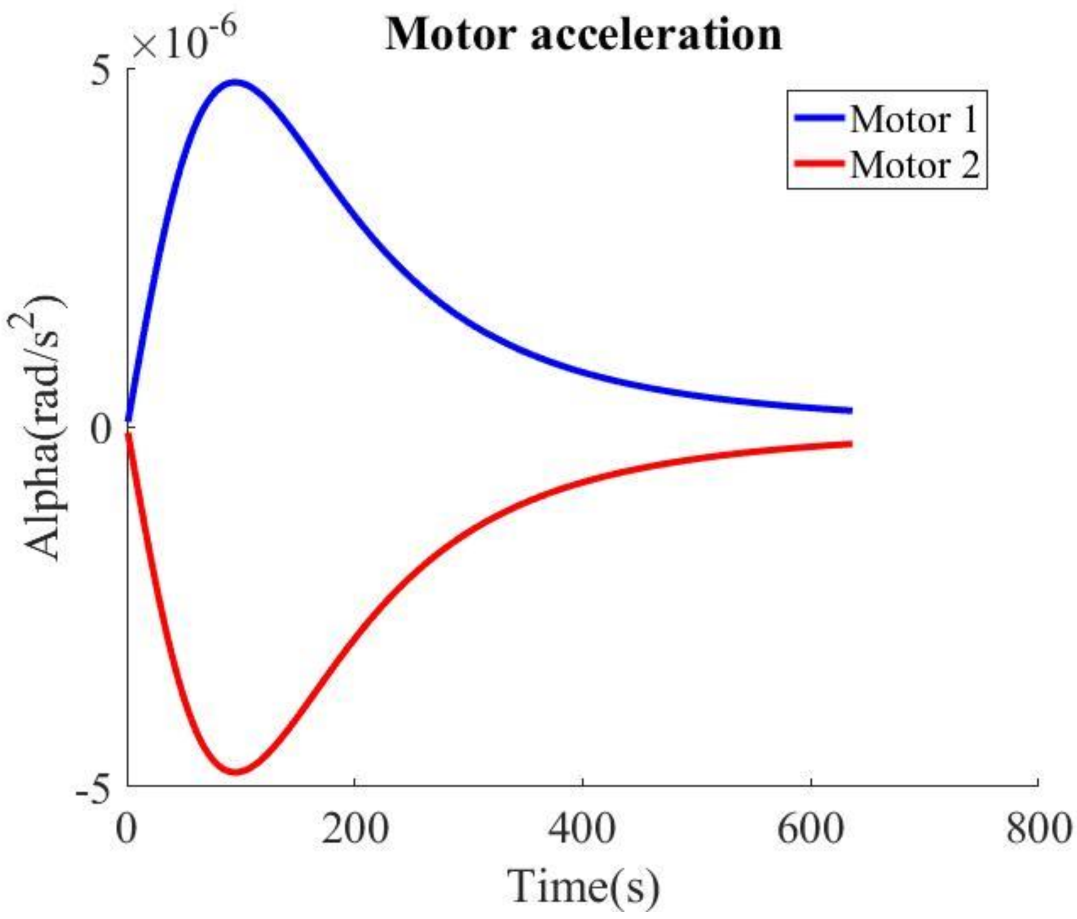

Torque Required

Solidworks estimate for moment of inertia for rotating components:

$2.776\ lb_m in^2 = 0.00599\ slug\ ft^2$

From maximum angular acceleration required
and $T = I\alpha$ (use 2I for margin)

$T_{max} =$ is on the order of 10^{-8} lb ft for both system level tests

This shows that the torque required for phasing is practically negligible

Any motor will be essentially unloaded during scanning process

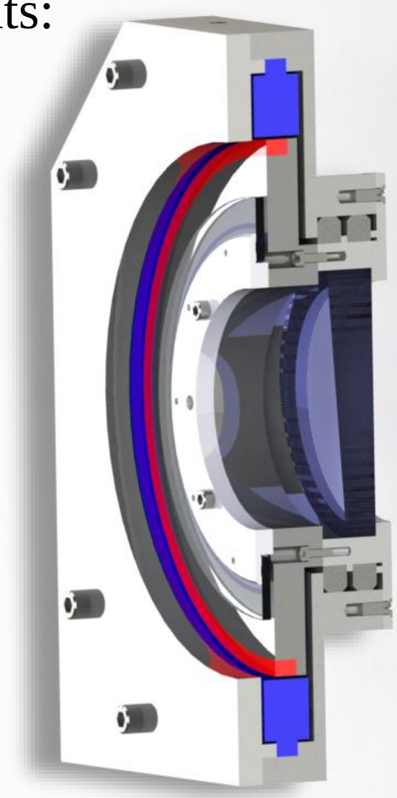

Motor Control

- From research: BLDC used for adjustable speed or precise precision control
- Position control performance difficult to estimate without full system parameters and detailed numerical modeling
- Need work to prove feasibility, currently showing establishment
- If control is not achievable on small scale (α) MOI can be increased or scan pattern can be analyzed with more phasing

Preliminary Control Concept

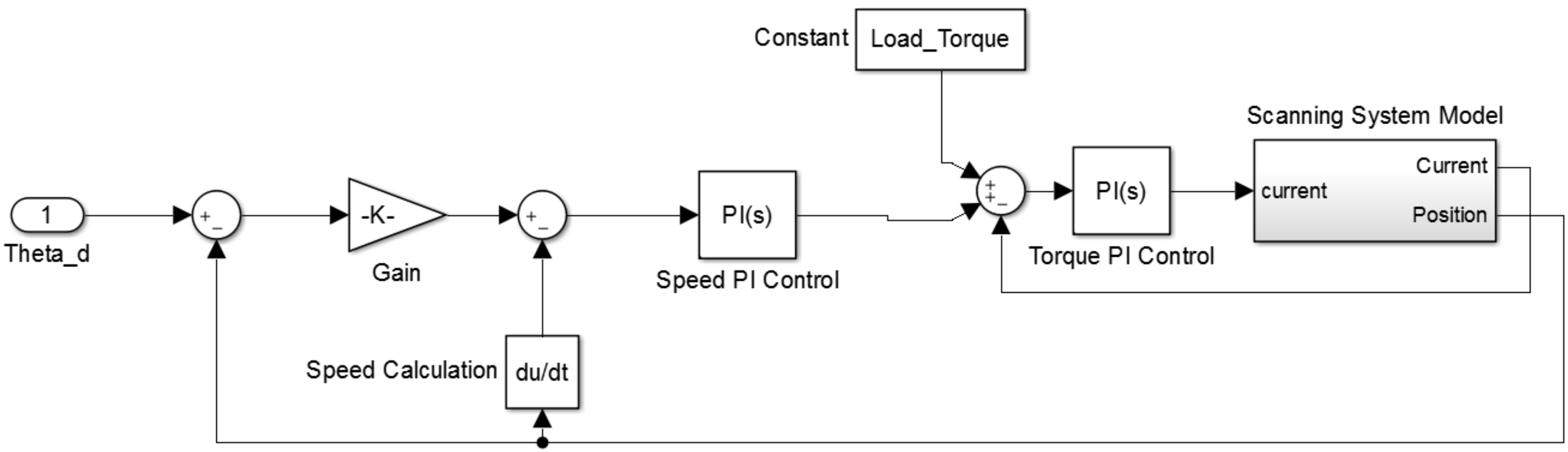

Retroreflector Feasibility

- Luminous Intensity [candela] – Quantity of luminous flux in given direction
- Illuminance [lux] – Measure of concentration of luminous flux falling on surface
- Luminance [candela/m^2] – Measure of flux emitted from or reflected by a uniform surface

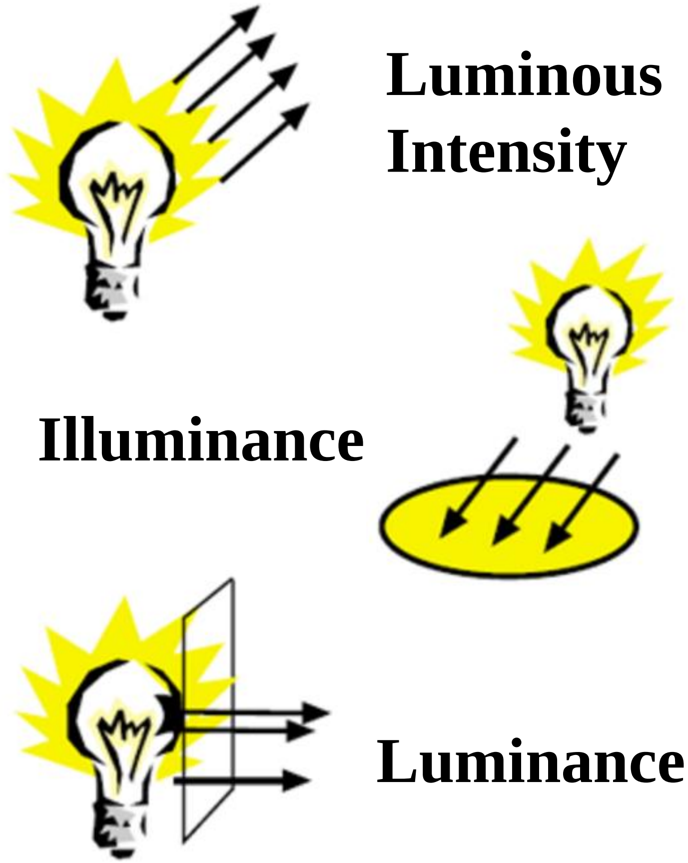

http://www.konicaminolta.com/instruments/knowledge/light/concepts/04.html

Retroreflector Feasibility

<u>Laser Emitter</u>

- Pulse: < 4 nJ
- Pulse length: 5 ns
- Beam divergence:
  - $\delta = 0.057°$
- Luminous Intensity:
  - 4.24e7 candela
- Illuminance on surface (15 m, 20° from nadir)
  - 1.89e5 lux

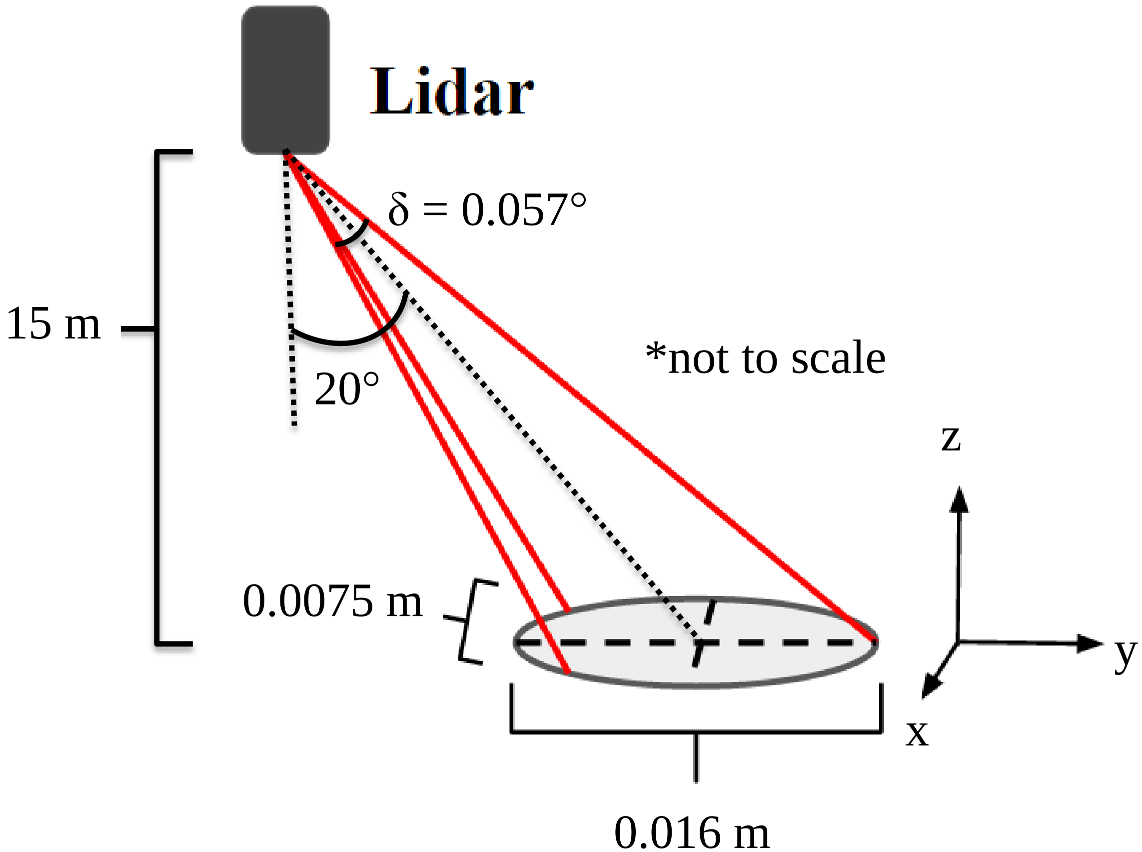

Retroreflector Feasibility

Reflexite Daybright V92

Observation Angles	Entrance Angles	White
0.2 °	-4 °	460
	30°	250
0.5 °	-4 °	100
	30 °	65

- Luminance of return:
  - 1.23e7 candela/m^2
- Luminance of Pepperl+Fuchs datasheet tests (90% Kodak White):
  - 1.70e5 candela/m^2

Prismatic Retroreflector

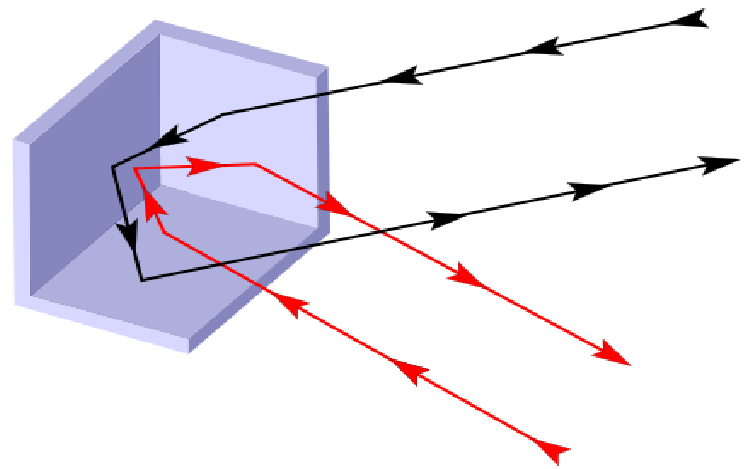

https://en.wikipedia.org/wiki/Retroreflector

Lidar Wavelength

Feasibility for MACULA

- Test surface can be constructed with white diffuse paint or white retroreflective tape

Why this sensor was selected

- Meets budget and accuracy constraints
- Test surface can be constructed to fit sensor

Benefits of Using 660 nm

- Visible spectrum (verification)

Lidar Wavelength

- Per **FR1**, MACULA is proof-of-concept system for CubeSat lander
  - Wavelength can be selected for custom-built sensors
  - Implemented systems will choose wavelength based upon landing surface

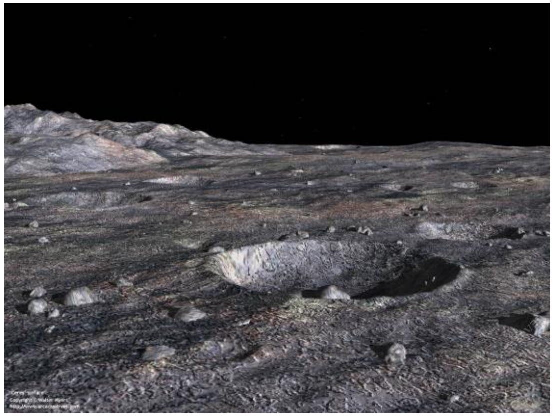

http://pics-about-space.com/asteroid-surface?p=1

http://pics-about-space.com/planet-mars-surface?p=1

Laser Wavelength vs. Cost

- Red lasers are the most common and cheapest to manufacture
- Laser colors other than red require specialized crystals with rare-earth elements such as Neodymium
  - These extra components can drive up the cost of other color lasers (yellow, blue, green) to dozens of times the cost of a red laser
- These colors can have better reflection on certain surfaces, but do not provide a general advantage over red lasers

Detector Functionality

- Parabolic mirror to collect diffuse returns
- Specular returns do not disperse

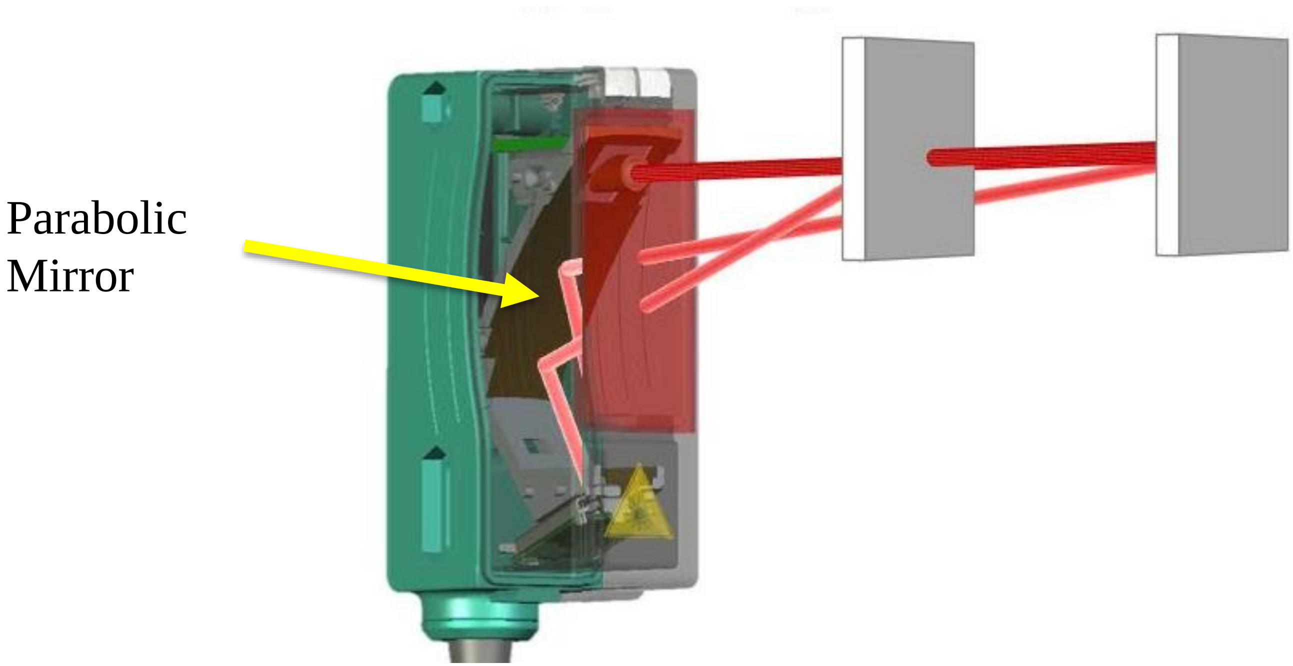

Prism Specifications

- Ross Optical P-WRC059
  - Diameter: 5.08 cm
  - 10° Maximum Beam Deviation (per prism)
  - Wedge Angle: 18° 8′
  - Angle Error: ± 30 arc seconds
  - Material: N-BK7 Grade A fine annealed
    - Transmission: 91% at 660 nm
    - Density: 2.51 g/cm³
    - Thermal Expansion: $7.1 \times 10^{-6}\ \mathrm{K}^{-1}$
  - Thin Edge Thickness: 3mm
  - Dimensional Tolerance ± 0.1 mm

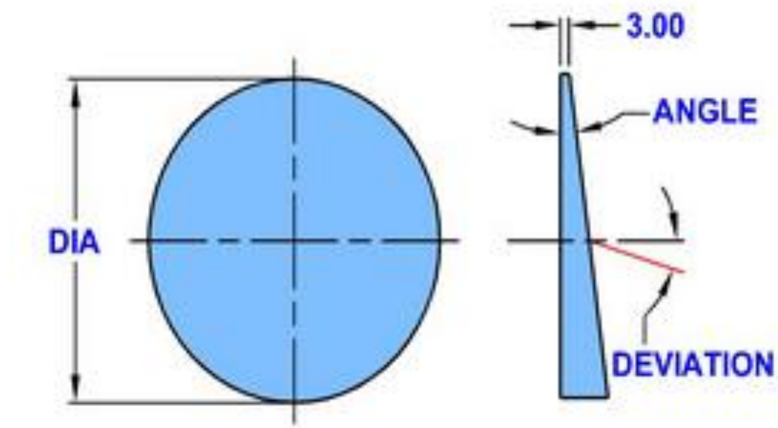

Index of Refraction

- N-BK7 has variable index of refraction

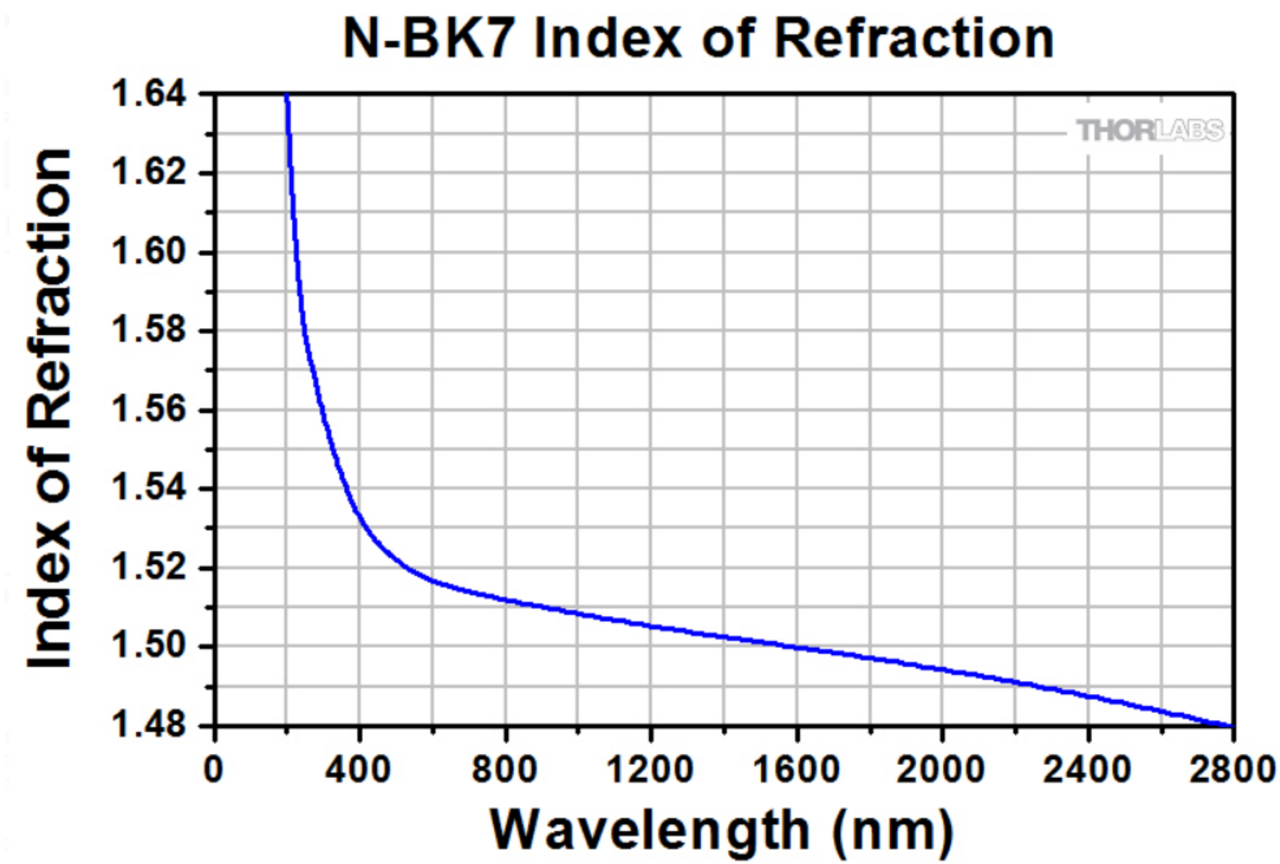

Coating Reflectance

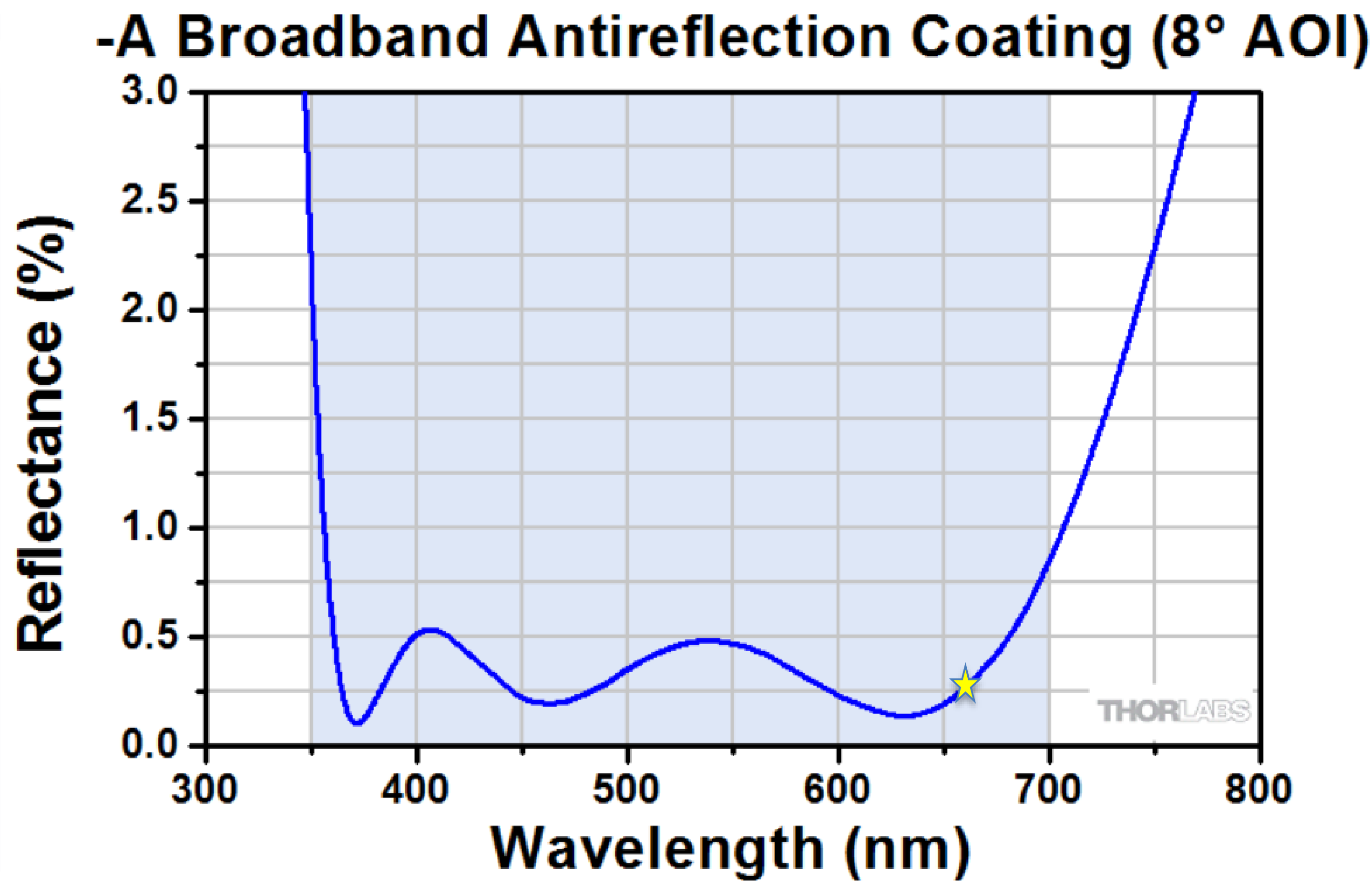

Error due to Reflections

- Lidar beam may reflect off prism surfaces into detector

To reduce this effect:

- Prisms can be coated
- Detector can be shielded
- System can be aligned such that reflections off prisms are angled away from detector

Prism Attenuation

- Material: N-BK7 Grade A fine annealed

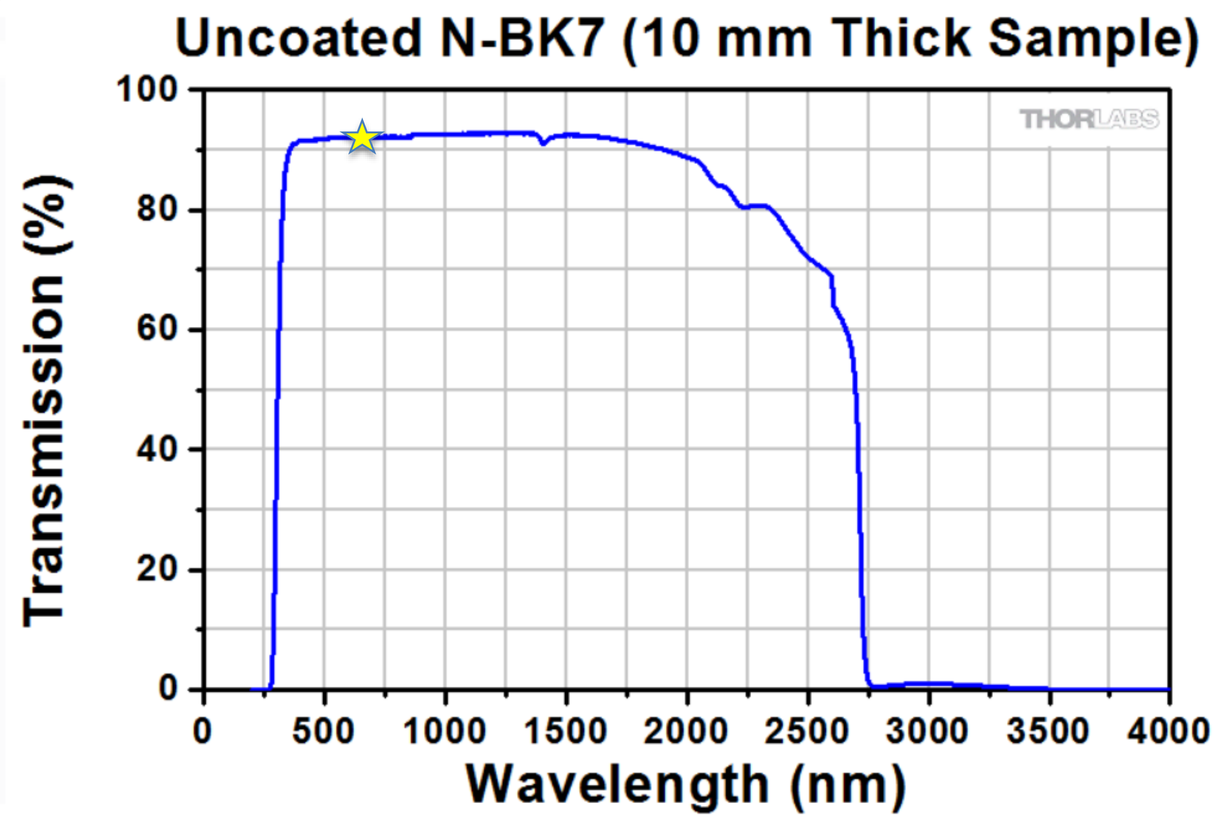

Prism Diameter

- Beam lines calculated for eight rotations of the prisms (rotated together to produce maximum deflection angle)
- Transmitter and two points on the edge of the receiver are projected straight and their refractions are calculated for each of the prism rotations
  - This is only part of the receiver field of view. The lidar is placed to maximize what the receiver can see, without clipping the transmitter
- Prism diameter based on the farthest point from the center axis for any beam on any prism face
- Resulting distance is divided by 0.9 to produce the prism diameter (for best refraction results from the prism)
- Modeled as blocks for ease of plotting only. Reported size is the diameter

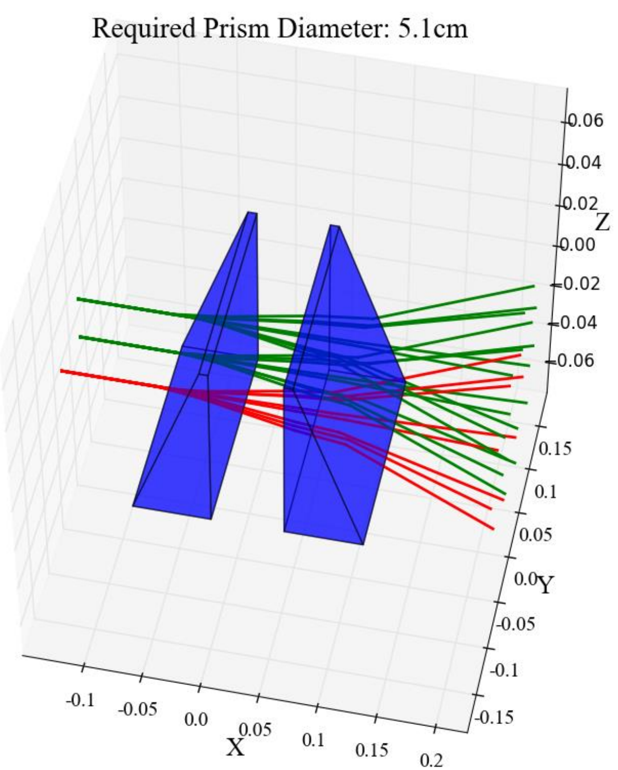

Embedded System

Motor Drivers

- Requirements
  - 12 V @ 1 A
  - Three Phase Brushless DC
  - Position Control → Encoder Feedback
- DZRALTE-020B080[2]

Microcontroller

- Requirements
  - TTL to RS-485/232 for Motor Drivers[1]
  - Two quadrature decoders[1]
  - One 12 bit minimum ADC[1]
  - UART, Ethernet, or USB → PC communication
  - FPU
  - 1 MB RAM (10 k points at 12 bytes each + hazard map and program margin)
- BeagleBone Black Rev C.1[2]

Incremental Rotary Encoder

- Requirements
  - Quadrature output with index
  - 0.1° Resolution
  - OPS Rotary Encoder[2]

1: May be a breakout board

2: Fits the requirements but need a trade study for actual selection

Power Requirements

- BeagleBone: 5 V 1 A max 500 mA normal operation – Can be powered by USB powers the TTL to RS485
- Motors and Motor Drivers: 12 V 1 A per pair
- VDM28: 10-30 V 100 mA max load current 20 mA max output current loop
- Encoder: 5 V 120 mA – can be powered by the BeagleBone; will require more than the USB can provide
- Need two 12 V 1 A power supply and one 5 V 1.5 A for 12 minutes.

- Total Wattage: 32.7 W
- Total Energy: 23,544 J

BeagleBone Black Rev C.1

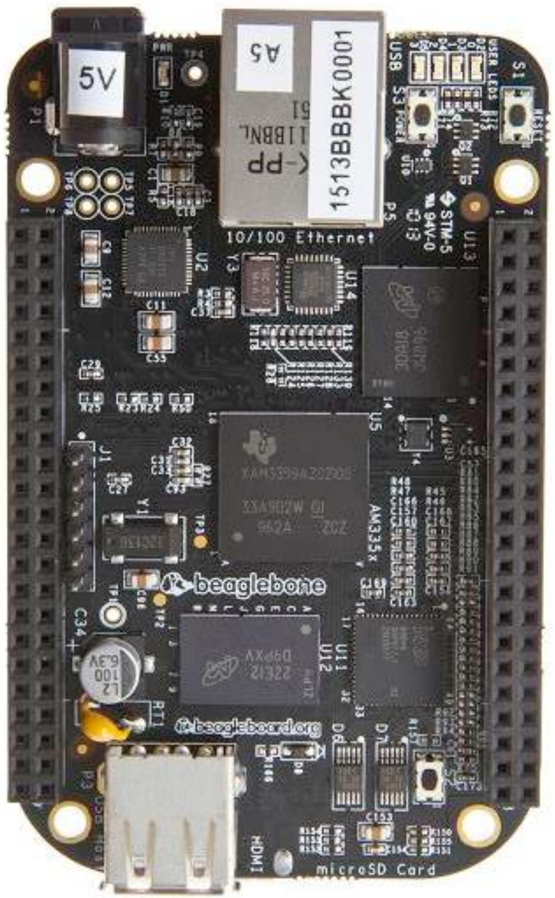

	Feature	
Processor	Sitara AM3358BZCZ100 1GHz, 2000 MIPS	
Graphics Engine	SGX530 3D, 20M Polygons/S	
SDRAM Memory	512MB DDR3L 800MHZ	
Onboard Flash	4GB, 8bit Embedded MMC	
PMIC	TPS65217C PMIC regulator and one additional LDO.	
Debug Support	Optional Onboard 20-pin CTI JTAG, Serial Header	
Power Source	miniUSB USB or DC Jack	5VDC External Via Expansion Header
PCB	3.4" x 2.1"	6 layers
Indicators	1-Power, 2-Ethernet, 4-User Controllable LEDs	
HS USB 2.0 Client Port	Access to USB0, Client mode via miniUSB	
HS USB 2.0 Host Port	Access to USB1, Type A Socket, 500mA LS/FS/HS	
Serial Port	UART0 access via 6 pin 3.3V TTL Header. Header is populated	
Ethernet	10/100, RJ45	
SD/MMC Connector	microSD , 3.3V	
User Input	Reset Button Boot Button Power Button	
Video Out	16b HDMI, 1280x1024 (MAX) 1024x768,1280x720,1440x900 ,1920x1080@24Hz w/EDID Support	
Audio	Via HDMI Interface, Stereo	
Expansion Connectors	Power 5V, 3.3V , VDD_ADC(1.8V) 3.3V I/O on all signals McASP0, SPI1, I2C, GPIO(69 max), LCD, GPMC, MMC1, MMC2, 7 AIN(1.8V MAX), 4 Timers, 4 Serial Ports, CAN0, EHRPWM(0,2),XDMA Interrupt, Power button, Expansion Board ID (Up to 4 can be stacked)	
Weight	1.4 oz (39.68 grams)	
Power	Refer to Section 6.1.7	

Expansion Header P8 Pinout

PIN	PROC	NAME	MODE0	MODE1	MODE2	MODE3	MODE4	MODE5	MODE6	MODE7
1,2						GND				
3	R9	GPIO1_6	gpmc_ad6	mmc1_dat6						gpio1[6]
4	T9	GPIO1_7	gpmc_ad7	mmc1_dat7						gpio1[7]
5	R8	GPIO1_2	gpmc_ad2	mmc1_dat2						gpio1[2]
6	T8	GPIO1_3	gpmc_ad3	mmc1_dat3						gpio1[3]
7	R7	TIMER4	gpmc_advn_ale		timer4					gpio2[2]
8	T7	TIMER7	gpmc_oen_ren		timer7					gpio2[3]
9	T6	TIMER5	gpmc_be0n_cle		timer5					gpio2[5]
10	U6	TIMER6	gpmc_wen		timer6					gpio2[4]
11	R12	GPIO1_13	gpmc_ad13	lcd_data18	mmc1_dat5	mmc2_dat1	eQEP2B_in		pr1_pru0_pru_r30_15	gpio1[13]
12	T12	GPIO1_12	gpmc_ad12	Lcd_data19	mmc1_dat4	Mmc2_dat0	Eqep2a_in		pr1_pru0_pru_r30_14	gpio1[12]
13	T10	EHRPWM2B	gpmc_ad9	lcd_data22	mmc1_dat1	mmc2_dat5	ehrpwm2B			gpio0[23]
14	T11	GPIO0_26	gpmc_ad10	lcd_data21	mmc1_dat2	mmc2_dat6	ehrpwm2_tripzone_in			gpio0[26]
15	U13	GPIO1_15	gpmc_ad15	lcd_data16	mmc1_dat7	mmc2_dat3	eQEP2_strobe		pr1_pru0_pru_r31_15	gpio1[15]
16	V13	GPIO1_14	gpmc_ad14	lcd_data17	mmc1_dat6	mmc2_dat2	eQEP2_index		pr1_pru0_pru_r31_14	gpio1[14]
17	U12	GPIO0_27	gpmc_ad11	lcd_data20	mmc1_dat3	mmc2_dat7	ehrpwm0_synco			gpio0[27]
18	V12	GPIO2_1	gpmc_clk_mux0	lcd_memory_clk	gpmc_wait1	mmc2_clk			mcasp0_fsr	gpio2[1]
19	U10	EHRPWM2A	gpmc_ad8	lcd_data23	mmc1_dat0	mmc2_dat4	ehrpwm2A			gpio0[22]
20	V9	GPIO1_31	gpmc_csn2	gpmc_be1n	mmc1_cmd			pr1_pru1_pru_r30_13	pr1_pru1_pru_r31_13	gpio1[31]
21	U9	GPIO1_30	gpmc_csn1	gpmc_clk	mmc1_clk			pr1_pru1_pru_r30_12	pr1_pru1_pru_r31_12	gpio1[30]
22	V8	GPIO1_5	gpmc_ad5	mmc1_dat5						gpio1[5]
23	U8	GPIO1_4	gpmc_ad4	mmc1_dat4						gpio1[4]
24	V7	GPIO1_1	gpmc_ad1	mmc1_dat1						gpio1[1]
25	U7	GPIO1_0	gpmc_ad0	mmc1_dat0						gpio1[0]
26	V6	GPIO1_29	gpmc_csn0							gpio1[29]
27	U5	GPIO2_22	lcd_vsync	gpmc_a8				pr1_pru1_pru_r30_8	pr1_pru1_pru_r31_8	gpio2[22]
28	V5	GPIO2_24	lcd_pclk	gpmc_a10				pr1_pru1_pru_r30_10	pr1_pru1_pru_r31_10	gpio2[24]
29	R5	GPIO2_23	lcd_hsync	gpmc_a9				pr1_pru1_pru_r30_9	pr1_pru1_pru_r31_9	gpio2[23]
30	R6	GPIO2_25	lcd_ac_bias_en	gpmc_a11						gpio2[25]
31	V4	UART5_CTSN	lcd_data14	gpmc_a18	eQEP1_index	mcasp0_axr1	uart5_rxd		uart5_ctsn	gpio0[10]
32	T5	UART5_RTSN	lcd_data15	gpmc_a19	eQEP1_strobe	mcasp0_ahclkx	mcasp0_axr3		uart5_rtsn	gpio0[11]
33	V3	UART4_RTSN	lcd_data13	gpmc_a17	eQEP1B_in	mcasp0_fsr	mcasp0_axr3		uart4_rtsn	gpio0[9]
34	U4	UART3_RTSN	lcd_data11	gpmc_a15	ehrpwm1B	mcasp0_ahclkr	mcasp0_axr2		uart3_rtsn	gpio2[17]
35	V2	UART4_CTSN	lcd_data12	gpmc_a16	eQEP1A_in	mcasp0_aclkr	mcasp0_axr2		uart4_ctsn	gpio0[8]
36	U3	UART3_CTSN	lcd_data10	gpmc_a14	ehrpwm1A	mcasp0_axr0			uart3_ctsn	gpio2[16]
37	U1	UART5_TXD	lcd_data8	gpmc_a12	ehrpwm1_tripzone_in	mcasp0_aclkx	uart5_txd		uart2_ctsn	gpio2[14]
38	U2	UART5_RXD	lcd_data9	gpmc_a13	ehrpwm0_synco	mcasp0_fsx	uart5_rxd		uart2_rtsn	gpio2[15]
39	T3	GPIO2_12	lcd_data6	gpmc_a6		eQEP2_index		pr1_pru1_pru_r30_6	pr1_pru1_pru_r31_6	gpio2[12]
40	T4	GPIO2_13	lcd_data7	gpmc_a7		eQEP2_strobe	pr1_edio_data_out7	pr1_pru1_pru_r30_7	pr1_pru1_pru_r31_7	gpio2[13]
41	T1	GPIO2_10	lcd_data4	gpmc_a4		eQEP2A_in		pr1_pru1_pru_r30_4	pr1_pru1_pru_r31_4	gpio2[10]
42	T2	GPIO2_11	lcd_data5	gpmc_a5		eQEP2B_in		pr1_pru1_pru_r30_5	pr1_pru1_pru_r31_5	gpio2[11]
43	R3	GPIO2_8	lcd_data2	gpmc_a2		ehrpwm2_tripzone_in		pr1_pru1_pru_r30_2	pr1_pru1_pru_r31_2	gpio2[8]
44	R4	GPIO2_9	lcd_data3	gpmc_a3		ehrpwm0_synco		pr1_pru1_pru_r30_3	pr1_pru1_pru_r31_3	gpio2[9]
45	R1	GPIO2_6	lcd_data0	gpmc_a0		ehrpwm2A		pr1_pru1_pru_r30_0	pr1_pru1_pru_r31_0	gpio2[6]
46	R2	GPIO2_7	lcd_data1	gpmc_a1		ehrpwm2B		pr1_pru1_pru_r30_1	pr1_pru1_pru_r31_1	gpio2[7]

Expansion Header P9 Pinout

PIN	PROC	NAME	MODE0	MODE1	MODE2	MODE3	MODE4	MODE5	MODE6	MODE7
1,2						GND				
3,4						DC_3.3V				
5,6						VDD_5V				
7,8						SYS_5V				
9						PWR_BUT				
10	A10					SYS_RESETn				
11	T17	UART4_RXD	gpmc_wait0	mii2_crs	gpmc_csn4	rmii2_crs_dv	mmc1_sdcd		uart4_rxd_mux2	gpio0[30]
12	U18	GPIO1_28	gpmc_be1n	mii2_col	gpmc_csn6	mmc2_dat3	gpmc_dir		mcasp0_aclkr_mux3	gpio1[28]
13	U17	UART4_TXD	gpmc_wpn	mii2_rxerr	gpmc_csn5	rmii2_rxerr	mmc2_sdcd		uart4_txd_mux2	gpio0[31]
14	U14	EHRPWM1A	gpmc_a2	mii2_txd3	rgmii2_td3	mmc2_dat1	gpmc_a18		ehrpwm1A_mux1	gpio1[18]
15	R13	GPIO1_16	gpmc_a0	gmii2_txen	rmii2_tctl	mii2_txen	gpmc_a16		ehrpwm1_tripzone_input	gpio1[16]
16	T14	EHRPWM1B	gpmc_a3	mii2_txd2	rgmii2_td2	mmc2_dat2	gpmc_a19		ehrpwm1B_mux1	gpio1[19]
17	A16	I2C1_SCL	spi0_cs0	mmc2_sdwp	I2C1_SCL	ehrpwm0_synci	pr1_uart0_txd			gpio0[5]
18	B16	I2C1_SDA	spi0_d1	mmc1_sdwp	I2C1_SDA	ehrpwm0_tripzone	pr1_uart0_rxd			gpio0[4]
19	D17	I2C2_SCL	uart1_rtsn	timer5	dcan0_rx	I2C2_SCL	spi1_cs1	pr1_uart0_rts_n		gpio0[13]
20	D18	I2C2_SDA	uart1_ctsn	timer6	dcan0_tx	I2C2_SDA	spi1_cs0	pr1_uart0_cts_n		gpio0[12]
21	B17	UART2_TXD	spi0_d0	uart2_txd	I2C2_SCL	ehrpwm0B	pr1_uart0_rts_n		EMU3_mux1	gpio0[3]
22	A17	UART2_RXD	spi0_sclk	uart2_rxd	I2C2_SDA	ehrpwm0A	pr1_uart0_cts_n		EMU2_mux1	gpio0[2]
23	V14	GPIO1_17	gpmc_a1	gmii2_rxdv	rgmii2_rxdv	mmc2_dat0	gpmc_a17		ehrpwm0_synco	gpio1[17]
24	D15	UART1_TXD	uart1_txd	mmc2_sdwp	dcan1_rx	I2C1_SCL		pr1_uart0_txd	pr1_pru0_pru_r31_16	gpio0[15]
25	A14	GPIO3_21*	mcasp0_ahclkx	eQEP0_strobe	mcasp0_axr3	mcasp1_axr1	EMU4_mux2	pr1_pru0_pru_r30_7	pr1_pru0_pru_r31_7	gpio3[21]
26	D16	UART1_RXD	uart1_rxd	mmc1_sdwp	dcan1_tx	I2C1_SDA		pr1_uart0_rxd	pr1_pru1_pru_r31_16	gpio0[14]
27	C13	GPIO3_19	mcasp0_fsr	eQEP0B_in	mcasp0_axr3	mcasp1_fsx	EMU2_mux2	pr1_pru0_pru_r30_5	pr1_pru0_pru_r31_5	gpio3[19]
28	C12	SPI1_CS0	mcasp0_ahclkr	ehrpwm0_synci	mcasp0_axr2	spi1_cs0	eCAP2_in_PWM2_out	pr1_pru0_pru_r30_3	pr1_pru0_pru_r31_3	gpio3[17]
29	B13	SPI1_D0	mcasp0_fsx	ehrpwm0B		spi1_d0	mmc1_sdcd_mux1	pr1_pru0_pru_r30_1	pr1_pru0_pru_r31_1	gpio3[15]
30	D12	SPI1_D1	mcasp0_axr0	ehrpwm0_tripzone		spi1_d1	mmc2_sdcd_mux1	pr1_pru0_pru_r30_2	pr1_pru0_pru_r31_2	gpio3[16]
31	A13	SPI1_SCLK	mcasp0_aclkx	ehrpwm0A		spi1_sclk	mmc0_sdcd_mux1	pr1_pru0_pru_r30_0	pr1_pru0_pru_r31_0	gpio3[14]
32						VADC				
33	C8					AIN4				
34						AGND				
35	A8					AIN6				
36	B8					AIN5				
37	B7					AIN2				
38	A7					AIN3				
39	B6					AIN0				
40	C7					AIN1				
41#	D14	CLKOUT2	xdma_event_intr1		tclkin	clkout2	timer7_mux1	pr1_pru0_pru_r31_16	EMU3_mux0	gpio0[20]
	D13	GPIO3_20	mcasp0_axr1	eQEP0_index		Mcasp1_axr0	emu3	pr1_pru0_pru_r30_6	pr1_pru0_pru_r31_6	gpio3[20]
42@	C18	GPIO0_7	eCAP0_in_PWM0_out	uart3_txd	spi1_cs1	pr1_ecap0_ecap_capin_apwm_o	spi1_sclk	mmc0_sdwp	xdma_event_intr2	gpio0[7]
	B12	GPIO3_18	Mcasp0_aclkr	eQEP0A_in	Mcaspo_axr2	Mcasp1_aclkx		pr1_pru0_pru_r30_4	pr1_pru0_pru_r31_4	gpio3[18]
43-46						GND				

VDM28

- Laser Class 2 → Do not stare into the beam
- 0.2 m to 15 m
- 660 nm wavelength
- 1 mrad beam divergence → <15 mm diameter spot at 15 m
- 10 ms response time; 250,000 Hz repetition rate, 5 ns pulse
- 30 VDC 100 mA max switching current
- Accuracy: ± 25 mm absolute; < 5 mm repeat
- 0/4 mA – 20 mA output

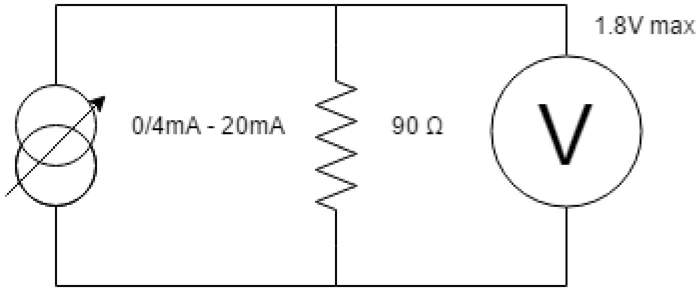

Resolution for a 12 Bit ADC
(15 m - 0.2 m) / 2^12 = 3.613 mm

OPS Encoder

- Quadrature output and index
- 163k cycles per revolution → 0.002209° resolution
- Maximum output frequency per channel: 5 MHz
- 30.67 revolutions per second maximum
- 5 V DC @ 120 mA

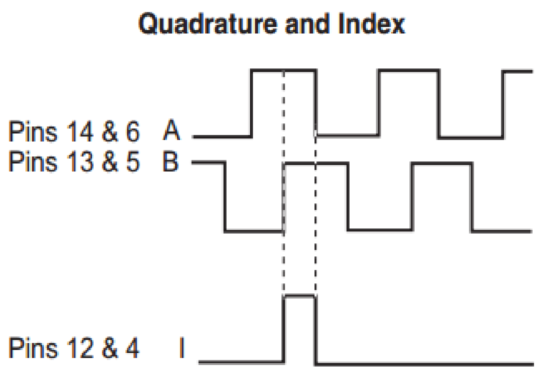

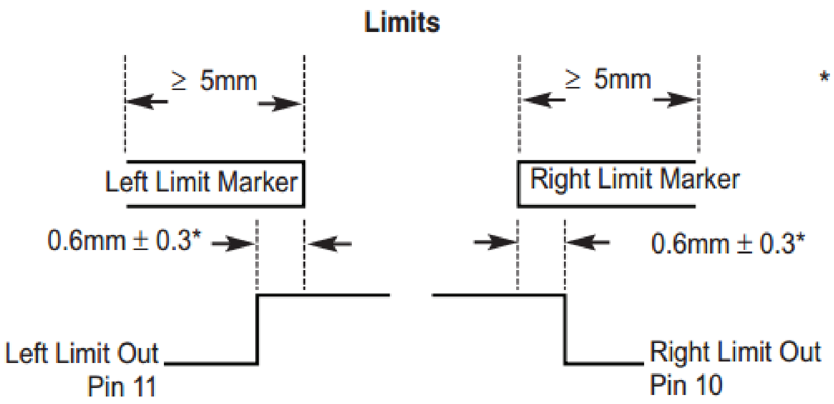

OPS Encoder Mounting Side

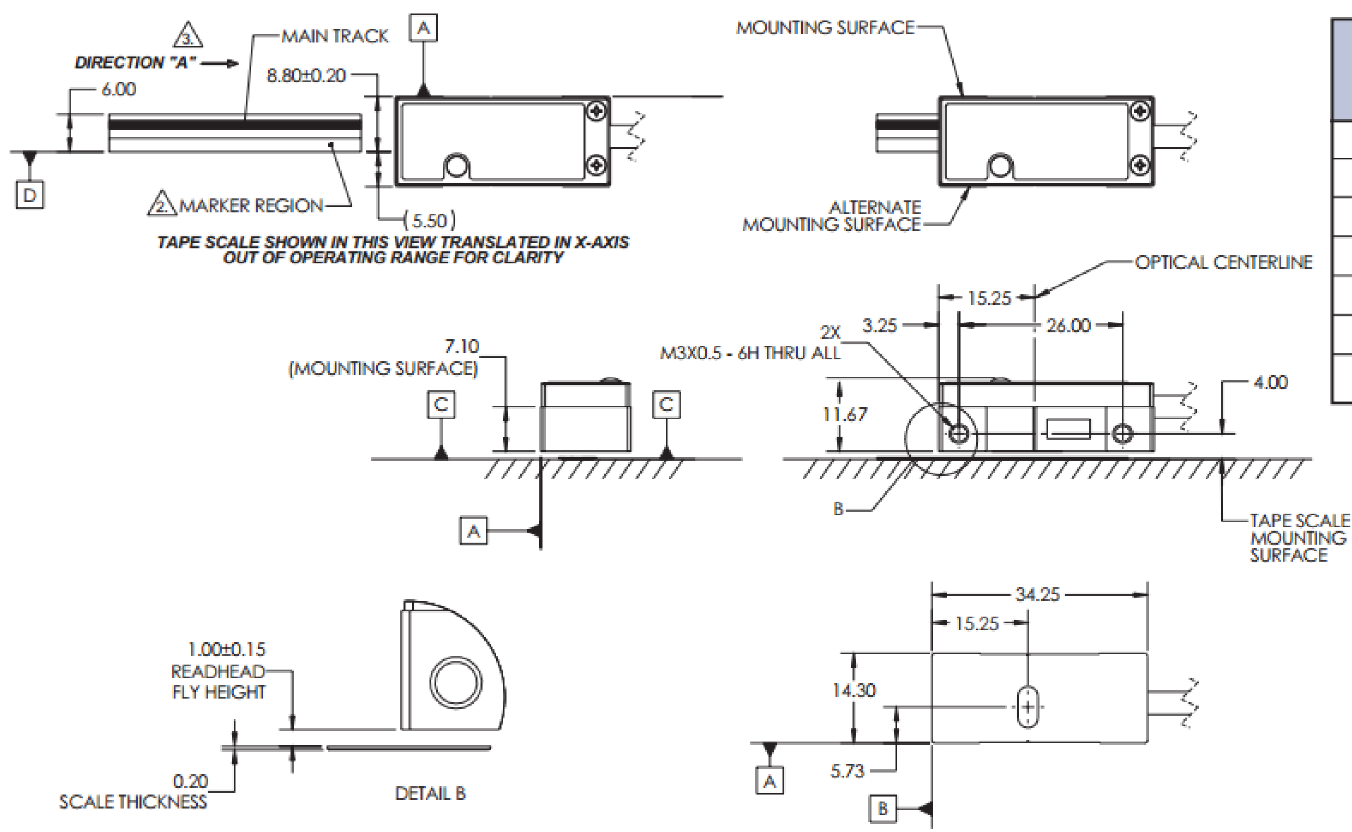

OPS Side Mount Configuration Sensor Alignment Tolerances	
Axis	**Alignment Tolerance**
X	Direction of Motion
Y	± 0.20mm
Z	± 0.15mm
θ_X	± 1.0°
θ_Y	± 1.0°
θ_Z	± 2.0°

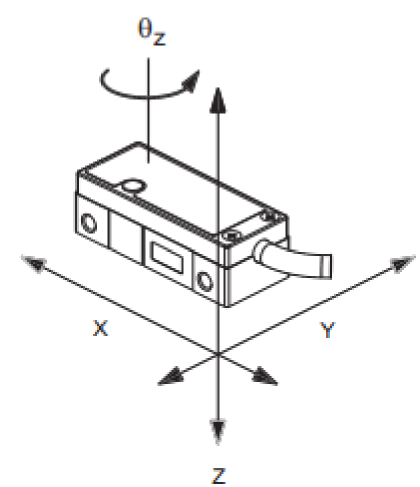

OPS Encoder Mounting Top

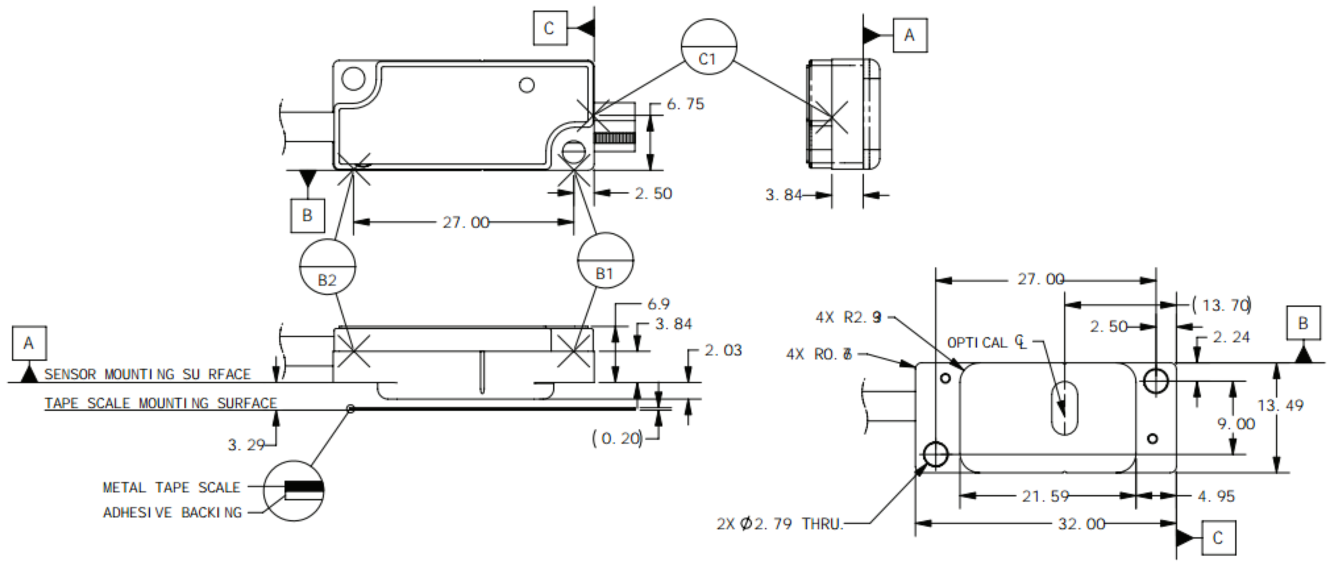

Wide Alignment Tolerances

OPS Top Mount Configuration Sensor Alignment Tolerances	
Axis	**Alignment Tolerance**
X	Direction of Motion
Y	± 0.20mm
Z	± 0.15mm
θ_X	± 1.0°
θ_Y	± 1.0°
θ_Z	± 2.0°

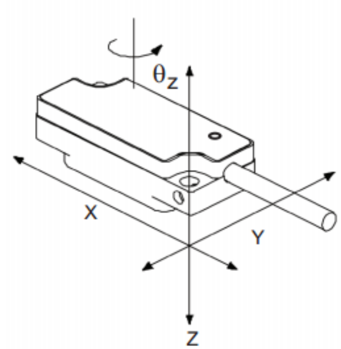

Sensor Size & Weight (top mount sensor)

Height	Width	Length
0.35[8.93mm]	0.53 [13.49mm]	1.26 [32.00mm]
Weight	6g (without cable)	

OPS Encoder Alignment

OPS Alignment Tool.

DPRALTE-020B080

- Communication: RS-485/232 / Modbus RTU
- Modes of Operation: Current, Hall Velocity, Position, Velocity
- 20-80 VDC 10 A, 20 A peak
- Command Sources: ±10 V Analog, 5 V Step and Direction, Encoder Following, Over the Network, Sequencing, Indexing, Jogging
- Max Encoder Frequency: 5 MHz pre-quad
- Position and Velocity Loop Sample Time: 100 µs
- Commutation: Sinusoidal, Trapezoidal

DZRALTE-012L080

- Communication: RS-485/232 / Modbus RTU
- Modes of Operation: Current, Hall Velocity, Position, Velocity
- 20-80 VDC 6 A, 12 A peak
- Command Sources: ±10 V Analog, 5 V Step and Direction, Encoder Following, Over the Network, PWM and Direction, Sequencing, Indexing, Jogging
- Max Encoder Frequency: 5 MHz pre-quad
- Position and Velocity Loop Sample Time: 100 μs
- Commutation: Sinusoidal, Trapezoidal

DZRALTE-020L080

- Communication: RS-485/232 / Modbus RTU
- Modes of Operation: Current, Hall Velocity, Position, Velocity
- 10-80 VDC 12 A, 20 A peak
- Command Sources: ±10 V Analog, 5 V Step and Direction, Encoder Following, Over the Network, PWM and Direction, Sequencing, Indexing, Jogging
- Max Encoder Frequency: 5 MHz pre-quad
- Position and Velocity Loop Sample Time: 100 μs
- Commutation: Sinusoidal, Trapezoidal

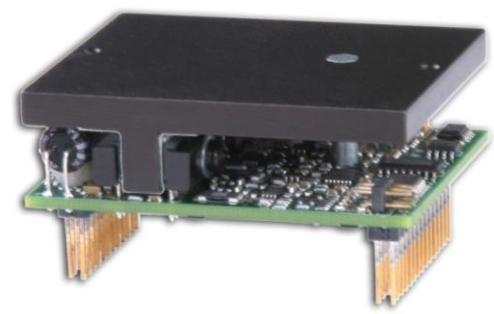

Communication Between Microcontroller and PC

- UART – 115200 bits / sec
- USB 2.0 – 480 Mbits / sec (high speed)
- Ethernet/IP – 10/100/1000 Mbits /sec

Controller-PC communication layer agnostic to protocol

Communication Packet Between PC and BeagleBone
4 to 65539 Bytes

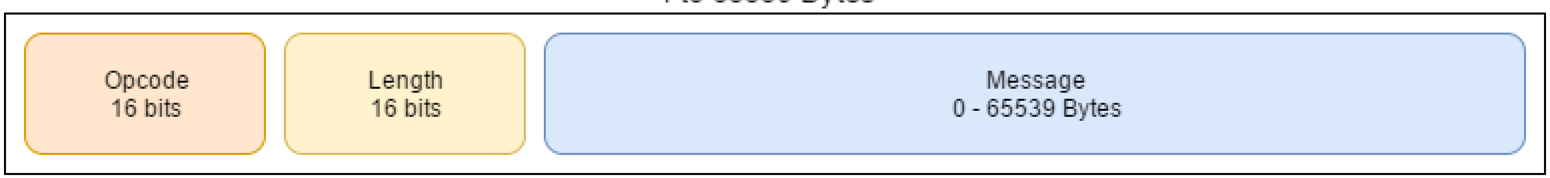

Sample Message Data

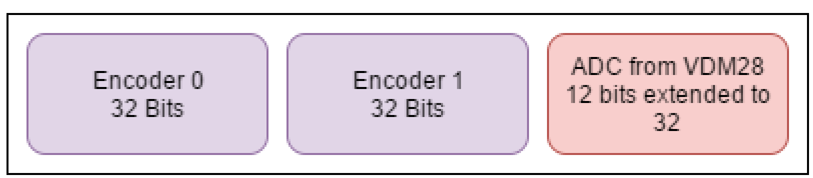

UART

- Will require an FTDI
- 115200 bits/s
- 8 data bits per packet
  1 start and 1 stop
- 11520 bytes/s

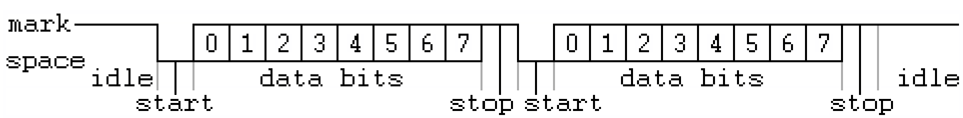

Ethernet data rate feasibility

IPv4

Max Ethernet packet 1518 bytes

68 bytes of UDP overhead (with IP and Ethernet frames)

1472 bytes left for data → 60 measurements per packet

1512 byte total packet size

100 Mb/s: 8127 frames/sec * 1512 bytes/frame =
12.288 Mbytes/s

1000 Mb/s: 81274 frames/sec * 1512 bytes/frame =
122.8 Mbytes/s

Ethernet UDP Overhead

Fast Ethernet (IEEE 802.3u) - UDP

Maximum Ethernet frames and data throughput rate calculations.

Fast Ethernet (IEEE 802.3u) Frame Structure with UDP Datagram

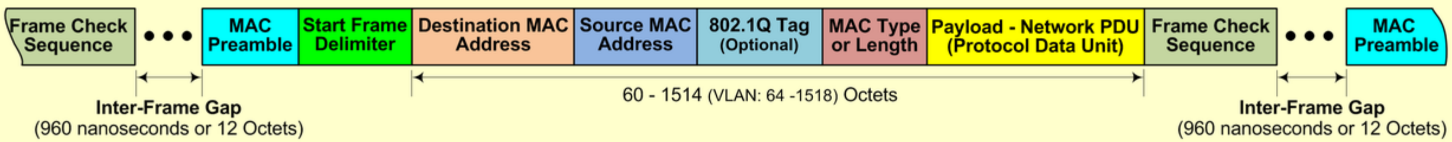

Fast Ethernet Frame Component Size With UDP Datagram

Frame Component		Component Size	
MAC Preamble		7 Octets of: **10101010**	
Start Frame Delimiter		1 Octet of: **10101011**	
Destination MAC Address		6 Octets	
Source MAC Address		6 Octets	
802.1Q VLAN TAG ID (Optional)		4 Octets (Optional)	
MAC Type or Length		2 Octets	
MTU (Maximum Transmission Unit) **Payload** Network PDU Protocol Data Unit:	Packet / Segment	**IP Header**	20 Octets
		UDP Header	8 Octets
		Data/Padding	18 - 1472 Octets
		Total:	**46 - 1500 Octets** (Max: 1504 – VLAN)
Frame Check Sequence (CRC)		4 Octets	
Inter-Frame Gap • • •		12 Octets (960 nanoseconds)	
Total Physical Frame Size:		**84 – 1538 Octets** (Max: 1544 -VLAN)	

Fast Ethernet Maximum Frame and Data Throughput Rate Calculation with UDP Datagram

Rate Term	Value
Fast Ethernet Bit Rate	100 Mbit/sec -or- 100Mb/sec
Fast Ethernet Bit Time	10 nanoseconds (.00000001 seconds)
1 Octet (Byte)	8 Bits
Max Octet Rate	(100Mb/sec)/((8 Bits) = **12,500,000 Octets/sec**
Max Frame Rate (84 Octet Frames) Min Packet (60 Bytes + 4 Bytes CRC)	(100Mb/sec)/((8 Bits)*(84 Octets/Frame)) = **148,810 Frames/sec (FPS)**
Max UDP Data Rate (84 Octet Frames) Min UDP Packet (60 Bytes + 4 Bytes CRC)	(148,810 Frames/sec)*(18 Bytes/Frame) = **2,678,571 Bytes/sec**
Max Frame Rate (1538 Octet Frames) Max Packet (1514 Bytes + 4 Bytes CRC)	(100Mb/sec)/((8 Bits)*(1538 Octets/Frame)) = **8,127 Frames/sec (FPS)**
Max UDP Data Rate (1538 Octet Frames) Max UDP Packet (1514 Bytes + 4 Bytes CRC)	(8,127 Frames/sec)*(1472 Bytes/Frame) = **11,963,589 Bytes/sec**
Max Fast Ethernet Frame Bandwidth Max Packet (60 Bytes + 4 Bytes CRC) Max Packet (60 Bytes)	(148,810 Frames/sec)*(64 Bytes/Frame) = **9,523,840 Bytes/sec** (9.082641 MiB/s) (148,810 Frames/sec)*(60 Bytes/Frame) = **8,928,600 Bytes/sec** (8.514977 MiB/s)
Max Fast Ethernet Frame Bandwidth Max Packet (1514 Bytes + 4 Bytes CRC) Max Packet (1514 Bytes)	(8,127 Frames/sec)*(1518 Bytes/Frame) = **12,336,786 Bytes/sec** (11.765276 MiB/s) (8,127 Frames/sec)*(1514 Bytes/Frame) = **12,304,278 Bytes/sec** (11.734274 MiB/s)

*** **Note 1:** Units – **M:** 1,000,000 **Mi:** 1,048,576

NST - 2011

Ethernet UDP Overhead

Gigabit Ethernet (IEEE 802.3ab) - UDP

Maximum Ethernet frames and data throughput rate calculations.

Gigabit Ethernet (IEEE 802.3ab) Frame Structure with UDP Datagram

Frame Check Sequence	• • •	MAC Preamble	Start Frame Delimiter	Destination MAC Address	Source MAC Address	802.1Q Tag (Optional)	MAC Type or Length	Payload - Network PDU (Protocol Data Unit)	Frame Check Sequence	• • •	MAC Preamble

Inter-Frame Gap (96 nanoseconds or 12 Octets)

60 - 1514 (VLAN: 64 -1518) Octets

Inter-Frame Gap (96 nanoseconds or 12 Octets)

Gigabit Ethernet Frame Component Size With UDP Datagram

Frame Component	Component Size	
MAC Preamble	7 Octets of: **10101010**	
Start Frame Delimiter	1 Octet of: **10101011**	
Destination MAC Address	6 Octets	
Source MAC Address	6 Octets	
802.1Q VLAN TAG ID (Optional)	4 Octets (Optional)	
MAC Type or Length	2 Octets	
MTU (Maximum Transmission Unit) — Packet	**IP Header**	20 Octets
Segment	**UDP Header**	8 Octets
Payload Network PDU Protocol Data Unit:	**Data/Padding**	18 - 1472 Octets
	*****Total:**	**46 - 1500 Octets** (Max: 1504 – VLAN)
Frame Check Sequence (CRC)	4 Octets	
Inter-Frame Gap • • •	12 Octets (96 nanoseconds)	
Total Physical Frame Size:	**84 – 1538 Octets** (Max: 1544 -VLAN)	

Gigabit Ethernet Maximum Frame and Data Throughput Rate Calculation with UDP Datagram

Rate Term	Value
Gigabit Ethernet Bit Rate	1000 Mbit/sec -or- 1000Mb/sec
Gigabit Ethernet Bit Time	1 nanosecond (.000000001 seconds)
1 Octet (Byte)	8 Bits
Max Octet Rate	(1000Mb/sec)/((8 Bits) = **125,000,000 Octets/sec**
Max Frame Rate (84 Octet Frames) Min Packet (60 Bytes + 4 Bytes CRC)	(1000Mb/sec)/((8 Bits)*(84 Octets/Frame)) = **1,488,095 Frames/sec (FPS)**
Max UDP Data Rate (84 Octet Frames) Min UDP Packet (60 Bytes + 4 Bytes CRC)	(1,488,095 Frames/sec)*(18 Bytes/Frame) = **26,785,714 Bytes/sec**
Max Frame Rate (1538 Octet Frames) Max Packet (1514 Bytes + 4 Bytes CRC)	(1000Mb/sec)/((8 Bits)*(1538 Octets/Frame)) = **81,274 Frames/sec (FPS)**
Max UDP Data Rate (1538 Octet Frames) Max UDP Packet (1514 Bytes + 4 Bytes CRC)	(81,274 Frames/sec)*(1472 Bytes/Frame) = **119,635,891 Bytes/sec**
Max Gigabit Ethernet Frame Bandwidth Max Packet (60 Bytes + 4 Bytes CRC)	(1,488,095 Frames/sec)*(64 Bytes/Frame) = **95,238,080 Bytes/sec** (90.876031 MiB/s)
Max Packet (60 Bytes)	(1,488,095 Frames/sec)*(60 Bytes/Frame) = **89,285,700 Bytes/sec** (85.149477 MiB/s)
Max Gigabit Ethernet Frame Bandwidth Max Packet (1514 Bytes + 4 Bytes CRC)	(81,274 Frames/sec)*(1518 Bytes/Frame) = **123,373,932 Bytes/sec** (117.658550 MiB/s)
Max Packet (1514 Bytes)	(81,274 Frames/sec)*(1514 Bytes/Frame) = **123,048,836 Bytes/sec** (117.348515 MiB/s)

*** **Note 1:** IEEE 802.3ab – Gigabit Ethernet over copper twisted-pair cabling.
*** **Note 2:** Gigabit Ethernet allows for larger MTUs (Jumbo or Super Jumbo Frames).
*** **Note 3:** Units – **M:** 1,000,000 **Mi:** 1,048,576

NST - 2011

USB Data Rate Feasibility

- **Universal Serial Bus Specification Revision 2.0**

Table 5-10. High-speed Bulk Transaction Limits

Protocol Overhead (55 bytes)		(3x4 SYNC bytes, 3 PID bytes, 2 EP/ADDR+CRC bytes, 2 CRC16, and a 3x(1+11) byte interpacket delay (EOP, etc.))				
	Data Payload	Max Bandwidth (bytes/second)	Microframe Bandwidth per Transfer	Max Transfers	Bytes Remaining	Bytes/ Microframe Useful Data
	1	1064000	1%	133	52	133
	2	2096000	1%	131	33	262
	4	4064000	1%	127	7	508
	8	7616000	1%	119	3	952
	16	13440000	1%	105	45	1680
	32	22016000	1%	86	18	2752
	64	32256000	2%	63	3	4032
	128	40960000	2%	40	180	5120
	256	49152000	4%	24	36	6144
	512	53248000	8%	13	129	6656
Max		60000000				7500

21 measurements for the maximum data payload produces a 508-byte data payload

Speeds should be over 50 million bytes a second

USB 2.0

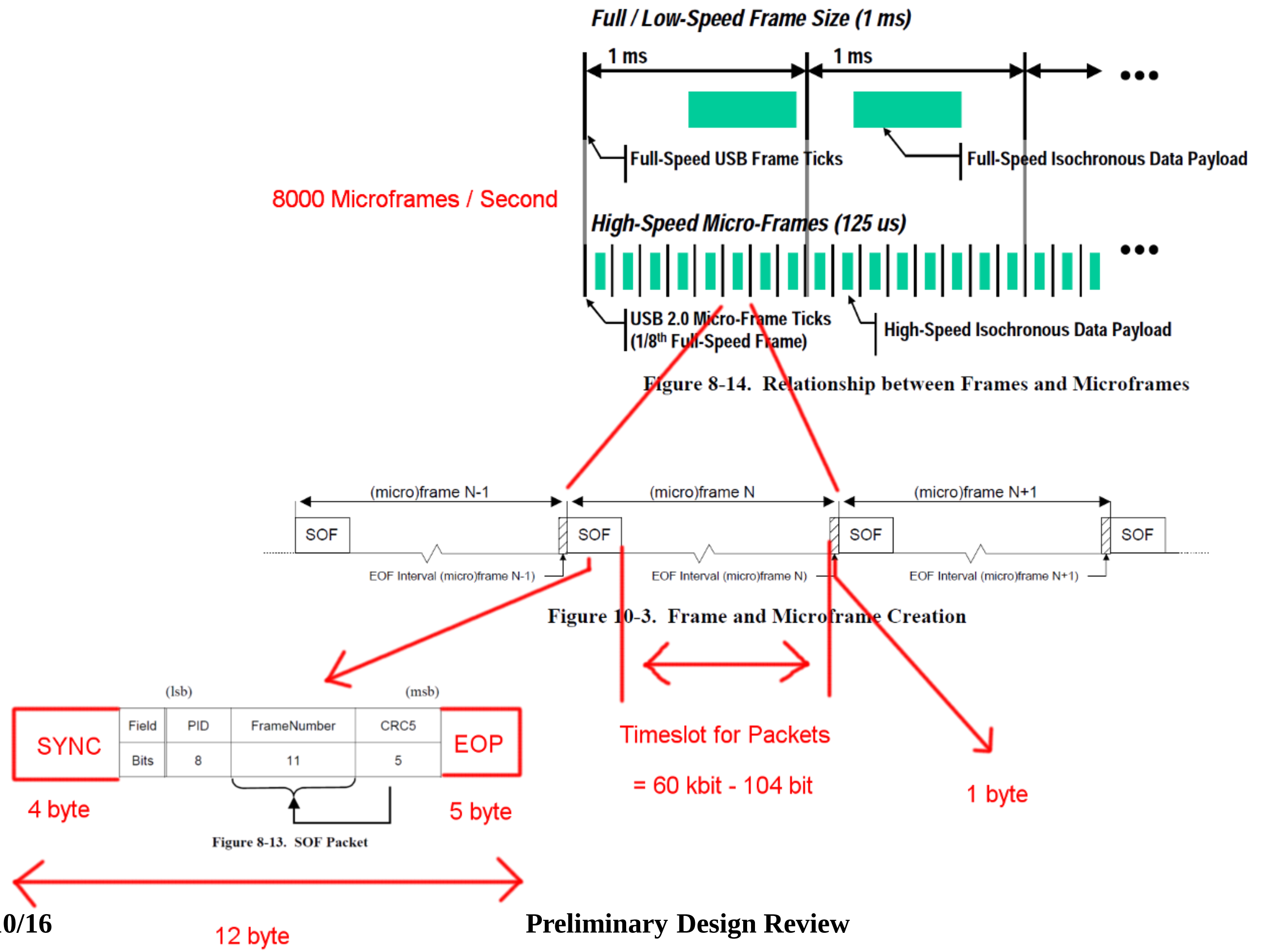

Figure 8-14. Relationship between Frames and Microframes

Figure 10-3. Frame and Microframe Creation

Figure 8-13. SOF Packet

USB 2.0

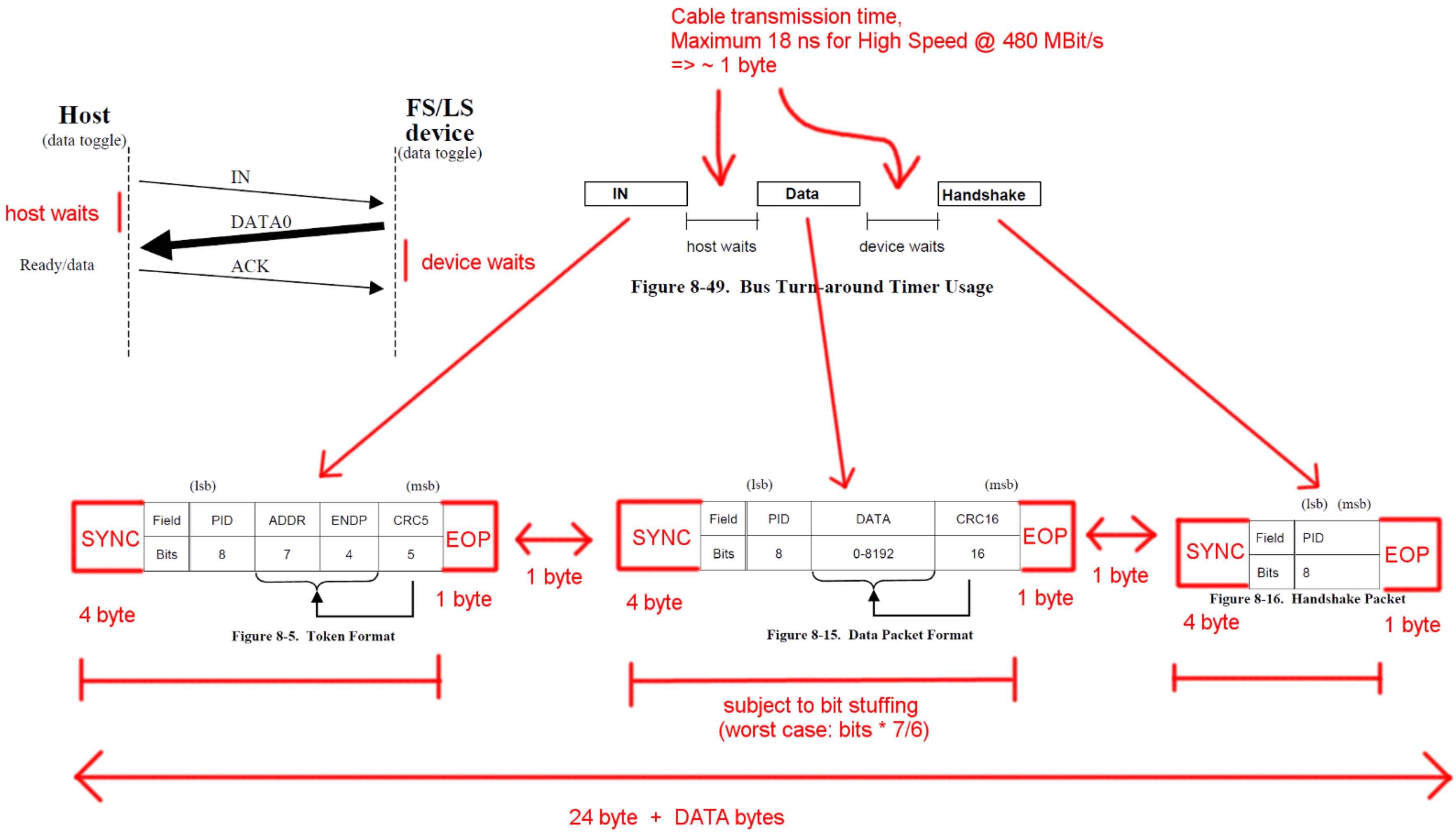

Figure 8-49. Bus Turn-around Timer Usage

Figure 8-5. Token Format

Figure 8-15. Data Packet Format

Figure 8-16. Handshake Packet

Drawings

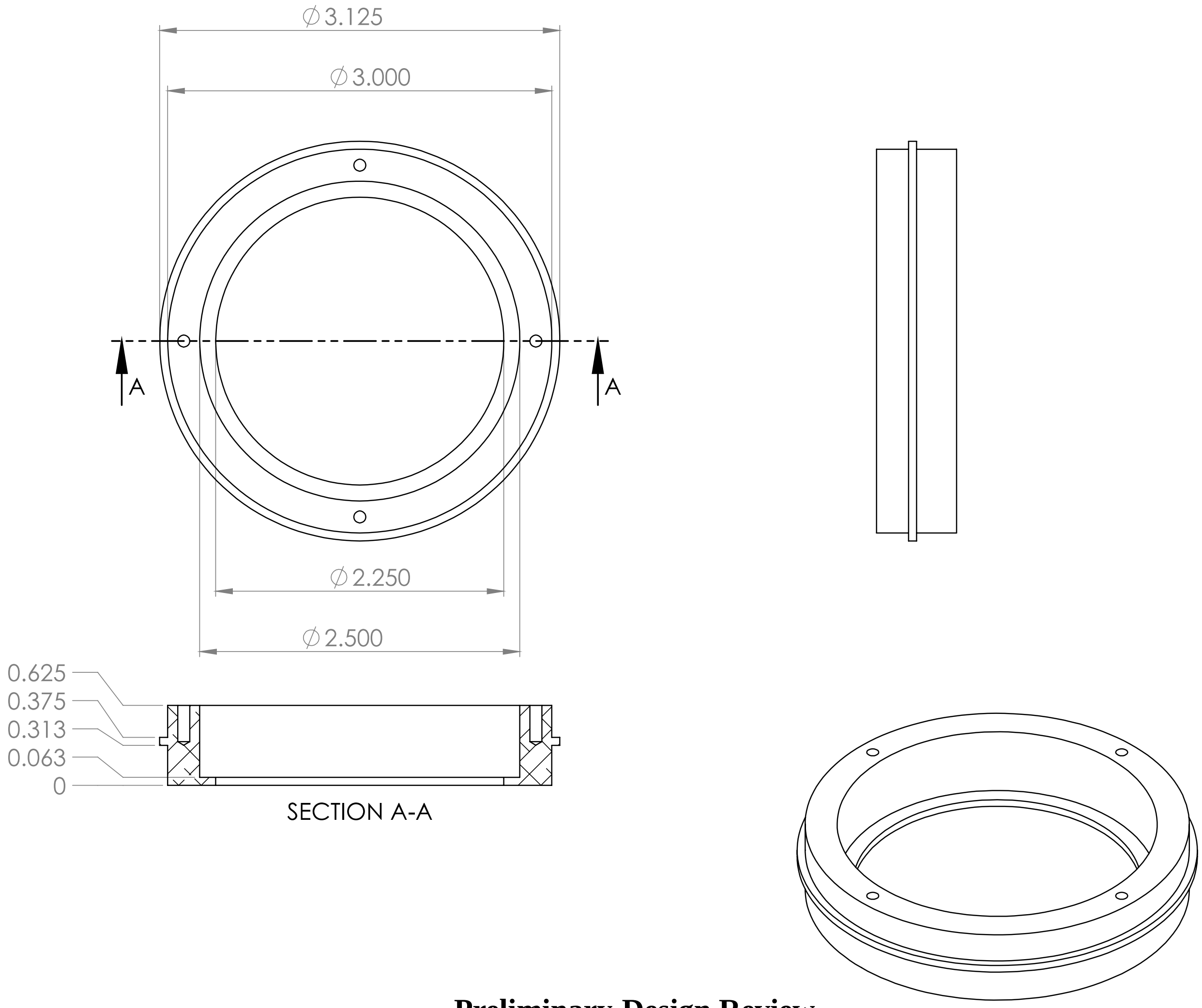

Drawings

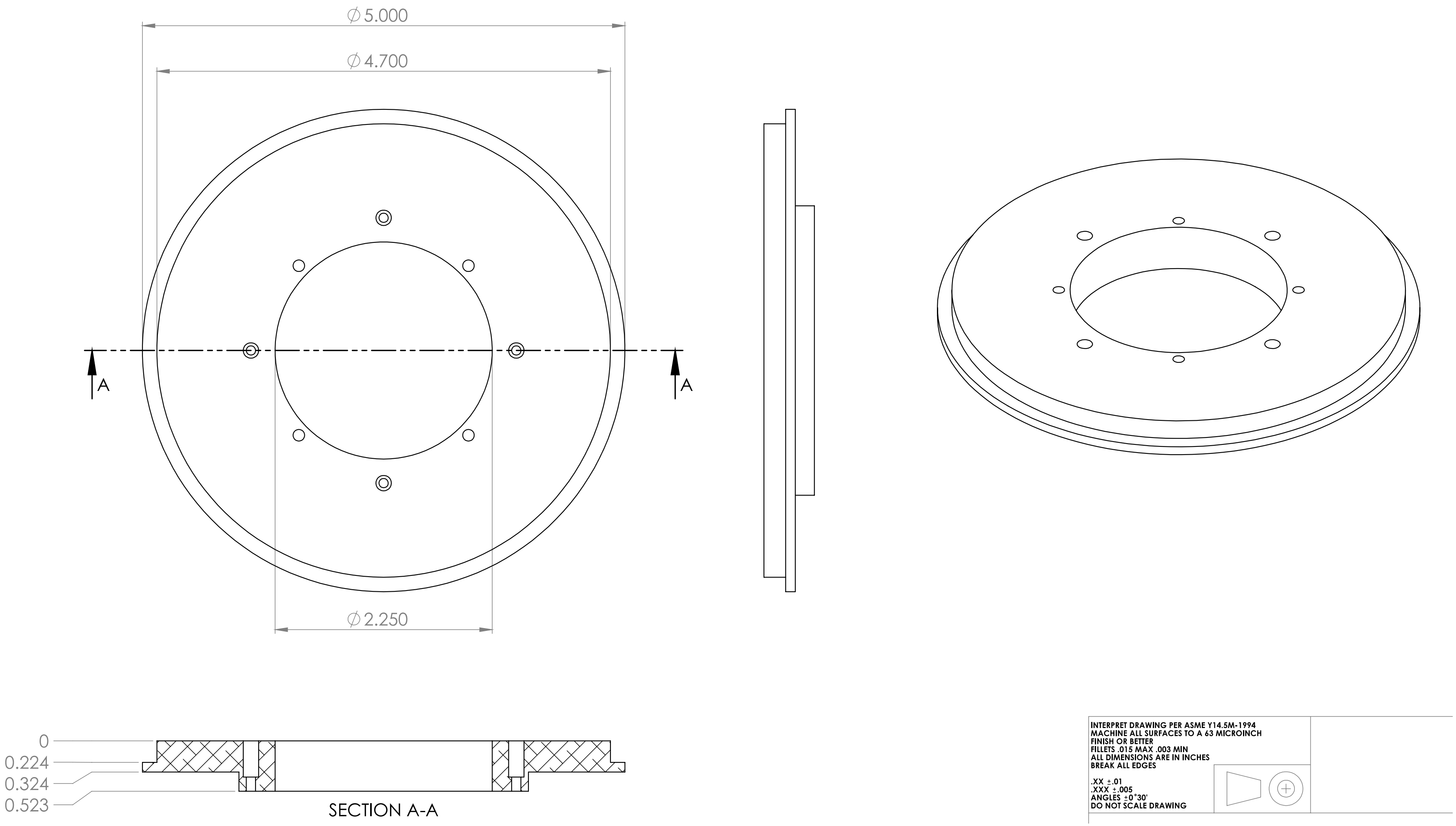

∅5.000
∅4.700
A
A
∅2.250
0
0.224
0.324
0.523
SECTION A-A
INTERPRET DRAWING PER ASME Y14.5M-1994
MACHINE ALL SURFACES TO A 63 MICROINCH
FINISH OR BETTER
FILLETS .015 MAX .003 MIN
ALL DIMENSIONS ARE IN INCHES
BREAK ALL EDGES
.XX ±.01
.XXX ±.005
ANGLES ±0°30'
DO NOT SCALE DRAWING

Drawings

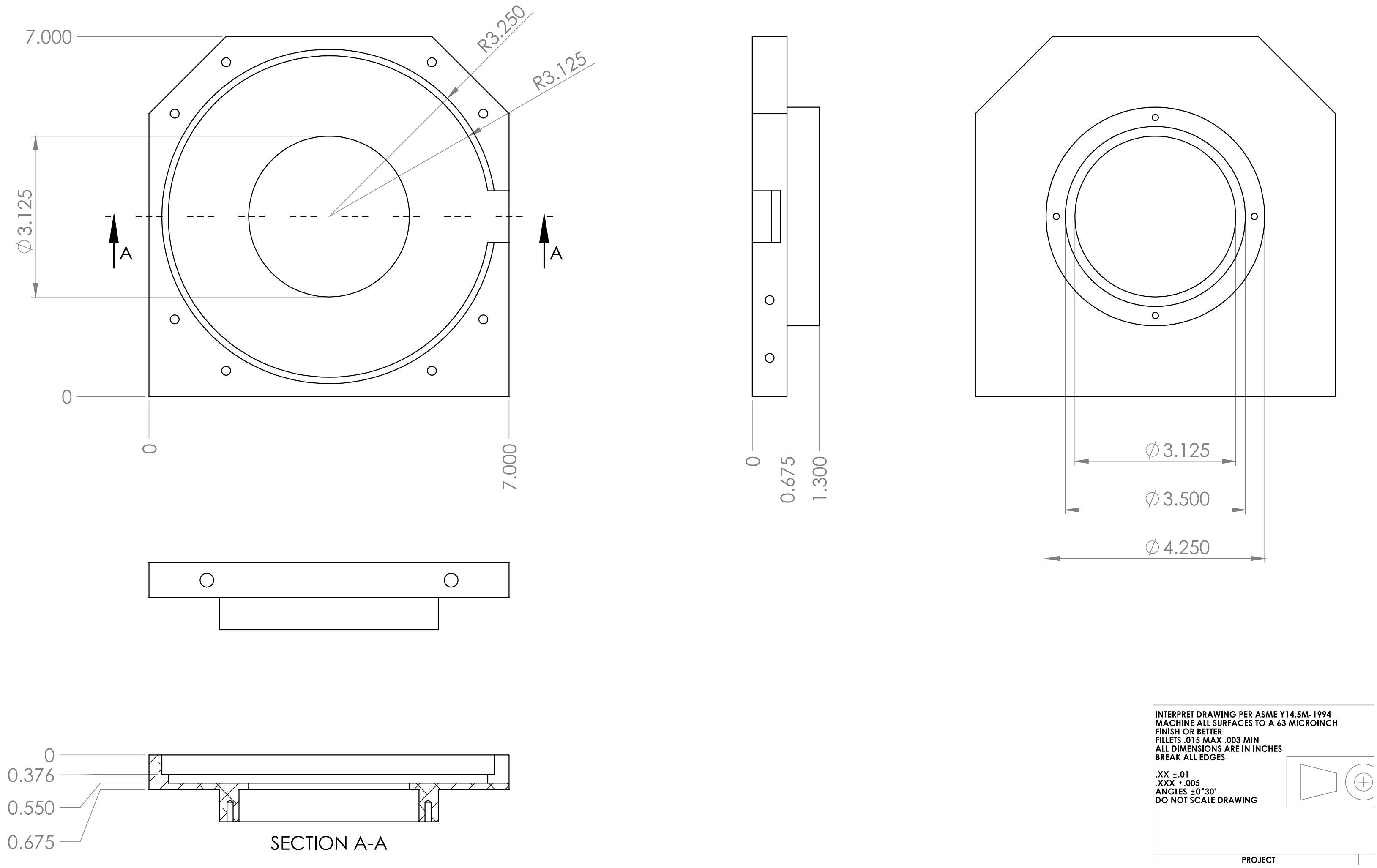

7.000
R3.250
R3.125
∅3.125
A
A
0
0
7.000
0
0.675
1.300
∅3.125
∅3.500
∅4.250
0
0.376
0.550
0.675
SECTION A-A
INTERPRET DRAWING PER ASME Y14.5M-1994
MACHINE ALL SURFACES TO A 63 MICROINCH
FINISH OR BETTER
FILLETS .015 MAX .003 MIN
ALL DIMENSIONS ARE IN INCHES
BREAK ALL EDGES
.XX ±.01
.XXX ±.005
ANGLES ±0°30'
DO NOT SCALE DRAWING
PROJECT

Drawings

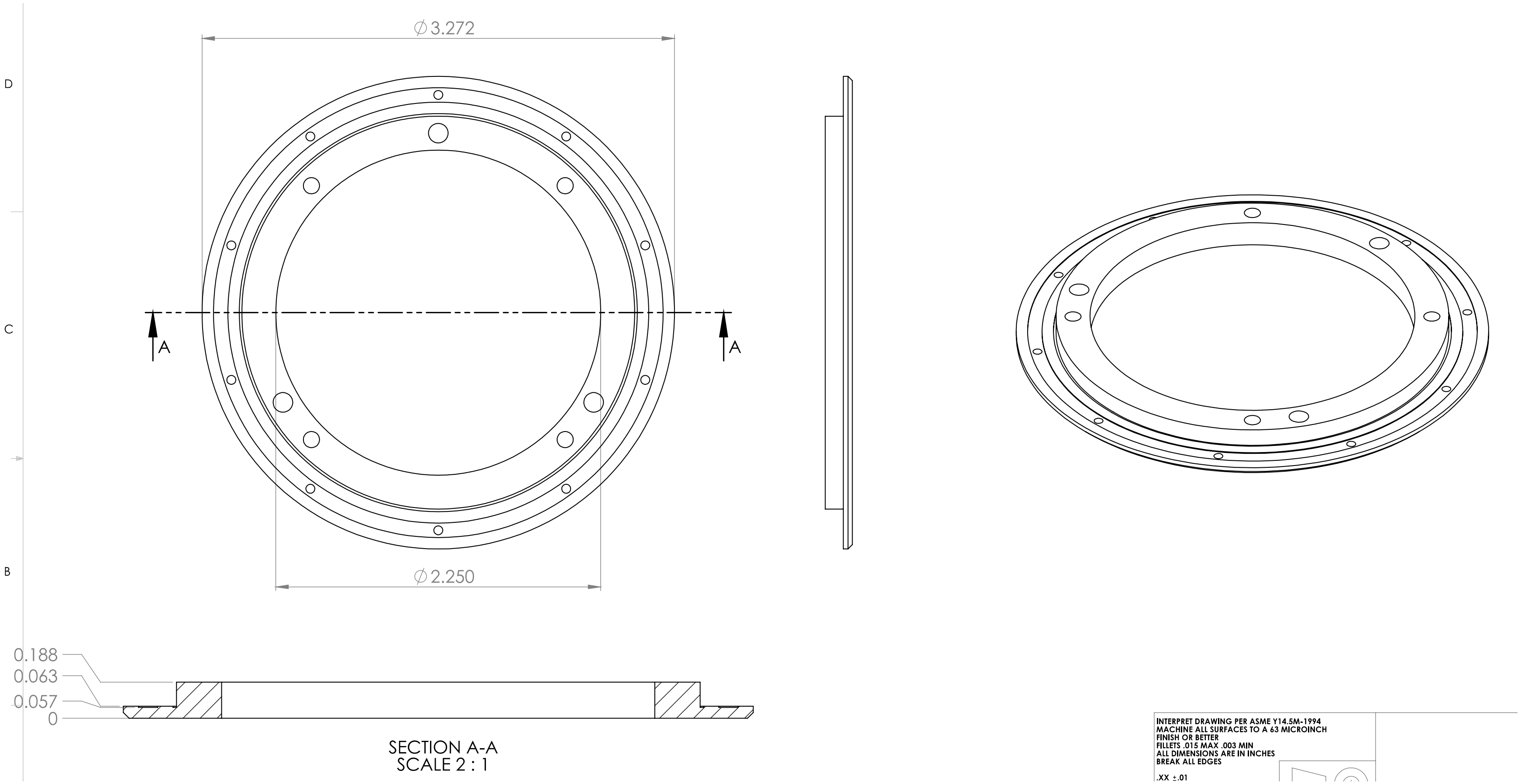

D
C
B
⌀3.272
A
A
⌀2.250
0.188
0.063
0.057
0
SECTION A-A
SCALE 2 : 1
INTERPRET DRAWING PER ASME Y14.5M-1994
MACHINE ALL SURFACES TO A 63 MICROINCH
FINISH OR BETTER
FILLETS .015 MAX .003 MIN
ALL DIMENSIONS ARE IN INCHES
BREAK ALL EDGES
.XX ±.01

Helical Gears

<u>Pros</u>

- Less noise at high speeds than more traditional spur gears
- Cheap to manufacture
- High machine efficiency

<u>Cons</u>

- Higher noise than other motor types
- Large gears necessary for use with prisms
- Backlash hinders change of torque direction
- Limited in terms of size
- Requires low torque conversions

Belt & Pulley Motors

Pros

- Shafts do not need to be axially aligned
- Damps noise and vibration
- High tolerance for misalignment

Cons

- Higher speeds reduce belt lifespan
- Slip and stretch reduces control capability for prisms
- Continuous adjustments needed to account for belt wear and stretch
- Performance decreases with closely spaced shafts

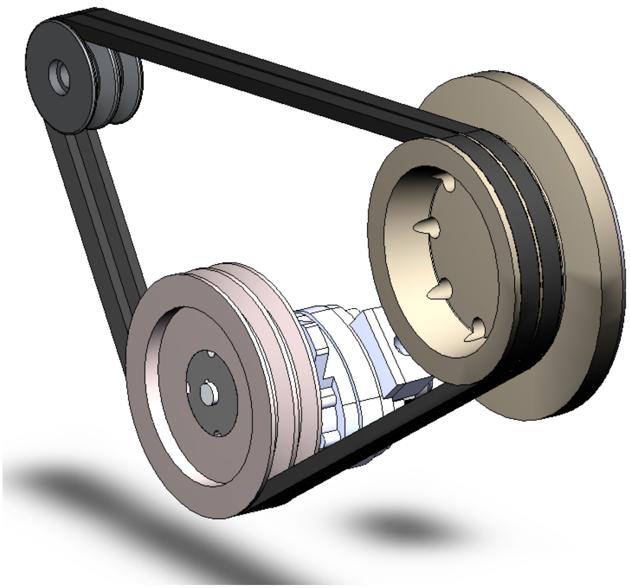

Rotational Concept

<u>Direct drive with brushless DC motors</u>

Advantages over other rotational concepts

- Hollow Core for optical path
- Fast and precise positioning or rate control
- No backlash, hysteresis, or elasticity
- Can be operated at both low (1 rpm or less), and high (up to 50000 rpm)
- Simple two-part design

Stator

Rotor

Angular Position Measurement

Rotary Glass Scale Encoder

- Size: 1.26 x 0.53 x 0.35 inches
- Accuracy: +/- 3.9 arc-sec
- Max Speed: 1600 rpm
- Output: Standard A quad B with index
- 163k CPR

Optical over magnetic provides required accuracy

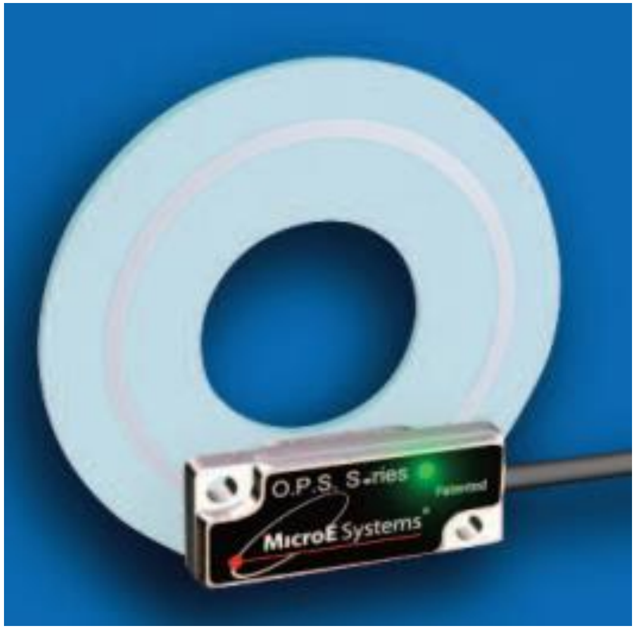

Motor Driving

<u>Two COTS Digital Servo Drives</u>

Drive motors based on position control

Accept angular position data from
rotary encoders

Support “electrical gearing” to control the
phase of the prisms

Digital Servo Driver With
Mounting Card

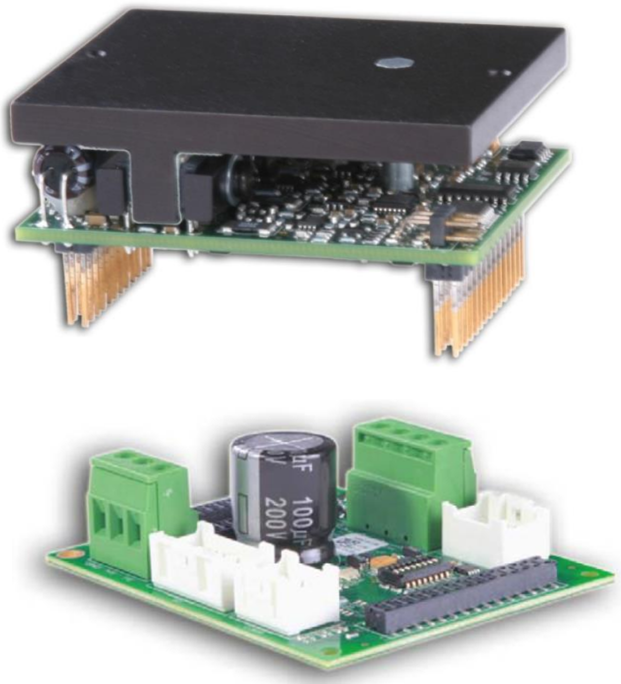

SENSITIVITY ANALYSIS (BACKUP)

Prism Axial Rotation

Ground scan distribution due to rotary encoder errors

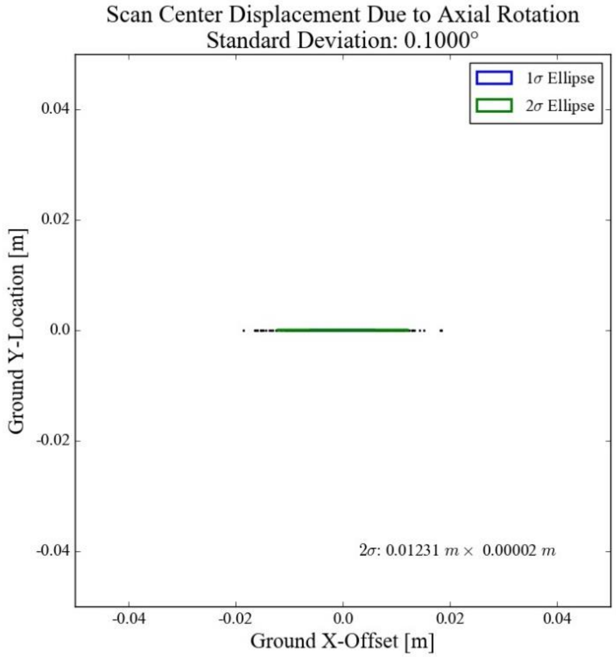

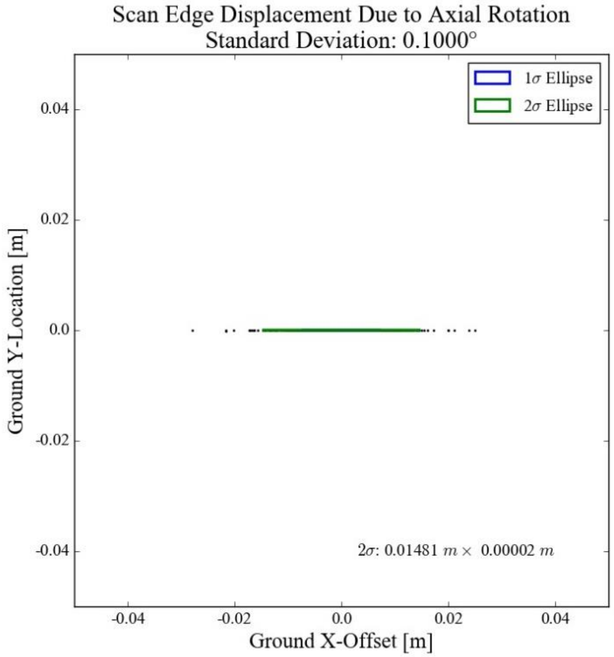

Prism Face Parallelism

Ground scan distribution due to prism mounting rotation and wedge angle

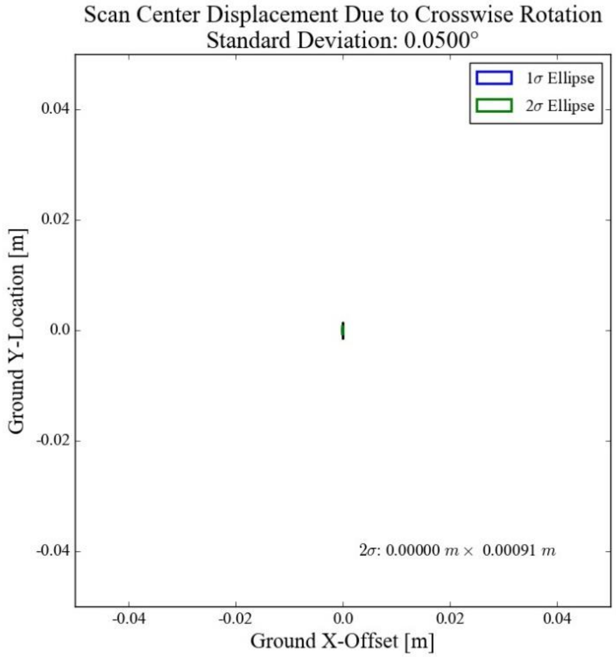

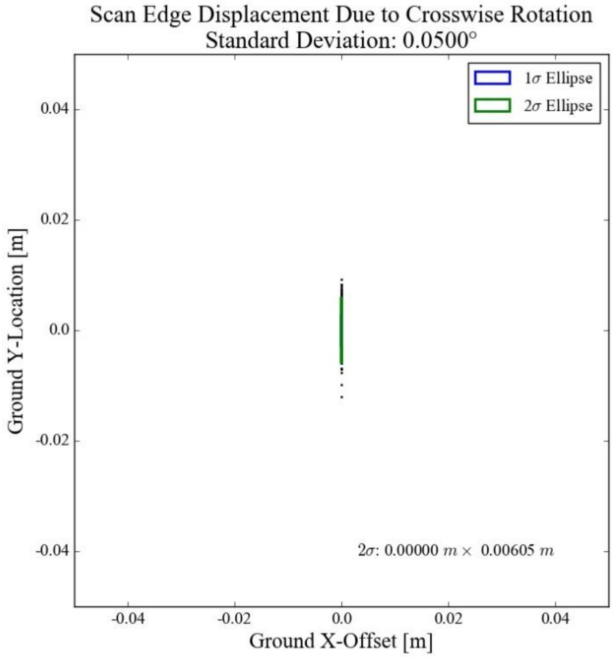

Two-Axis Prism Rotation

Ground scan distribution due to combined axial and crosswise rotations

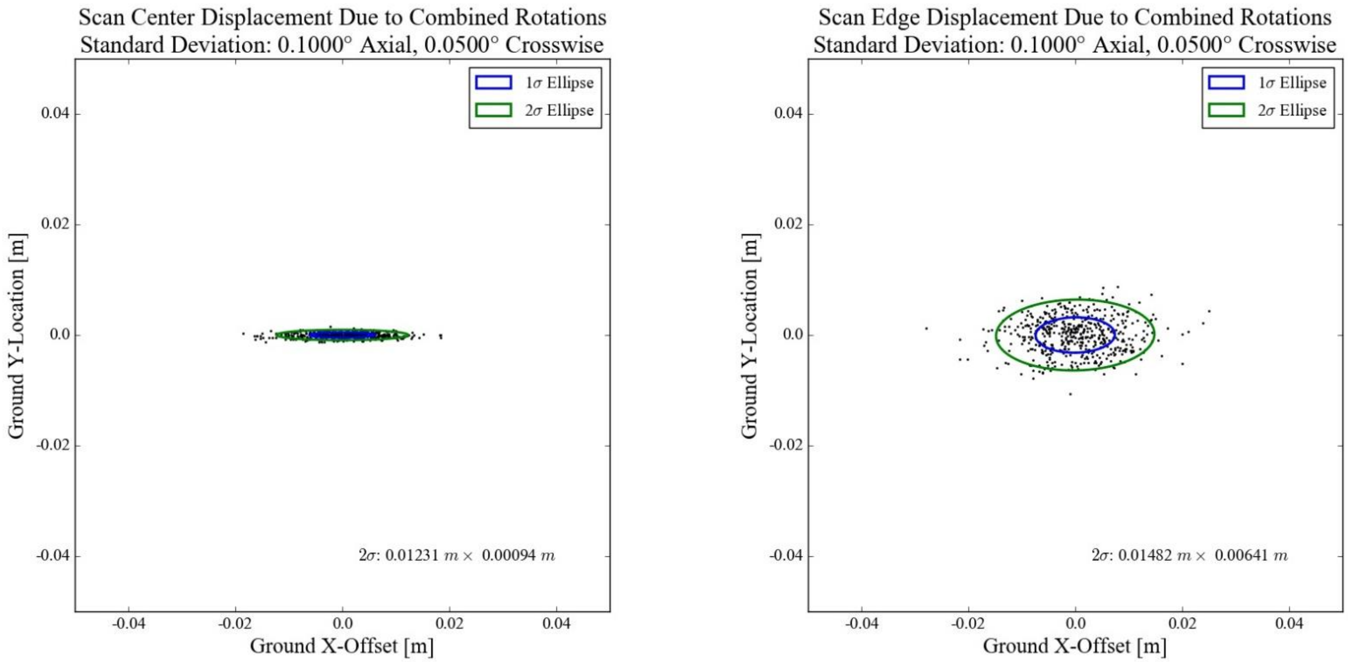

Axial (X) Prism Placement

Ground scan distribution due to prism placement along the beam axis

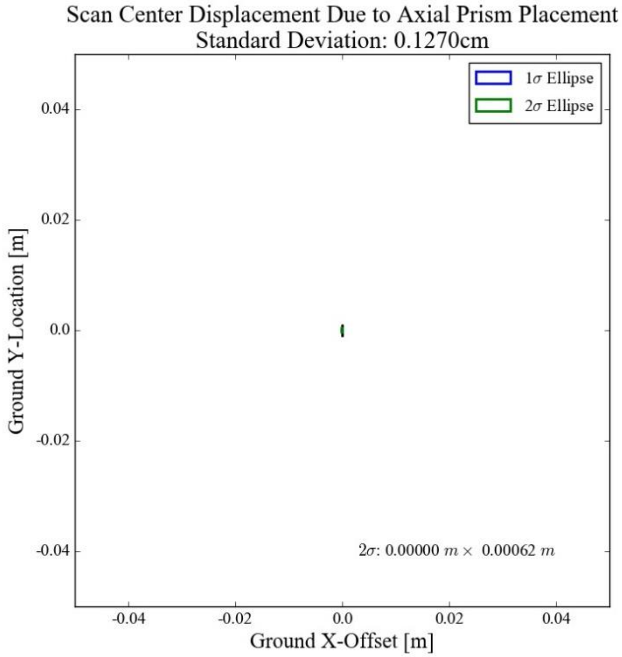

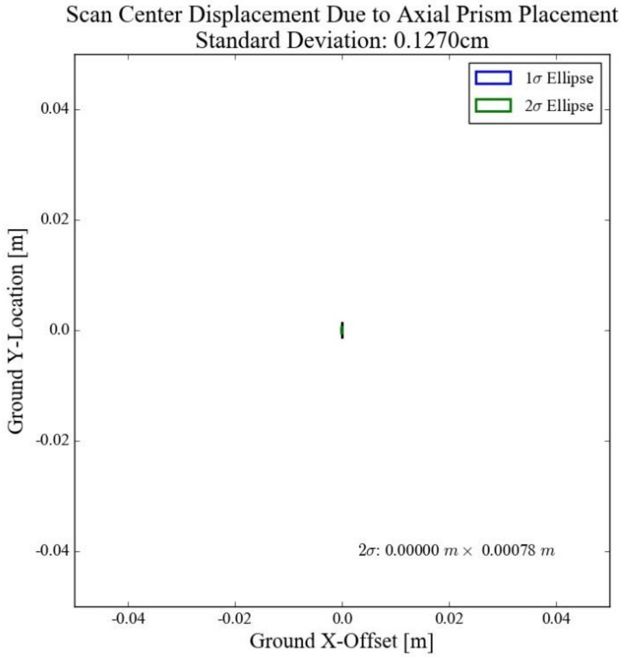

Y-Z Plane Prism Placement

Ground scan distribution due to prism placement on the plane normal to the beam

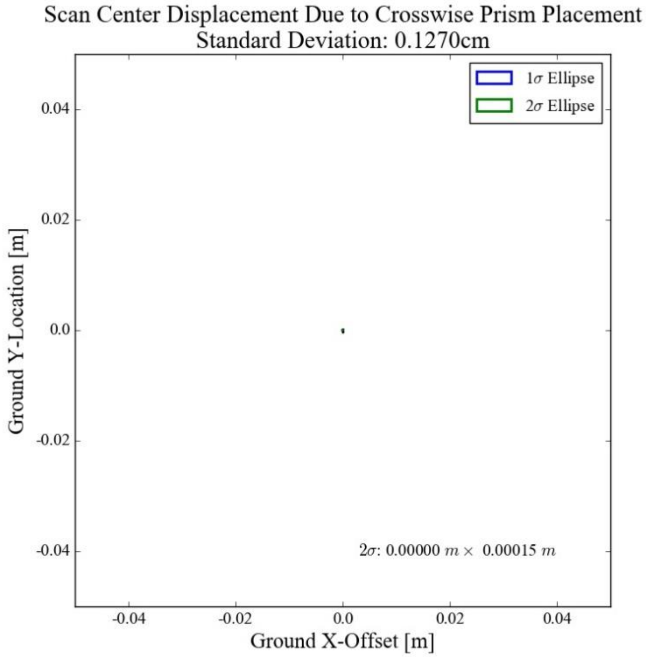

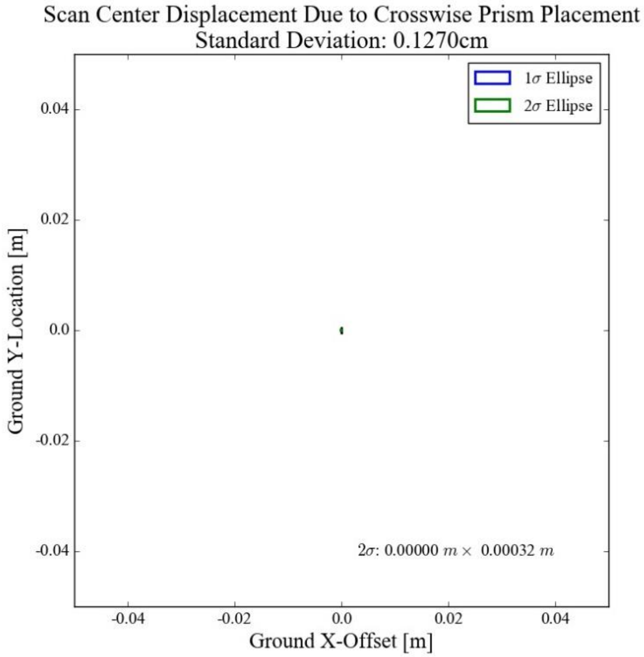

Transmitter 3D Placement

Ground scan distribution due to prism placement on the plane normal to the beam

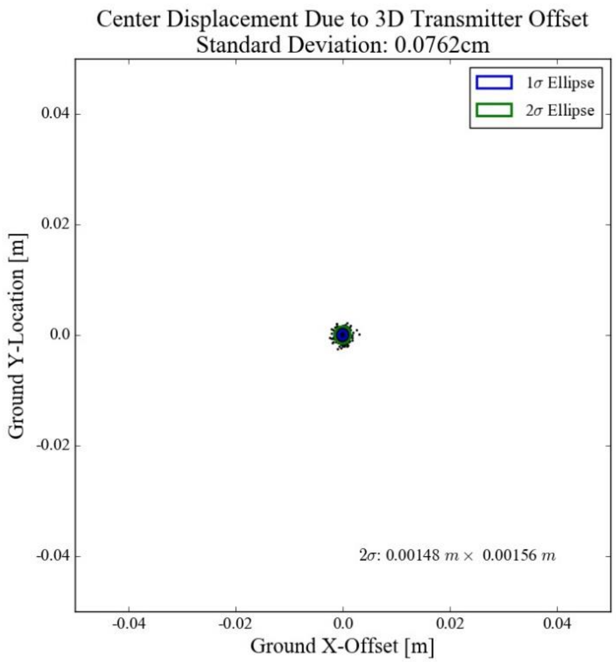

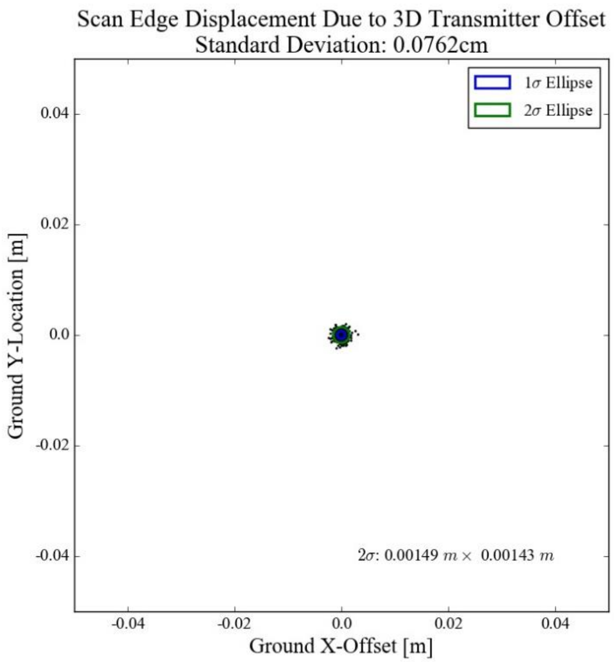

Beam Divergence

Spot size of laser beam on ground plane

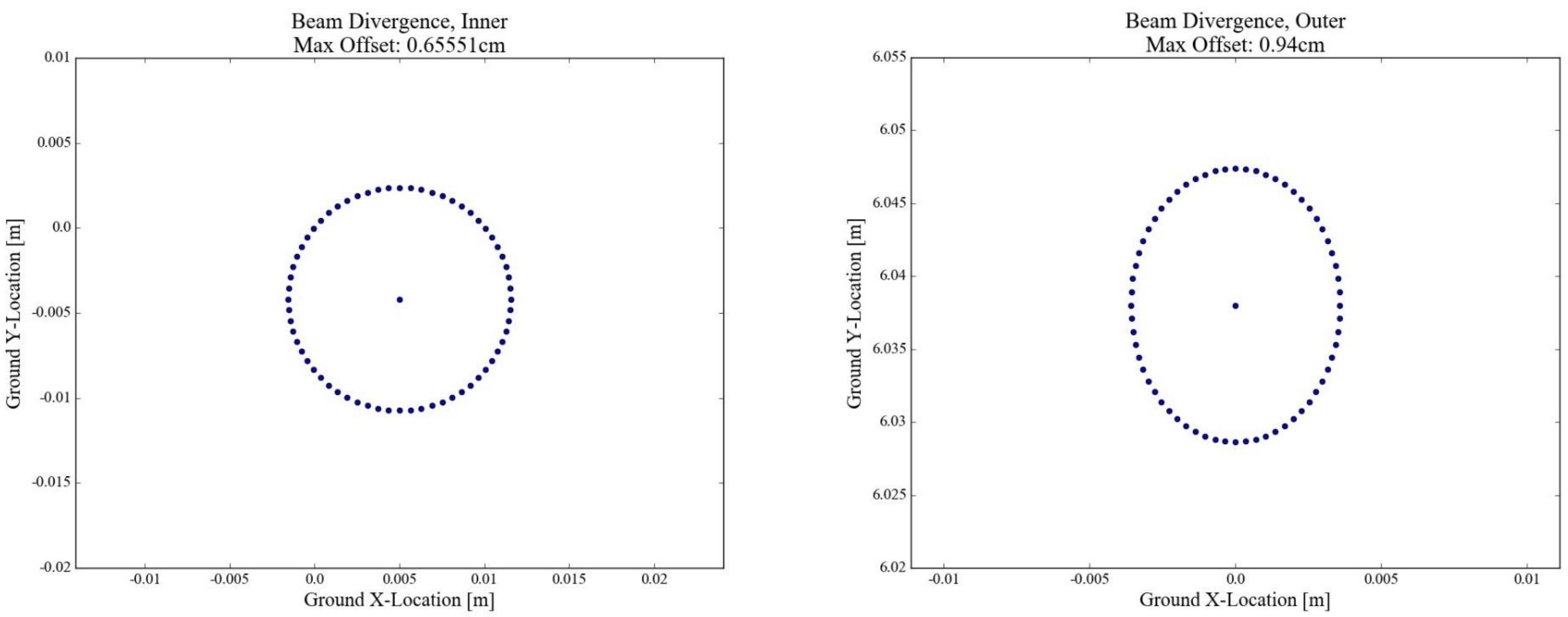

Sources of Error: Derivation

Sources of Error

Expected Final Uncertainty

Must be Calibrated
System Inherent

Lidar:

- Translational deviations — +/- 0.030 inch (ALL directions)
  - Tolerance stack-up between lidar stand, main baseplate, and lidar fastening method (0.005 inch assumed for all machine cut faces, 0.020 inch assumed for fastening slop)
- Rotational deviations — +/- 0.05°
  - Error that must be achieved to meet required projected error based on Monte Carlo results. A test must be developed that can calibrate this error
- Beam divergence — 0.06°

Sources of Error

Prisms:

Acceptable / Easily Mitigated
Must be Calibrated

Expected Final Uncertainty

- Uncertainty in wedge angle +/- 0.008°

  Manufacturer specification: error is acceptable, and we would have no hope of measuring the wedge angle without auxiliary optical equipment

- Uncertainty in index of refraction +/- 0.0002

  This uncertainty can be bounded by the expected error of the index of refraction of air

  The prism material is less susceptible to temperature gradients or deviations from isotropicity than air

Sources of Error

Prisms:

Expected Final Uncertainty

Acceptable / Easily Mitigated
Must be Calibrated

– Uncertainty in angular position +/- 0.1°

This error stems directly from error in encoder measurement (0.001°), and error in the orientation of the prism relative to its defined reference on the encoder glass scale

– Deviation from parallelism +/- 0.05°

These deviations will result from seating tolerances during integration

Accurate seating methods and calibration must bring this error source to within 0.05°

Sources of Error

Prisms:

Expected Final Uncertainty

Acceptable / Easily Mitigated
Must be Calibrated

- Translational deviations
  - X: +/- 0.050 inch Y: +/- 0.025 inch Z: +/- 0.025 inch
  - X: axial tolerance stack-up in rotational components (0.005 inch for all faces)
  - Y: concentricity tolerance tolerance stack-up
  - Z: concentricity tolerance and main housing outer dimension tolerance stack-up

Error Mitigation Methods

Lidar

Translational and rotational deviations can be calibrated using optical testing

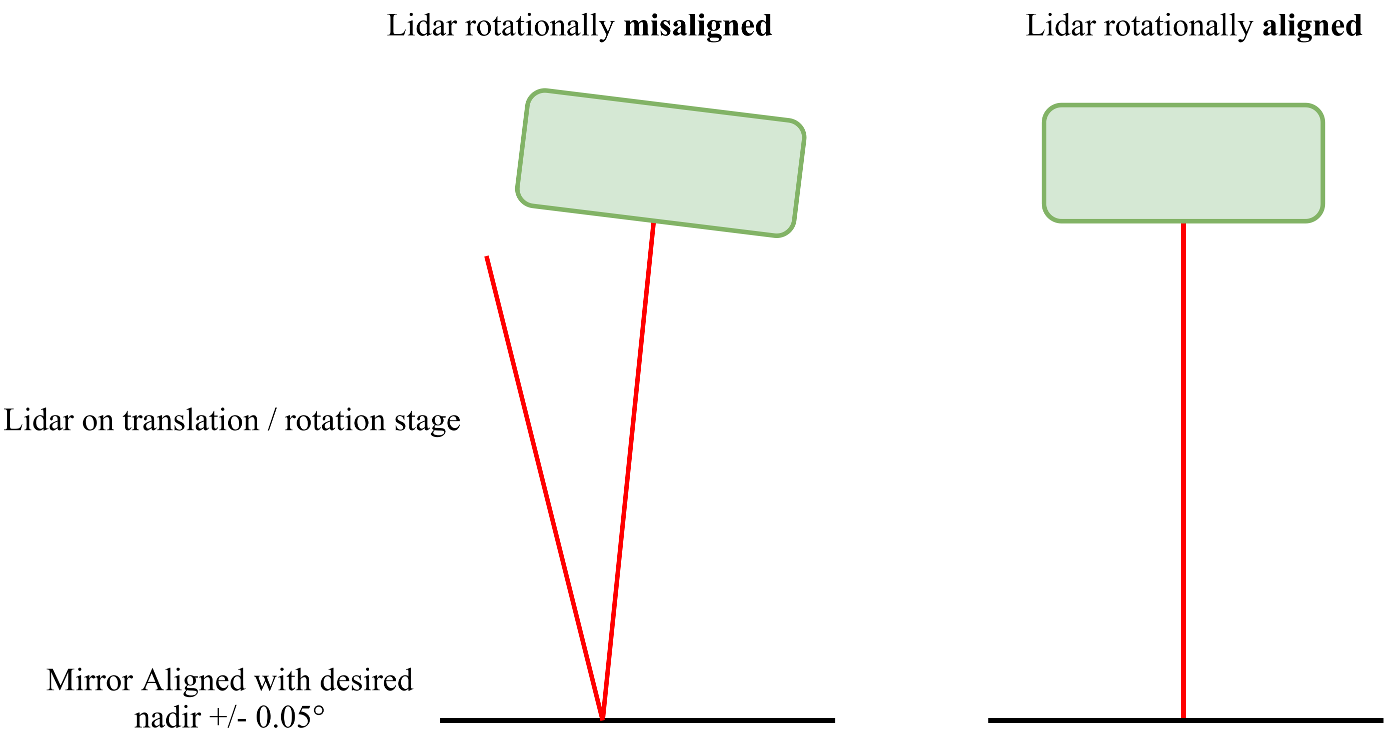

Error Mitigation Methods

Lidar

Translational and rotational deviations can be calibrated using optical testing

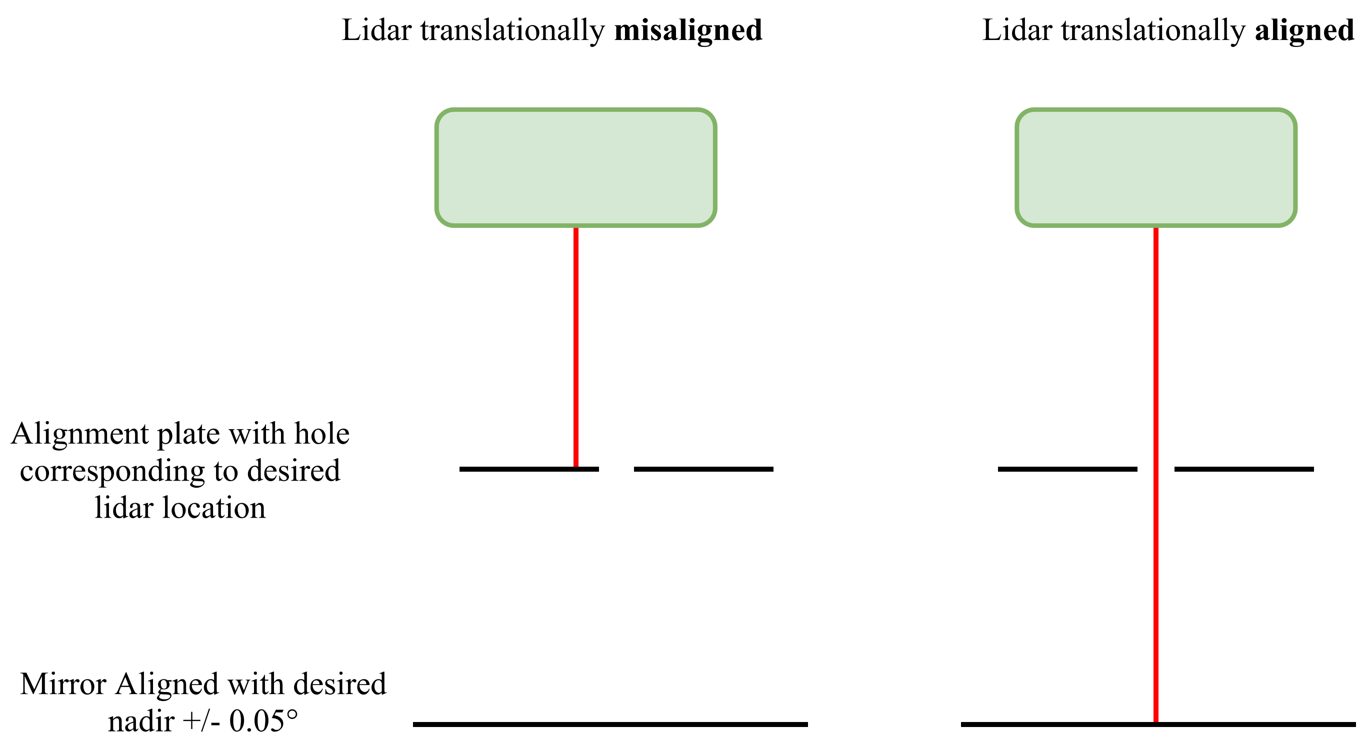

Error Mitigation Methods

Prisms Parallelism Deviations

Translational deviations can be accounted for by increasing prism size

Deviations in parallelism will be reduced using seating methods that are improved from standard fastening methods

Remaining deviations will require mechanical adjustment mechanisms (yet to be designed) to align the prisms within requirement

Relevant Frames

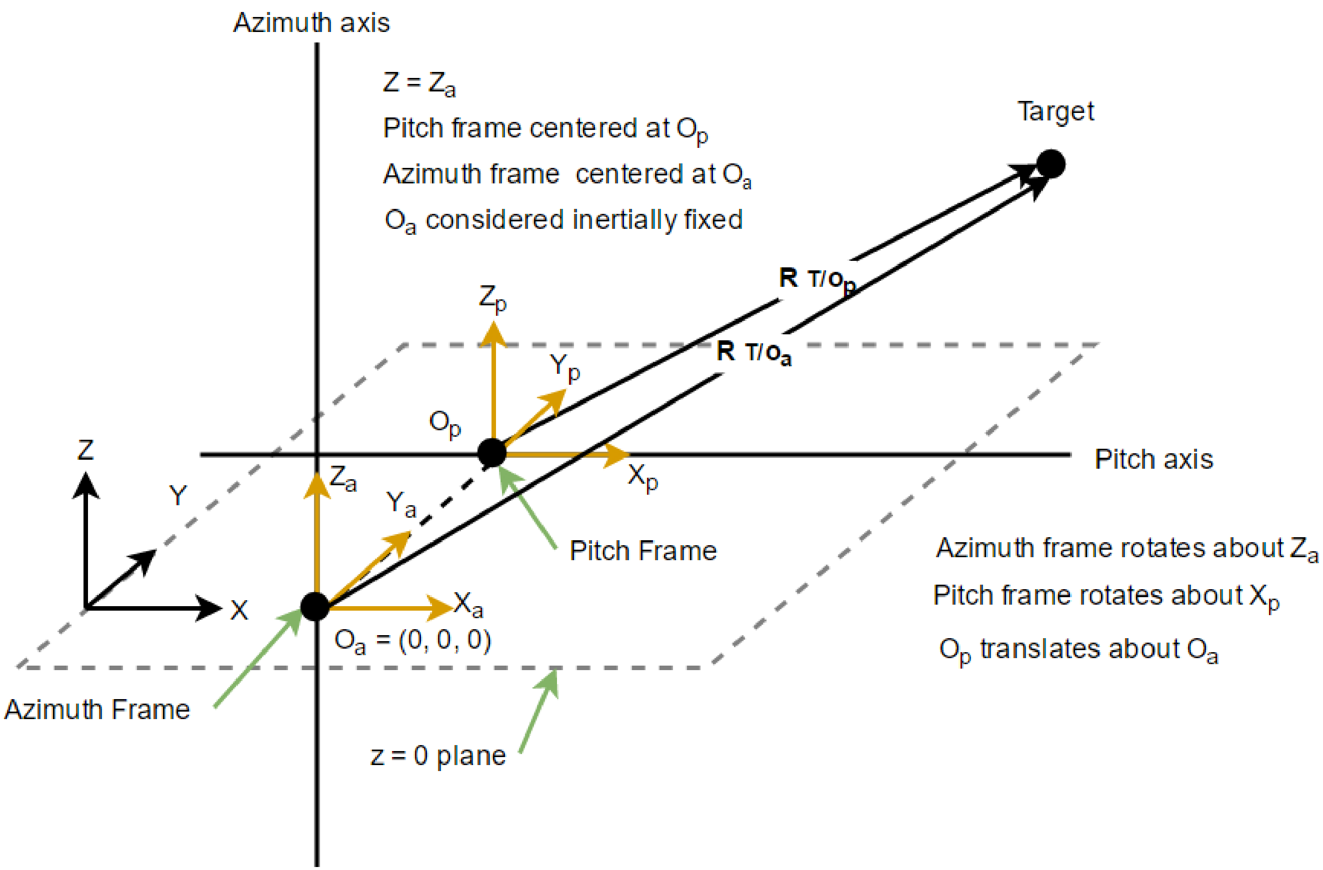

Relevant Vectors

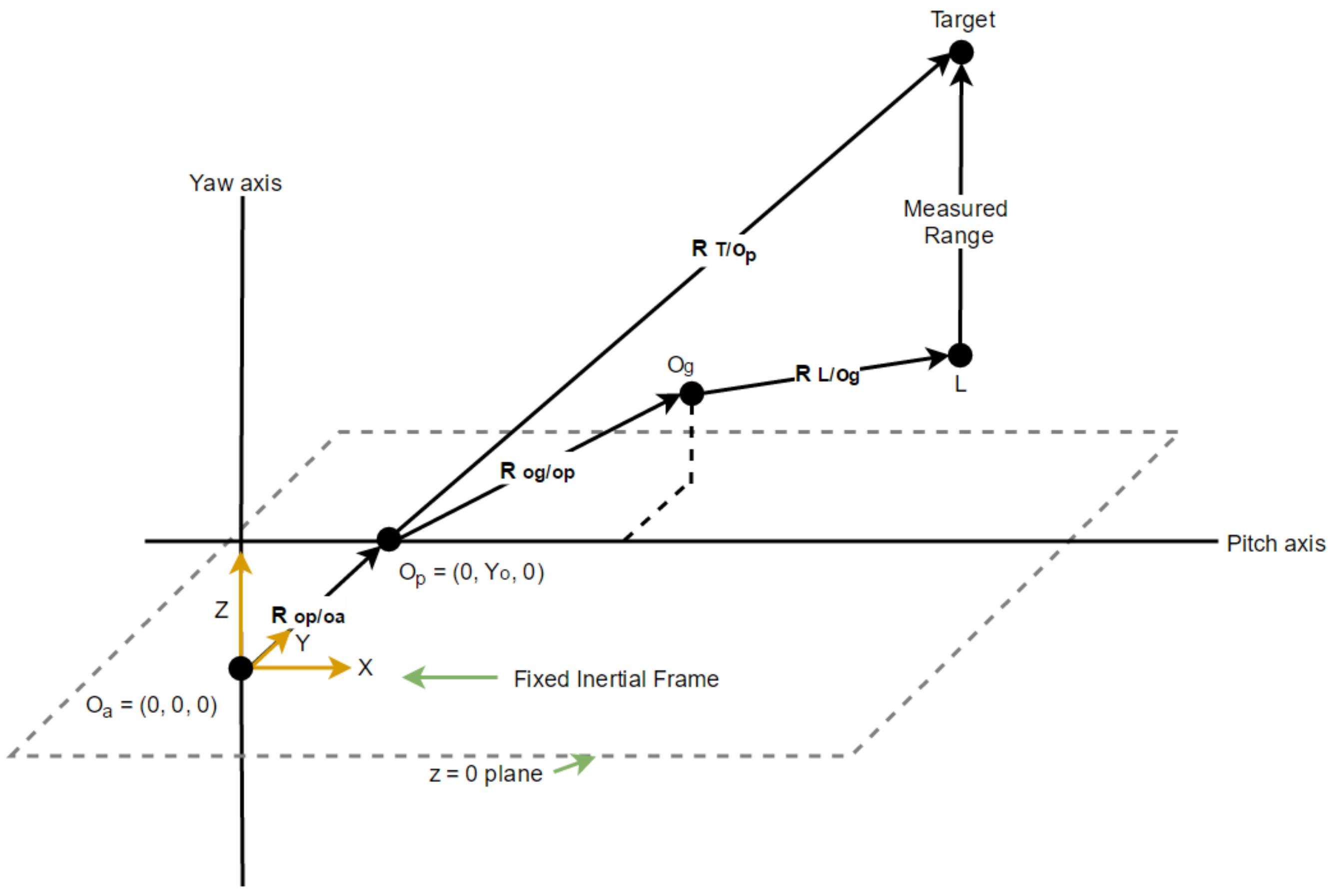

Frame Transformations

$$[R_{T/O_a}]_I = C_3(-\psi)\Bigg(Y_o + C_1(-\phi)\Big([R_{O_g/O_p}]_p + [R_{L/O_g}]_p + [r]_p\Big)\Bigg)$$

where

$$C_1(x) = \begin{pmatrix} 1 & 0 & 0 \\ 0 & \cos(x) & \sin(x) \\ 0 & -\sin(x) & \cos(x) \end{pmatrix}$$

$$C_3(x) = \begin{pmatrix} \cos(x) & \sin(x) & 0 \\ -\sin(x) & \cos(x) & 0 \\ 0 & 0 & 1 \end{pmatrix}$$

Hazard Detection Algorithms

Simple Filter

- Identifies safe/unsafe points purely by their height value
- Mainly used as a baseline comparison

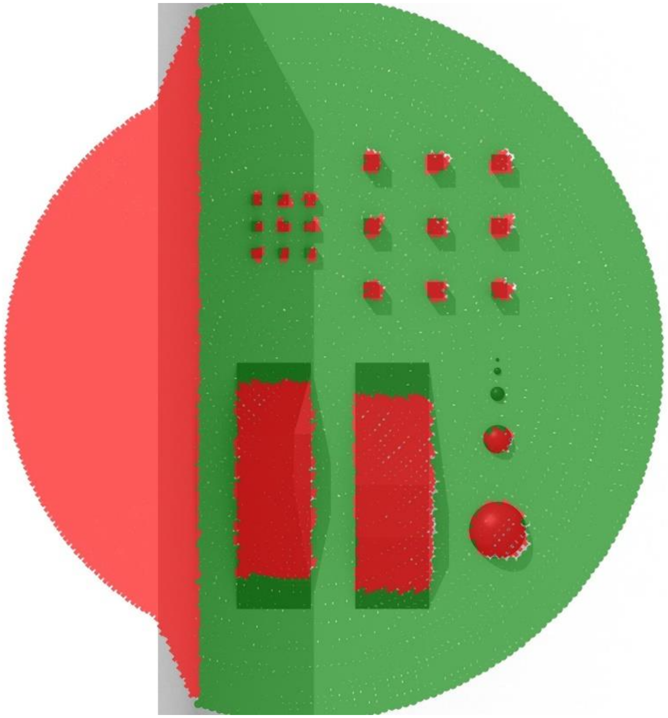

Hazard Detection Algorithms

Point Displacement Filter

- Identifies hazards where scanned points are far away from their expected location (on a flat plane)

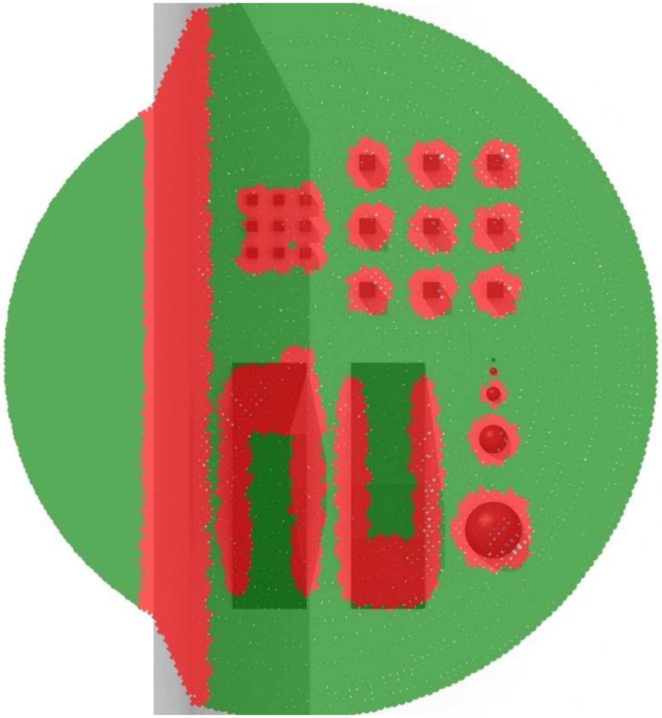

Simulated Lidar Scan

- Simple terrain map with obstacles, made in Blender
- Simulated lidar scans at 10 cm resolution and outputs 3D point cloud
- Point cloud is fed to hazard detection algorithms to test their feasibility

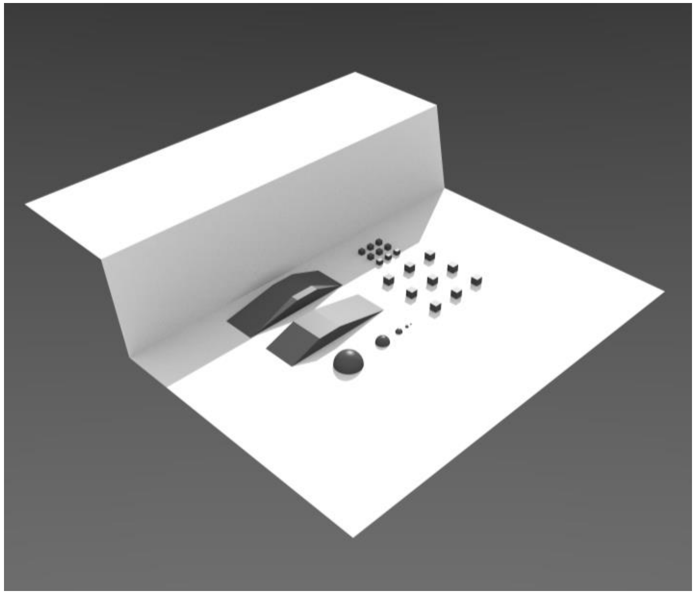

Blender Lidar Simulator

- Uncertainties in the Blender point projection are much smaller than they will be for the physical system
  - Comparison of defined scan pattern to re-projected ground scan shows an average error of less than 2 micrometers over a 14.1 meter distance

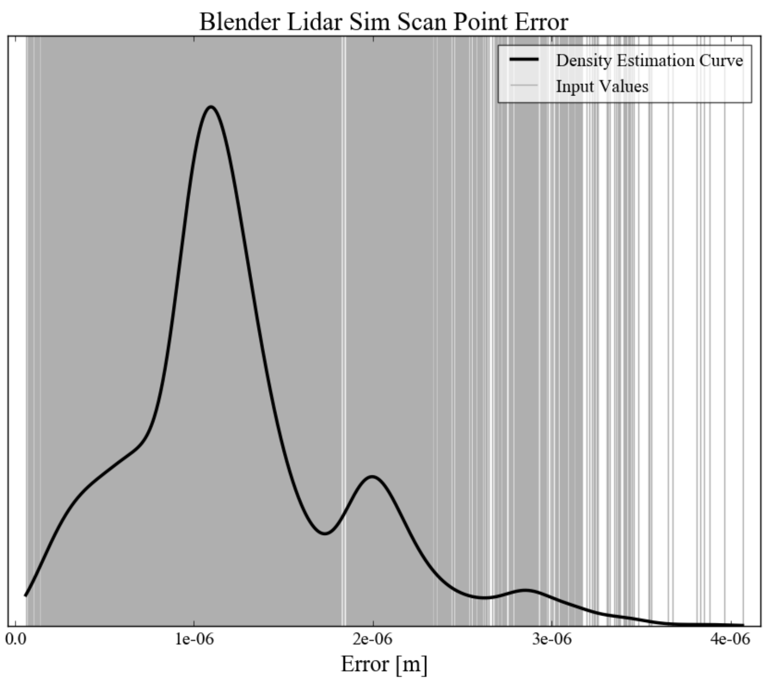

Stroking

Stroking bloats object boundary contours

Voronoi Diagrams

A Voronoi diagram shows the cells whose edges are defined as the locus of points equidistant from their nearest neighbors. Algorithms for computing such a diagram are readily available. Calculating the area of the of the cells may be accomplished by triangulation, with areas of triangles calculated by Heron's formula

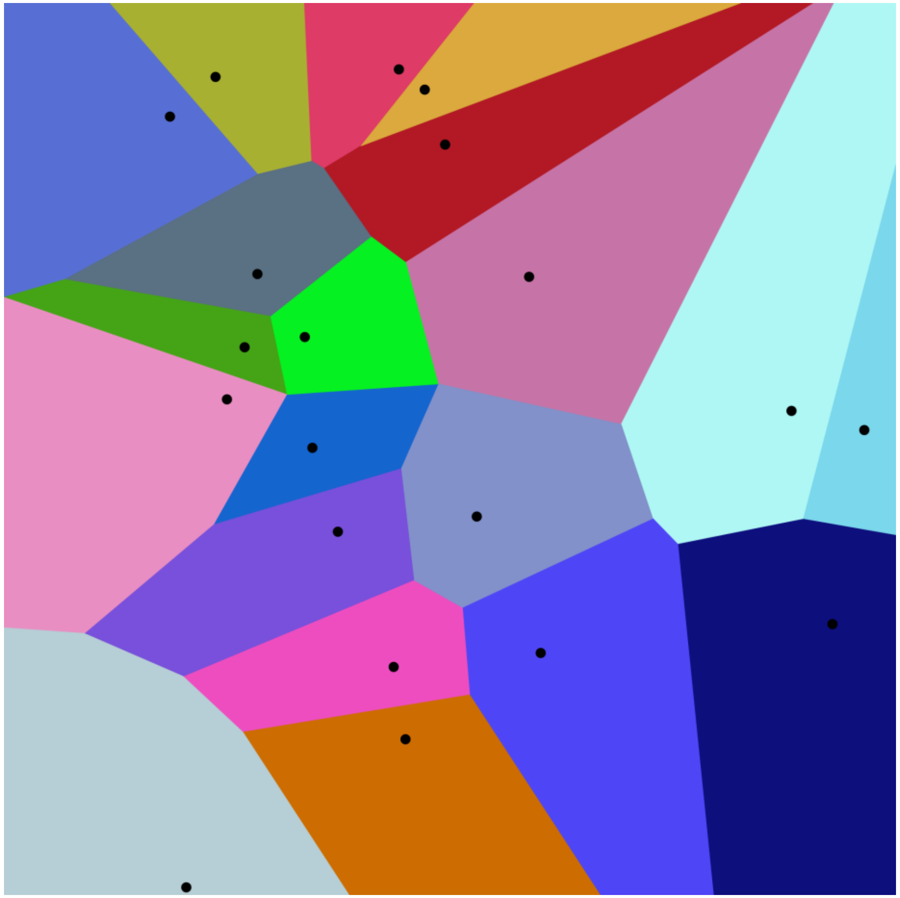

https://upload.wikimedia.org/wikipedia/commons/thumb/5/54/Euclidean_Voronoi_diagram.svg/2000px-Euclidean_Voronoi_diagram.svg.png

Centroid Finding

In the continuous setting for a 2D object with area A

$$\bar{x} = \frac{1}{A}\int_{\Omega} x\,dA \qquad \bar{y} = \frac{1}{A}\int_{\Omega} y\,dA$$

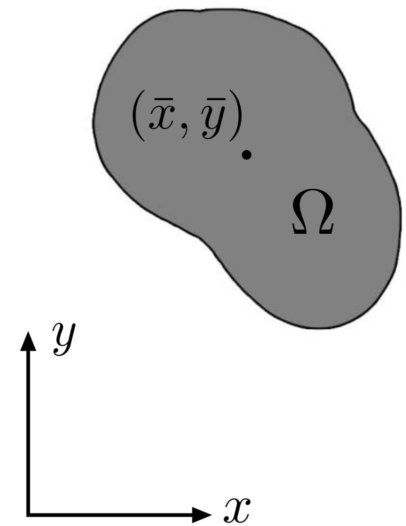

In the discrete setting

$$\bar{x} = \frac{1}{A}\sum_{i=1}^{n} x_i v_i \qquad \bar{y} = \frac{1}{A}\sum_{i=1}^{n} y_i v_i$$

Where v_i is the area of a Voronoi Diagram block

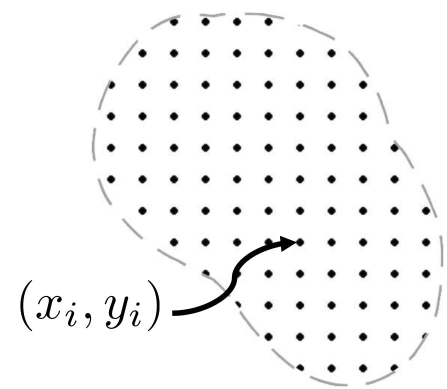

Nearest Neighbor

Nearest neighbor algorithms identify points close to a center

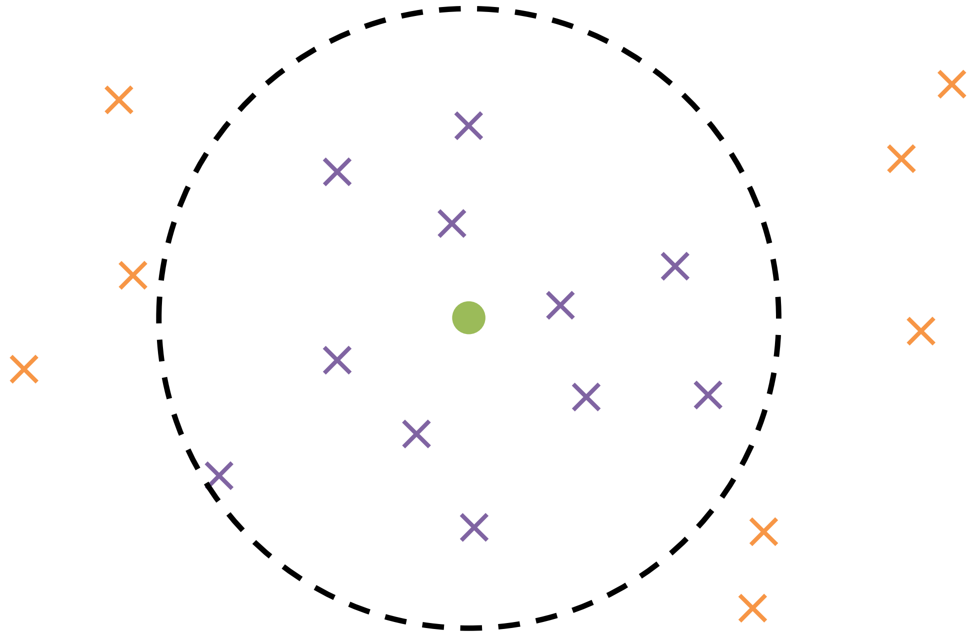

Stroking Neighbor

Stroking Neighbor:

1) Strokes the hazard map to find safe sites for lander center
2) Computes the centroids of these regions
3) Finds the nearest centroid to nadir

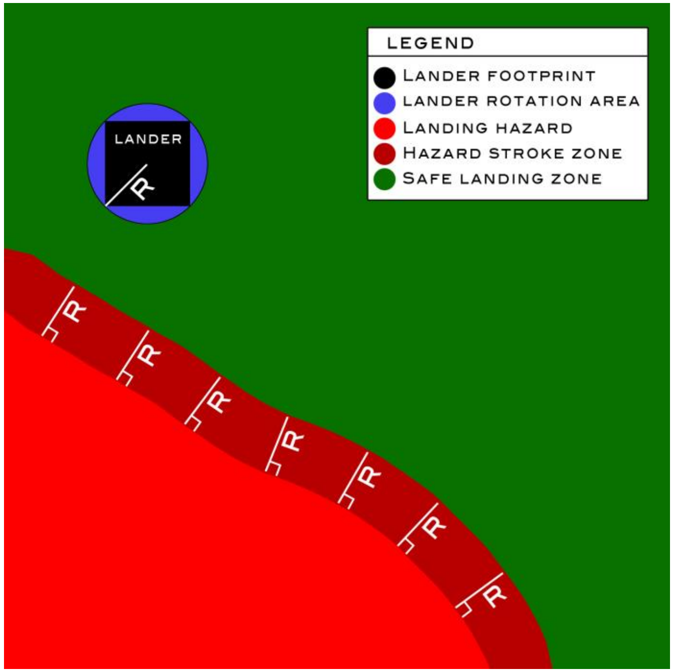

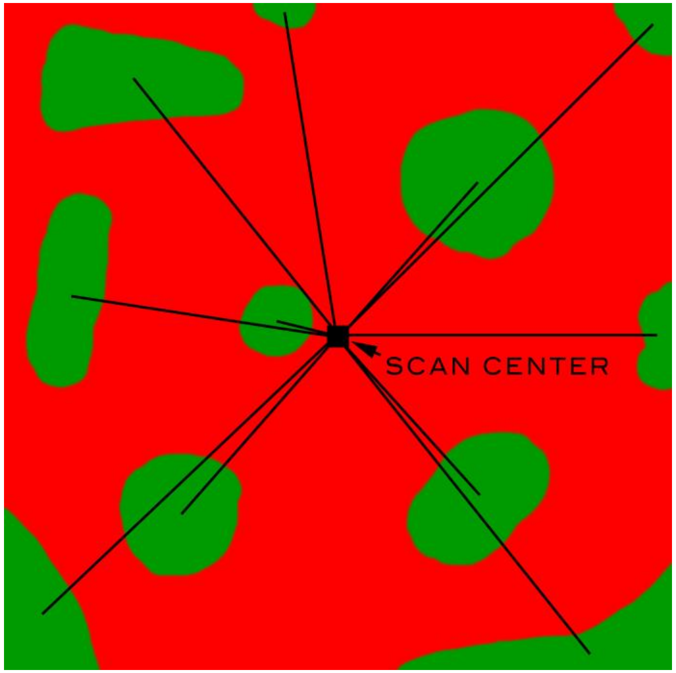

Computation Time

- Simple Filter:
  - Extremely fast but very poor performance
  - Time to run on laptop: 0.035 seconds for 10 cm grid
- Morphological Filter:
  - Finding neighboring points is an expensive operation, $O(n^2)$
  - Time to run on laptop: 0.31 seconds for 10 cm grid
- Point Displacement Filter
  - Also requires a distance matrix to find neighboring points
  - Time to run on laptop: 1.78 seconds for 10 cm grid

Full Budget

Item	Quantity	Cost per (USD)	Total cost (USD)	Source/Notes
Lidar:				
Pepperl-Fuchs VDM28-15-L-IO/73c/110/122	1	470.17	470.17	https://www.carltonbates.com/Photoelectric-Sensors-Reflex-Reflective-Block-Style-/PEPPERL-
Motors:				
ULT100B11AH000 (without halls)	1	833	833	Requested quote from "http://www.celeramotion.com/"
Encoders:				
OPS read head (OD 3.937" ID 2.756")	2	560	1120	Requested quote from "http://www.celeramotion.com/"
Bearings:				
VA030CP0 Thin Section Bearing 3"x3 1/2"x1/4" inch Open	4	81.77	327.08	http://www.vxb.com/VA030CP0-Thin-Section-3-x3-1-2-x1-4-inch-Open-p/kit8779.htm
Microprocessor:				
BeagleBone Black Rev C.1	1	55	55	https://www.adafruit.com/products/1996
Test setup:				
Manufactured in-house	1	100	100	
Motor Drivers:				
DZRALTE - 010B080	2	400	800	Requested quote from "http://www.a-m-c.com/"
Risley prism:				
P-WRC059 coated with BBAR 400-700 nm	2	108	216	Requested quote from "http://www.rossoptical.com/"
Materials				
			500	
Shipping			210	Assuming $15 per item
Total			**4631.25**	Tax exempt
Budget			**5000**	Provided by the CU Aerospace Engineering department
Percent Margin			**7.375**	

Alternate motors:

ULT100B11AH000	2	965	1930	http://www.celeramotion.com/

Alternate bearings:

VA030XP0 3"x3 1/2"x1/4" inch 4 Point Contact Thin Bearing	4	173.49	693.96	http://www.vxb.com/VA030XP0-3-x3-1-2-x1-4-inch-4-Point-Contact-Thin-p/kit9225.htm

Alternate Motor Drivers:

DPRALTE - 020B080	2	605	1210	https://www.servo2go.com/product.php?ID=101890#details